COMPARISON BETWEEN WEAK AND STRONG GROUND MOTIONS AT SELECTED LOCATIONS OF BANGLADESH.

A Thesis Submitted by

MD. SAMSUR RAHMAN
STUDENT NO: 0412042208

In partial fulfillment of requirement for the degree of

MASTER OF SCIENCE IN CIVIL ENGINEERING (GEOTECHNICAL)

MARCH 14, 2016

DEPARTMENT OF CIVIL ENGINEERING
BANGLADESH UNIVERSITY OF ENGINEERING AND TECHNOLOGY
Dhaka-1000, Bangladesh

The thesis titled "Comparison between weak and strong ground motion at selected locations of Bangldesh." Submitted by Md. Samsur Rahman, Roll No. 0412042208, Session April 2012 has been accepted as satisfactory in partial fulfillment of the requirement for the degree of Master of Science in Civil Engineering on 14th March 2016.

BOARD OF EXAMINERS

(Dr. Mehedi Ahmed Ansary) — Chairman (Supervisor)
Professor
Department of Civil Engineering
Bangladesh University of Engineering and Technology.
Dhaka-1000

(Dr. K.A.M. Abdul Muqtadir) — Member
Professor and Head
Department of Civil Engineering
Bangladesh University of Engineering and Technology.
Dhaka-1000

(Dr. Mohammad Shariful Islam) — Member
Professor
Department of Civil Engineering
Bangladesh University of Engineering and Technology.
Dhaka-1000

(Dr. Md. Mahmudur Rahman) — Member (External)
Professor and Head
Department of Civil Engineering
Ahsanullah University of Science and Technology.
Dhaka-1208

DECLARATION

It is hereby declared that except for the contents where specific references have been made to the work of others, the studies contained in this thesis are the result of investigation executed by the author under the supervision of Dr. Mehedi Ahmed Ansary, Professor, Department of Civil Engineering, Bangladesh University of Engineering and Technology.

It is hereby declared that this thesis or any part of it has not been submitted elsewhere for the award of any degree or diploma.

(Signature of the Author)

ACKNOWLEDGEMENT

"In the name of Almighty Allah, the most Beneficent and the mostMerciful"

The author wishes to express his profound gratitude and sincere appreciation to his supervisor, Dr. Mehedi Ahmed Ansary, Professor, Department of Civil Engineering, Bangladesh University of Engineering & Technology (BUET), Dhaka for his dynamic assistance, constant guidance, invaluable suggestions, enthusiastic encouragement, strong support, generous help, persistent simulation and unfailing enthusiasm at all stages to fulfill this extensive study. It would have been impossible for the author to carry out this study without his guidance and inspiration.

The author wants to express his sincere thanks to Dr. K.A.M Abdul Muqtadir, Professor and Head, Department of Civil Engineering, BUET, for his co-operation.

The author would like to express sincere appreciation to Dr. Mohammad Shariful Islam, Professor, Department of Civil Engineering, BUET and Dr. Md. Mahmudur Rahman, Professor, Department of Civil Engineering, AUST for their interest and suggestions during the present research.

The author conveys special thanks to BUET-Japan Institute of disaster Prevention and Urban Safety (BUET-JIDPUS) and Bangladesh Network Office for Urban Safety (BNUS) staffs for providing microtremor equipment as well as assistance to fulfill this research. The author is also very grateful to the Civil Engineering Department, BUET for providing all the necessary supports and funds for this whole work.

Finally, the author wishes to express his gratitude to all the members of his family especially his parents for their continuous support and utmost sacrifice without which this thesis work would not come into reality.

ABSTRACT

Microtremor recordings for weak ground motion and Earthquake recordings for strong ground motions are the easiest and cheapest way to understand the dynamic characteristics of soil. The purpose of this research is to apply Horizontal to Vertical Spectral ratio (H/V) of Microtremor and Earthquakes at six locations namely Bogra, Natore, Jamuna Bridge east at Sirajganj, Police staff college at Mirpur, Haji camp at Ashkona and BUET campus to assess site amplification of those sites.

For spectral analysis of Microtremor, five low noise segments each having window of 41s (data recordings) have considered at 100 Hz instrumental sampling. Fast Fourier Transformation (FFT) has been applied on the time domain records. Then, non-reference spectral ratio (H/V) technique has been applied. The resultant of two horizontal components of H/V ratio have been digitally filtered using suitable average smoothing point. After calculating five sets of the H/V ratios at selected location, the H/V ratio has been plotted with respect to their frequency at selected locations. Similarly for Earthquakes, ground motion records of Sikim earthquake 2006 and 2011, Bengal earthquake 2006, Assam earthquake 2010 and Nepal earthquake 2015 have been used. These accelerometers provide data in North-South, East-West and Up-Down directions. Then Fourier spectrum ratio (Horizontal versus Vertical) for various free field stations is computed.

Comparing between H/V ratio of Microtremor and Earthquake recordings, it has been observed that the peak H/V ratio of earthquake moved into left side or right side and slightly upwards or downwards with respect to microtremor. From these result, it can be said that although amplitude values of the ratios are close, the predominant frequency for the three cases differs slightly. The reason of this difference is that microtremor and earthquake consists of different types of waves, but the H/V ratio is based on shear-wave only.

Damage assessment of soils using Nakamura's Vulnerability Index (Kg) has been used in the investigated locations. The seismic Vulnerability Index (Kg) at those six locations varies from 6.72 to 20.88 for microtremor observations. The estimated vulnerability Index from earthquakes is always higher than the microtremor due to high input energy. Microtremor vulnerability Index (Kg) values show higher value for reclaimed area which provides evidence that those sites need some kind of soil improvement if they want to sustain earthquake load.

CONTENTS

		Page
BOARD OF EXAMINEERS		**I**
DECLARATION		**II**
ACKNOWLEDGEMENT		**III**
ABSTRACT		**IV**
TABLE OF CONTENTS		**V**
LIST OF TABLES		**IX**
LIST OF FIGURES		**X**
NOTATION		**XVII**
CHAPTER 1	**INTRODUCTION**	
1.1	General	1
1.2	Objective of the Research	2
1.3	Study Area and Site Selection	3
1.4	Outline of Methodology	4
1.5	Overview of the Thesis	9
CHAPTER 2	**LITERATURE REVIEW**	
2.1	General	10
2.2	Regional Tectonics	12
2.3	Seismotectonic Setup	14
2.4	Major Seismic Sources	15
2.5	Seismic Zoning map of Bangladesh	19
2.6	Past Research on Microtremor	23
2.6.1	Earthquake and Microtremor Spectral Ratio	25
2.6.2	Observed and Analytical	29

Page

Amplitude Ratio

2.7 Microtremor and Earthquake ground motion of H/V Technique 32

2.7.1 Method of Microtremor and Earthquake Ground Motion in the H/V Technique 33

2.7.2 Theory of Microtremor and Earthquake H/V Technique 34

2.8 Relationship Between Shear Wave Velocity (V_s) and SPT (N) Value 37

2.9 Damage Assessment 41

2.9.1 Seismic Vulnerability Index for soil 41

2.10 Summary 44

CHAPTER 3 DATA COLLECTION AND ANALYSIS

3.1 General 45

3.2 Study Locations 46

3.3 Some earthquakes have affected Bangladesh of the last decay 48

3.4 Methodology of microtremor and earthquake data analysis 49

3.5 Sub-Soil Investigation on SPT-N values and Microtremor Array analysis 50

3.6 Microtremor data collection 57

Page

3.7 Earthquake data analysis 59
3.7.1 Time history and Fourier spectrum Microtremor data analysis at selected locations of Bangladesh 60
3.8 Earthquake data analysis 67
3.8.1 Time History and Fourier Spectrum analysis of different Earthquake at Selected Locations 67
3.9 Stability check of Microtremor Data 71
3.10 Smoothing Effect on Microtremor and Earthquake Data 71
3.11 Horizontal versus Vertical (HVSR) and Smoothed HVSR analysis of Microtremor and Earthquake at Selected Locations 72
3.12 Summary 84

CHAPTER 4 COMPARISON OF MICROTREMOR AND EARTHQUAKE GROUND MOTION ANALYSIS

4.1 General 85
4.2 Comparison of Microtremor and Earthquake ground motion 85
4.3 Vulnerability Assessment 92
4.3.1 Seismic damage assessment of soil using Nakamura's Technique 92
4.4 Summary 93

Page

CHAPTER 5 CONCLUSIONS AND RECOMMENDATIONS

5.1 General 95
5.2 Conclusions 95
5.3 Recommendations 96

REFERENCES 97

LIST OF TABLES

page

Table 2.1 Great historical earthquakes in and around Bangladesh 15

Table 2.2 Significant Seismic Sources and Maximum Likely Earthquake Magnitude in Bangladesh (After Bolt, 1987) 17

Table2.3 Operational Basis Earthquake, Maximum Credible Earthquake and Depth of Focus of Earthquakes for Different Seismic Sources (After Ali And Chowdhury, 1992) 18

Table 2.4 Magnitude,EMS Intensities and distances of some major historical earthquakes around Dhaka (after Ansary, 2001) 18 38

Table 2.5 Empirical correlation between SPT N-value and Shear-wave Velocity (After TC4, ISSMFE, 1993) 47

Table3.1 Location of Digital Seismic Measuring Device Station (ETNA) 48

Table 3.2 Most recently some earthquakes that have affected in and around Bangladesh 86

Table 4.1 The predominant frequency and H/V ratio of microtremor and earthquake at Bogra 87

Table4.2 The predominant frequency and H/V ratio of microtremor and earthquake at Natore. 88

Table4.3 The predominant frequency and H/V ratio of microtremor and earthquakes Jamuna Bridge East at Sirajganj. 89

Table4.4 The predominant frequency and H/V ratio of microtremor and earthquakes Haji-Camp at Ashkona. 90

Table4.5 The predominant frequency and H/V ratio of microtremor and earthquakes Police Staff College at Mirpur. 91

Table4.6 The predominant frequency and H/V ratio of microtremor and earthquakes at BUET-Campus. 92

Table 4.7 Damage assessment of site soil using Nakamura's empirical formula

LIST OF FIGURES

		Page
Figure1.1	Select Study Location of Microtremor observation and Earthquake Measuring Devices in and around of Bangladesh	3
Figure1.2	Microtremor data collection procedure (Array Mode) in (a) Horizontal line in one way direction and (b) Plus sign (+Ve) shape	6
Figure1.3	Flow chart of the Thesis for study area.	7
Figure 2.1	Microtremor observation and damage assessment.	11
Figure 2.2	Estimated slip potential along the Himalaya (after Bilham et al., 2001)	12
Figure 2.3	India's northward drift over the last 70 million years (after Molnar and Tapponnier, 1975)	13
Figure2.4	Generalized tectonic map of Bangladesh and adjoining areas (after GSB, 1991)	13
Figure 2.5	Seismic Zoning Map of Bangladesh (after BNBC, 1993)	21
Figure 2.6	Proposed (Updating) Seismic Zoning Map of Bangladesh	22
Figure2.7	Comparision of (1) the average earthquake site-to-reference spectral ratios (SSR) with (2) the average earthquake H/V spectral ratios (HVSR) of up to seven earthquakes, and (3) the average microtremor H/V spectral ratio at three strong-motion instrument sites in greater Victoria. (After Molnar et al., 2007)	27
Figure 2.8	Comparision of the H/V spectral ratio from up to four weak-motion earthquakes and microtremors at four sites across SW British Columbia.(after Molnar et al, 2007)	28
Figure 2.9	Amplitude ratios of microtremor and theoretical Rayleigh-wave plotted with transfer function of shear wave. (After Ansary et al., 1996)	30
Figure2.10	Amplitude ratios of microtremor and theoretical transfer function of shear wave at National University Tongi, Gazipur (after Rahman, 2011)	31

LIST OF FIGURES

		Page
Figure2.11	Amplitude ratios of microtremor and theoretical transfer function of shear wave at Block-D, Bashundhara. (after Rahman, 2011)	32
Figure2.12	Typical geological structure of sedimentary basin	34
Figure2.13	Relationship between charactersistics of RayleighWave and Impedance Ratio. (After Nakamura, 2000	36
Figure2.14	Schematic comparison of Horizontal (H_f), Vertical (V_f), H_f/H_b (spectral ratio of sediment site to the reference(After Nakamura, 2000)	37
Figure2.15	Recommended Curves for Correction Factor from EffectiveOverburden Pressure. (After Murthy, 1991)	39
Figure2.16	Proposed Shear Wave Velocity and SPT N-value correlations for clay and sand (After Ansary et al., 2010)	40
Figure 2.17	Surface ground deformation.	41
Figure2.18	$K_g$values calculated for Loma Prieta Earthquake. (After Nakamura et al., 1990)	43
Figure 3.1	Location of Digital Seismic Measuring Devices (29-ETNA) in and around Bangladesh	46
Figure 3.2	Flow Chart for Methodology of Microtremor and Strong Motion Data Analysis.	49
Figure 3.3	Depth, SPT-N Values and Soil Profile at Bogra LGED office	51
Figure 3.4	Depth and Shear Wave Velocity at Bogra LGED office	52
Figure 3.5	Depth, SPT-N Values and Soil Profile at Natore LGED office	53

LIST OF FIGURES

		Page
Figure 3.6	Depth and Shear Wave Velocity at Bogra LGED office	54
Figure3.7	Depth, SPT-N Values and Soil Profile at Jamuna Bridge East Side, Serajgnj	55
Figure3.8	Depth and Shear Wave Velocity at Jamuna Bridge East Side, Serajgnj	56
Figure 3.9	Microtremor measurement apparatus	58
Figure 3.10	Field data collection Process for Microtremor and Seismic Measuring devices.	58
Figure3.11	Time history of Microtremor obseravation LGED office at Bogra.	59
Figure3.12	(a)Total time history (0-1800) sec. (b) Segment-1 (0-41) sec (c) Segment-2(41-82) sec. (d) Segment-3 (82-123) sec .(e) Segment-4123-164) sec. and (f) Segment-5 (164-205) sec for Time History and of Microtremor analysis at LGED office Bogra.	61
Figure3.13	(a)Total time history (0-1800) sec. (b) Segment-1 (200-241) sec .(c) Segment-2 (241-282) sec. (d) Segment-3 (282-323)sec (e) Segment-4 (323-364)sec. and (f) Segment-5 (364-405)sec for Time History and FFT of Microtremor analysis at LGED office Natore	62
Figure3.14	(a) Total time history (0-600)sec. (b)Segment-1 (200-241)sec (C) Segment- 2 (241-282)sec. (d) Segment-3 (282-323)sec .(e) Segment-4 (323-364)sec.and (f) Segment-5 (364-405)sec for Time History and FFT of Microtremor analysis at Jamuna Bridge East Side.	63
Figure3.15	(a)Total time history (0-1800)sec. (b)Segment-1 (900-941)sec.(C)Segment-2(941-982)sec.(d)Segment-3 (982-1023)sec .(e) Segment-4(1023-1064)sec and (f) Segment-5 (1064-1105)sec for Time History and FFT of Microtremor analysis at Airport, Ashkona Haji-Camp, Dhaka.	64

LIST OF FIGURES

Page

Figure3.16 Figure 3.16 (a)Total time history.(0-1800)sec. (b)Segment-1 (400-441)sec .(C) Segment-2 (441-482)sec. (d) Segment-3 (482-523)sec .(e) Segment-4(523-564)sec. and (f) Segment-5 (564-605)sec for Time History and FFT of Microtremor analysis at Police Staff College, Mirpur-Dhaka. 65

Figure3.17 Time history and FFT at (a) Sikim EQ in Acceleration, Velocity, Displacement and FFT at Bogra (b) Time history and FFT in the Sikim Earthquake at Bogra LGED office.(c) Sikim EQ Natore.(d) Sikim EQ J.B.East (e) Assam EQ Haji-Camp, Dhaka and (f) Monipu Earthquake at BUET-Campus, Dhaka. 66

Figure3.18 Time history and FFT at (a) Sikim EQ in Acceleration, Velocity, Displacement and FFT at Bogra (b) Time history and FFT in the Sikim Earthquake at Bogra LGED office.(c) Sikim EQ Natore.(d) Sikim EQ J.B.East (e) Assam EQ Haji-Camp, Dhaka and (f) Monipur Earthquake at BUET-Campus, Dhaka. 68

Figure3.19 Time history and FFT at (a) Jessore Earthquake at Bogra LGED office (b) Jessore Earthquake at Natore LGED office.(c) Jessore EQ J.B.East.(d) Bhutan-India Earthquake at Bogra LGED office (e) Bhutan-India Earthquake at Natore LGED office and (f) Mynmar-Assam Earthquake at PSC, Dhaka. 69

Figure3.20 Time history and FFT at (a) Bhutan-India EQ T at Natore LGED office, Natore. (b) Bhutan-India EQ at Bogra LGED office, Bogra LGED office.(c)) Bhutan-India EQ T at police Staff College,Mirpur-Dhaka.(d) Nepal EQ at LGED, Bogra (e) Nepal EQ Natore LGED office and (f) Nepal Earthquake at BUET-Campus, Dhaka. 70

Figure 3.21 H / V Ratio of Microtremor analysis at Bogra LGED office in (a) Segment 3: (82-123) Sec (b) Segment 2: (41-82) Sec (C) Segment 3: (82-123) Sec (d) Segment 4: (123-164) Sec (e) Segment 5: (164-205) Sec. and (f) Combined H/ V Ratio at Bogra. 73

.

76

LIST OF FIGURES

Page

Figure 3.22 H / V Ratio of Microtremor analysis at Natore LGED office in (a) Segment 1: (200-241) Sec (b) Segment 2: (241-282) Sec (C) Segment 3: (282-323) Sec (d) Segment 4: (323-364) Sec (e) Segment 5: (364-205) Sec. and (f) Combined H/ V Ratio at Natore 74

Figure3.23 H / V Ratio of Microtremor analysis at Jamuna Bridge East side in (a) Segment 1: (200-241) Sec (b) Segment 2: (241-282) Sec (c) Segment 3: (282-323) Sec (d) Segment 4: (323-464) Sec (e) Segment 5: (464-405) Sec. and (f) Combined H/ V Ratio at Jamuna Bridge East Site 75

Figure 3.24 H / V Ratio of Microtremor analysis at Haji-Camp in (a) Segment 1: (900-941) Sec (b) Segment 2: (941-982) Sec (C) Segment 3: (982-1023) Sec (d) Segment 4: (1023-1064) Sec (e) Segment 5: (1064-1105) Sec. and (f) Combined H/ V Ratio at Airport Haji-Camp, Dhaka. 76

Figure 3.25 H / V Ratio of Microtremor analysis at PSC in (a) Segment 1: (400-441) Sec (b) Segment 2: (441-482) Sec (C) Segment 3: (482-523) Sec (d) Segment 4: (523-564) Sec (e) Segment 5: (564-605) Sec. and (f) Combined H/ V Ratio at police Staff College, Mirpur- Dhaka. 77

Figure 3.26 H / V Ratio of Microtremor analysis at BUET in (a) Segment 3: (200-241) Sec (b) Segment 2: (241-282) Sec (C) Segment 3: (282-323) Sec (d) Segment 4: (323-364) Sec (e) Segment 5: (364-405) Sec. and (f) Combined H/ V Ratio at BUET-Campus, Dhaka.

Figure 3.27 H/ V Ratio and smoothed HVSR analysis of Sikim Earthquake analysis at (a) EW, NS and Average HVSR at Bogra (b) Average and smoothed HVSR at Bogra (c) ES, NS and Average HVSR at Natore (d) Average and smoothed HVSR at Natore (e) EW, NS and Average HVSR at BUET (f) Average and smoothed HVSR at BUET-Dhaka 78

LIST OF FIGURES

Page

Figure 3.28 H/ V Ratio and smoothed HVSR analysis of Jessore Earthquake at (a) EW, NS and Average HVSR at Bogra (b) Average and smoothed HVSR at Bogra (c) ES, NS and Average HVSR at Natore (d) Average and smoothed HVSR at Natore (e) EW, NS and Average HVSR at BUET (f) Average and smoothed HVSR at BUET 80

Figure3.29 H/ V Ratio and smoothed HVSR analysis of Assam-India and Myanmar-Assam Earthquake analysis at (a) H/ V Ratio at PSC, Mirpur (b) Average and smoothed HVSR at PSC, Mirpur (C) H/ V Ratio at Haji-Camp (d) Average and smoothed HVSR at Haji-Camp (e) H/ V Ratio at BUET (f) Average and smoothed HVSR at BUET, Dhaka. 81

Figure3.30 H/ V Ratio and smoothed HVSR analysis of Nepal Earthquake at (a) EW, NS and Average HVSR at Bogra (b) Average and smoothed HVSR at Bogra (c) ES, NS and Average HVSR at Natore (d) Average and smoothed HVSR at Natore (e) EW, NS and Average HVSR at PSC (f) Average and smoothed HVSR at PSC, Mirpur-Dhaka 82

Figure3.31 H/ V Ratio and smoothed HVSR analysis of Nepal, Monipur-India and Mynmar-Assam Earthquake analysis at (a) EW, NS and Average at BUET (b) Average and smoothed average HVR at BUET (c) EW, NS and Average at BUET (d) Average and smoothed average HVR at BUET (e) EW, NS and Average at BUET (f) Average and smoothed average HVR at BUET-Dhaka 83

Figure 4.1 Comparison of HVR in Microtremor and Earthquake at Bogra 86

Figure 4.2 Comparison of HVR in Microtremor and Earthquake at Natore 87

Figure 4.3 Comparison of Microtremor and Earthquake in the Jamuna Bridge East at Sirajganj 88

Haji-Camp at Ashkona.

Figure 4.5 Comparison of HVR in Microtremor and in the

LIST OF FIGURES

Page

Figure 4.4 Comparison of HVR in Microtremor and Earthquake in the Haji-Camp at Ashkona 89

Figure 4.5 Comparison of HVR in Microtremor and in the Police Staff College at Mirpur 90

Figure 4.6 Comparison of HVR in Microtremor and Earthquake At BUET-Campus 91

NOTATION

α_b	Acceleration of basement
N	Field SPT N-value
C_N	Correction factor for SPT N-value in terms of confining pressure
σ	Stress along any direction
γ	Shear strain deformation
ω	Frequency of motion
G	Shear modulus
v_p	P-Wave Velocity
v_s	S-Wave Velocity
Kg	Seismic Vulnerability Index
F_g	Predominant Frequency
A_g	H/V Ratio
g	Acceleration due to gravity
F	Natural frequency
FFT	Fast Fourier Transformation
SMAs	Strong Motion Accelerograph
ETNA	Electronic Transmission and Neumerical Analysis
SSMM	Small Scale Microtremor Measurement
MTobs	Microtremor Observation
EQ's	Earthquakes
(SWV) Vs_{30},	Shear Wave Velocity at 30 m Depth
SCS	Segmental Cross-Spectrum
M and I	Magnitude and Intensity of Earthquake
HVSR	Horizontal versus Vertical (H/V) spectral ratio

CHAPTER ONE

INTRODUCTION

1.1 GENERAL

Bangladesh is an earthquake prone country but in the recent past it has not suffered any damaging large earthquakes. In the past few hundred years, several large catastrophic earthquakes struck this area. So far, all the major recent earthquakes have occurred away from major cities, and have affected relatively sparsely populated areas. In 1897, an earthquake of magnitude 8.7 caused serious damages to buildings in the northeastern part of India (including Bangladesh) and 1542 people were killed. Bilham et al. (2001) pointed out that there is high possibility that a huge earthquake will occur around the Himalayan region based on the difference between energy accumulation in this region and historical earthquake occurrence.

The use of microtremor, an idea pioneered by Kanai et al. (1954) turns into one of the most appealing approaches in the site effects studies, due to its relatively low economic cost, and the possibility of recordings without strict spatial or time restrictions. The H/V spectral ratio determined from microtremors has shown a clear peak that is well correlated with the fundamental resonance frequency at “soft soil” sites after Bard (2004). Comparison of microtremor and earthquake spectral ratios at strong-motion instrument sites across SW British Columbia showed similar fundamental periods and in greater Victoria remarkably similar amplitudes, validating the use of the method for linear earthquake site response Molnar et al, (2007).

Further evidence was given by Suzuki et al. (1995) who used both microtremor and strong-motion data in Hokkaido, Japan, and ascertained that the peak frequency determined by the H/V ratio seemed to correspond with the predominant frequency estimated from the thickness of an alluvial layer.

The seismic damage is closely related to the ground structure. It is important to clarify the geological structure of the region, when designing earthquake-proof buildings and structures and in drawing up an earthquake disaster prevention plan for the region. Microtremor

measurement is effective as a method for conveniently and cheaply understanding the ground properties. Nakamura (1989) had determined that the horizontal and vertical spectrum (H/V spectrum) of the short cycle tremor was effective for analysis of the ground motion characteristics and for evaluation of the earthquake motion. The H/V spectral ratio technique of microtremors gained popularity in the early nineties, after the publication of several papers [Field and Jacob (1993); Lermo and Chávez-García (1994)], claiming the ability of this technique to estimate the site response of soft sedimentary deposits satisfactorily.

1.2 OBJECTIVE OF THE RESEARCH

The followings are the specific objectives of the research:

- To obtain weak ground motion (microtremor) at different location of Bangladesh
- To obtain strong ground motion (earthquake) at different location of Bangladesh
- Use Horizontal to Vertical Spectral Ratio (HVSR) from microtremor and SMA to estimate predominant frequency and amplification for Bangladesh
- To estimate damage of soils using Nakamura's (2000) Vulnerability Index (Kg)

1.3 STUDY AREA AND SITE SELECTION

To check the stability of microtremor observation six locations Bogra, Natore, Jamuna Bridge east side at Sirajganj, Police staff college at Mirpur, Haji camp at Ashkona and BUET campus have been selected. In all these locations as shown in Figure 1.1 SMA has been deployed since 2003.

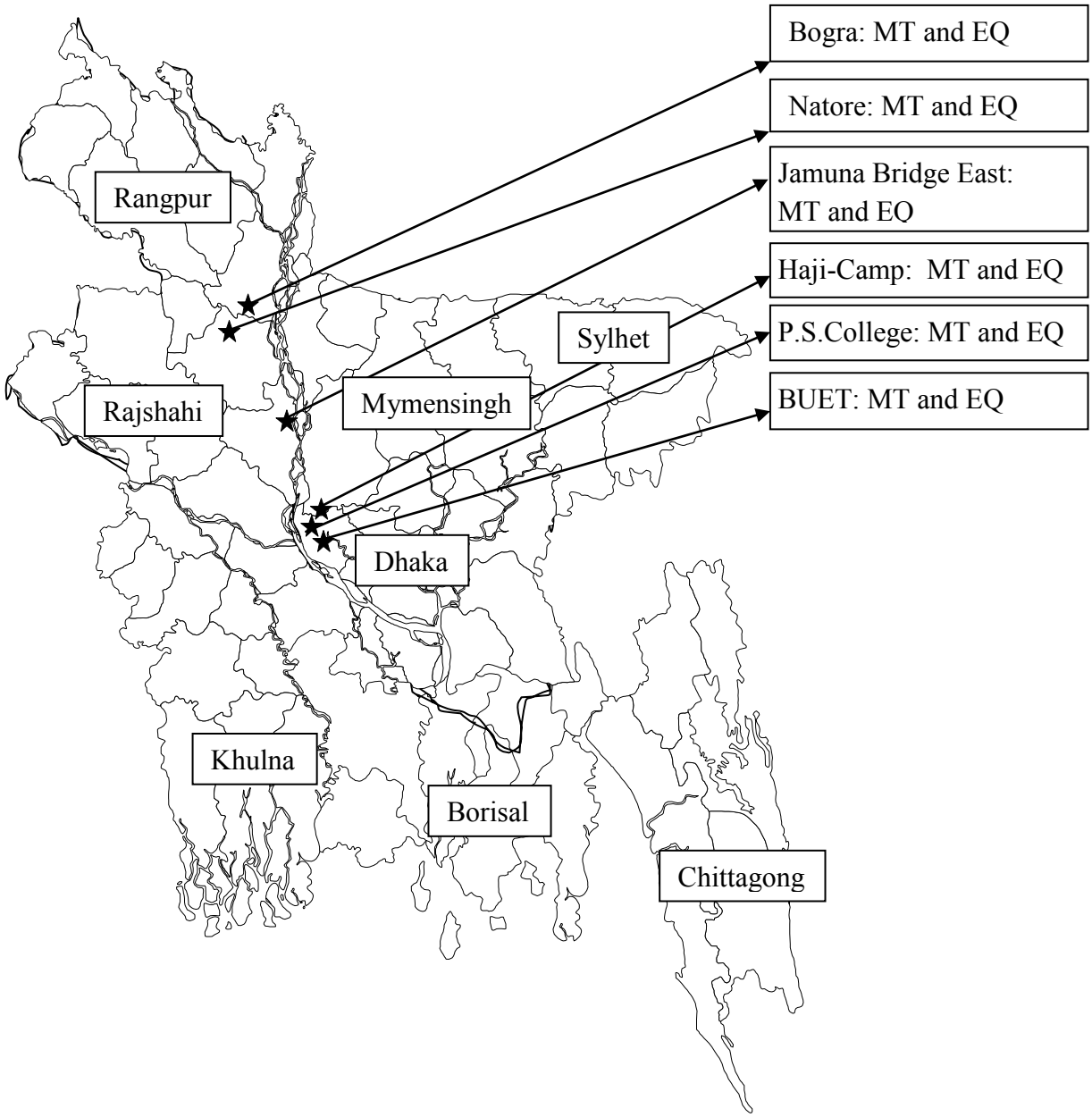

Figure 1.1 Selected Study Location of Microtremor observation and Earthquake Measuring Devices in and around Bangladesh

1.4 OUTLINE OF METHODOLOGY

The amplitude ratio (H/V) of horizontal to vertical spectra of microtremor has become popular to determine predominant period and amplification of a site. It is well known that, degree of damage during earthquakes strongly depends on dynamic characteristics of buildings as well as amplification of seismic waves. Among the other time consuming and expensive approaches, microtremor is the easiest and cheapest way to understand the dynamic characteristics of soil as well as structural element. In a short period of time it provides several information including natural frequency, amplification and vibration characteristics of soil and structure at different frequencies.

Following steps have been followed in this research:

A. Microtremor Data Collection and Analysis (Point mode)

Microtremor observation has been carried out in selected locations of Bangladesh. Each record comprises of three components, viz., EW, NS and UD. For spectral analysis five noise-free segments of 41s of the recordings have been taken at 100 Hz instrumental sampling. Time domain data is not suitable for the clear identification of soil response due to ambient noise. This is why First Fourier Transformation (FFT) has been applied on the time domain records. After smoothing the corresponding spectra, spectral ratio (H/V) technique have been applied to derive transfer functions. The applied sequences are given below:

1. **FFT Transformation**

At first, Fourier spectra of the two horizontal directions (East-West and North-South) and the vertical component (Up-Down) have been calculated. Fast Fourier Transformation (FFT) has been used to transfer time domain data to frequency domain data.

2. **Smoothing of the Spectra**

After Fast Fourier transformation (FFT), the combined horizontal and vertical spectra have been digitally filtered applying a logarithmic window with a suitable bandwidth coefficient. These filtering techniques have been applied to reduce the distortion of peak amplitudes.

3. **Calculation of the Soil Response functions**

The smoothed combined horizontal spectrum have been divided with the smoothed vertical component to plot Horizontal to vertical spectral ratio (H/V) which will provide the desired predominant frequency and corresponding amplification factor of the investigated portions (41s) of records.

4. **Estimation of Predominant Frequency and Amplification**

After calculating five sets of the H/V ratios at selected grid, they have been normalized to obtain a relatively non-biased site specific H/V ratio. Then, Normalized H/V ratios at different time of the day have been plotted in Logarithmic window. From this normalized H/V ratio the predominant frequency and corresponding amplification factor of this site have been taken.

B. SMA Data Collection and Analysis

The purpose of SMA data collection and analysis is to predict model for acceleration-attenuation for earthquakes in Bangladesh and its neighboring region. For this purpose, recently twenty five (29) digital accelerometers (Model-ETNA) were deployed in PWD and LGED offices all over Bangladesh. For this research, six locations Bogra, Natore, Jamuna Bridge east side at Sirajganj, Police staff college at Mirpur, Haji camp at Ashkona and BUET campus have been selected. These accelerometers provide data in North-South, East-West and Up-Down direction. Then Fourier spectrum ratio (Horizontal to Vertical) for various free field stations are computed.

C. Microtremor Data Collection and Analysis (Array Mode)

Array mode of Microtremor data collection process is shown in Figure 1.2. In one case, one sensor is located in central position and another four sensors was setup in the distance around fifty feet from the reference point of MT1. Each record comprises of three components, viz., EW, NS and UD. For spectral analysis five noise-free segments of 41s of the recordings have been taken at 100 Hz instrumental sampling. There are two methods of Microtremor Measurement Array systems such as (a) Horizontal line in one way directions and (b) Plus

sign shape in both directions

(a) Horizontal line in one way directions

In this Array, one Sensor (MT1) is fixed and other four sensors is setup in the Horizontal directions. Each sensor to sensor distance is 50′ (Fifty feet).

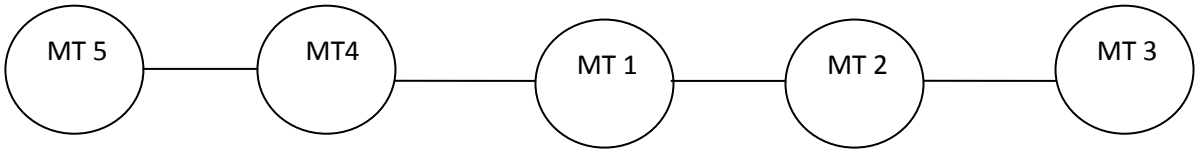

(a)

(b) Plus sign (+Ve) shape

In this Array, one Sensor (MT1) is fixed and other two sensor is setup in the Horizontal directions and another two sensor is setup in the vertical directions. Each sensor to sensor distance is 50′ (Fifty feet).

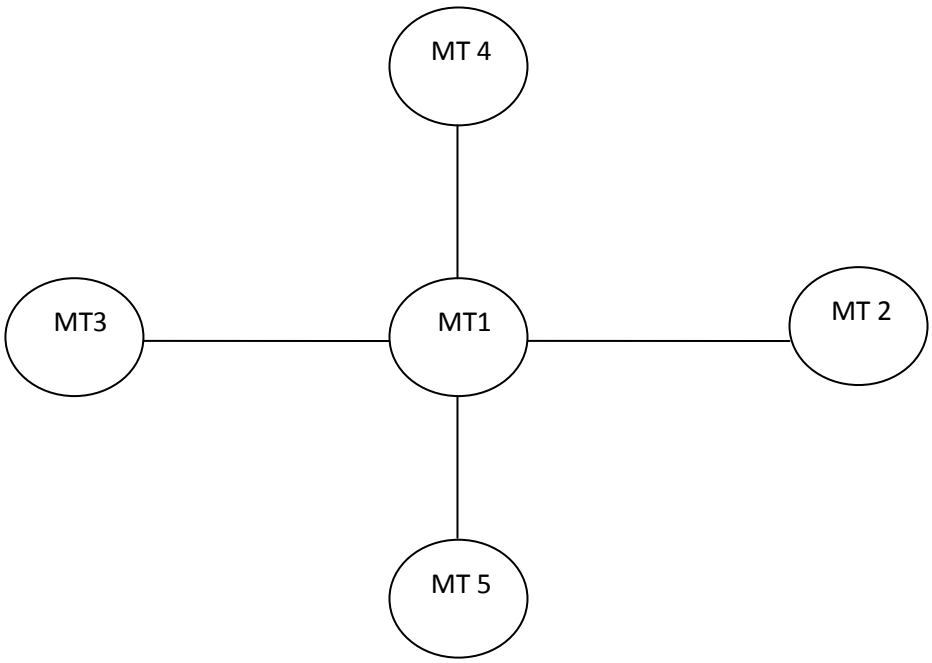

(b)

Figure 1.2 Microtremor data collection procedure (Array Mode) in (a) Horizontal line in one way direction and (b) Plus sign (+Ve) shape

D. Develop Soil condition with Site response Analysis

The characteristics of Soil investigated locations have been developed based on soil investigation report and analysis of Microtremor Array.

The brief methodology of this research and Thesis flow chart is shown in Figure 1.3. The ultimate target is to compare H/V ratio between Microtremor and Earthuqakes.

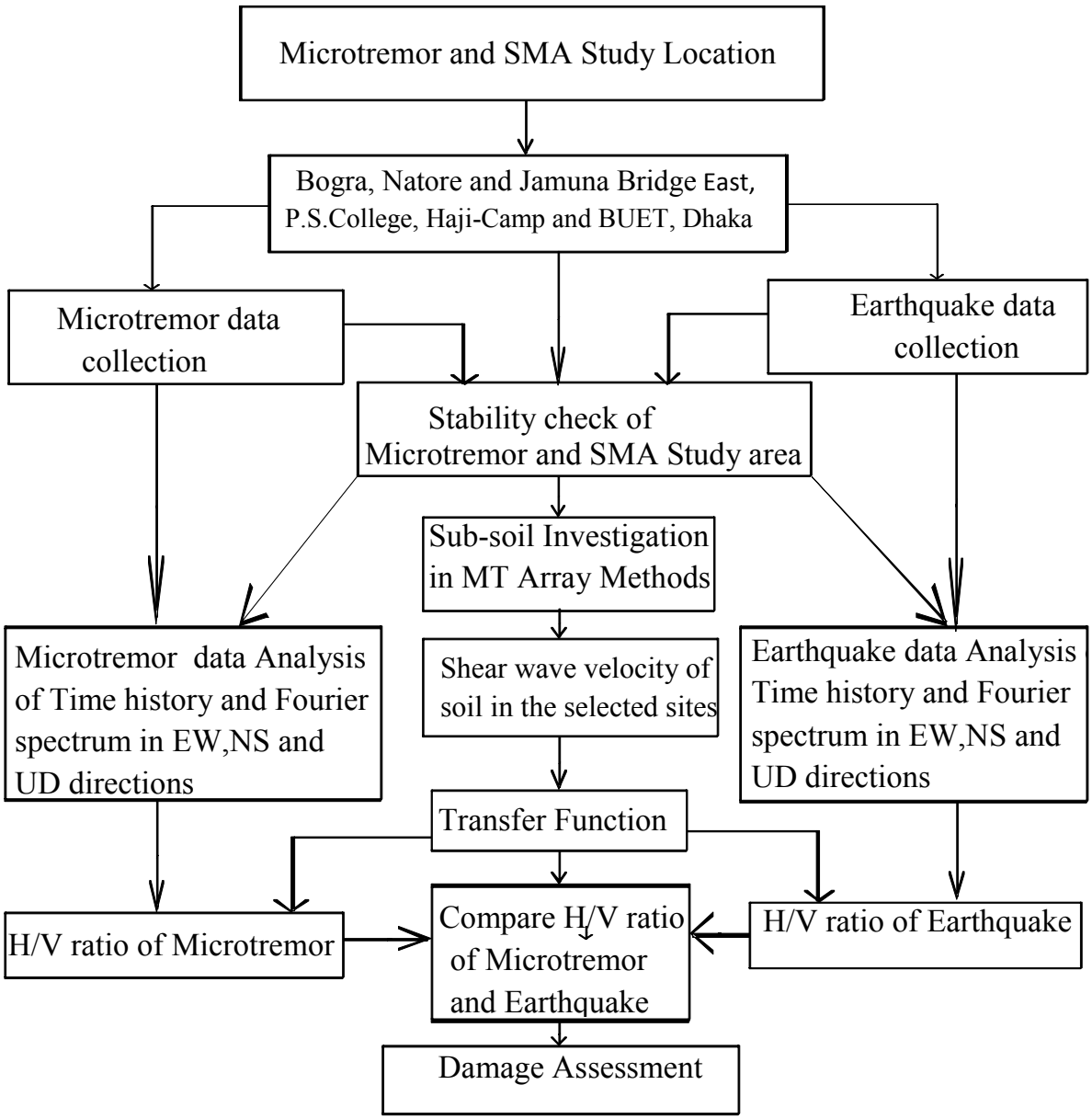

Figure 1.3 Flow chart of this Research

The whole research has been carried out in the following phases according to previous Figure 1.3

a. Stability of microtremor data has been carried out at six different locations. Time domain data has been converted to frequency domain data because time domain data do not show dynamic properties of soil. So, Fourier transformation of the segments of 41s long time history data along EW, NS and UD of these locations has been carried out. Then, the stability of Fourier spectra data has been checked at different time instants. Fourier spectra data do not show the amplification and stable data for site response. Therefore, Horizontal to Vertical spectral ratio data has been calculated from these Fourier spectra data. Stability of H/V ratio data at seven locations has been compared. H/V ratios are more stable than Fourier spectra data. From this conclusion, the analysis of Horizontal to Vertical spectra ratio (H/V) has been applied for microtremor and earthquake data analysis.

b. For details study of microtremor observations and earthquake data, six points in Bogra, Natore, Jamuna Bridge east side at Serajganj, Police staff college at Mirpur, Haji camp at Ashkona and BUET campus have been selected. These data are located in the same geological units. However, from the analysis of these data, most of the locations did not show significant amplification due to the presence of stiff soil within BUET campus. For this reason, six locations outside BUET have been selected.

c. Field investigations include three boreholes up to a depth of 30 m at Bogra and Natore LGED office and Jamuna Bridge East side. We have been collected for SPT-N value (Borehole data) from different sources and Microtremor (Observation) Array data for these point.

d. Among these locations, empirical soil correlations developed by Ansary et al. (2010) and other empirical correlations (After TC4, ISSMFE, 1993) and SPT-N have been used to estimate the shear-wave velocity in Vs30 equation will be applied.

e. The H/V ratio of Weak ground motion (Microtremor) and strong ground motion (SMA) have been compared at these locations.

f. For the damage assessment of soils at the observed locations Nakamura's (2000) Vulnerability Index (Kg) has been used.

1.5 OVERVIEW OF THE THESIS

The main purpose of this research is to estimate dynamic response of soils at different locations of Predominant frequency and Horizontal to Vertical spectral (H/V) ratio.

Chapter one describes in background idea of the current research, its scopes and objectives, and methodology of the study area.

Chapter 2 presents the literature review that includes geology and geomorphology, Past research of microtremor, Microtremor and Earthquakes Horizontal to Vertical spectral (H/V) ratio technique, relationship between microtremor and strong ground motion, Correlation between Field SPT N-value and Shear Wave Velocity.

Chapter 3 is the main part of this research which represents Microtremor and Earthquake data collection and analysis, Stability check of microtremor data, various effects on the result of microtremor and earthquakes. The SPT- N values, soil profile and other empirical correlations of soil have been used to estimate the shear wave velocity at six selected locations.

.

Chapter 4 represents the comparison of microtremor and earthquake data analysis. The main part of this chapter is the analysis result and comparison between weak motion (Microtremor) and Strong ground motion (Earthquakes) and Nakamura damage assessment of the study locations.

Chapter 5 is a summary of the weak ground motion in Microtremor and Strong ground motion of Earthquake and these H/V technique, Comparison of predominant frequency and amplification factor at selected locations. The specific conclusions and recommendations have been discussed in this chapter.

CHAPTER TWO

LITERATURE REVIEW

2.1 GENERAL

Microtremor and Earthquake consists of different types of waves producing in soil from various sources. The common noise sources are vibrating machine, traffic, environment and human movement. Microtremor observation is carried out to record time history of noise data. Horizontal to Vertical (H/V) Fourier spectral ratio technique is applied to assess the vulnerability of soil and building. Figure 2.1 shows various sources of microtremor for site response analysis. Microtremor is composed of fundamental mode of Rayleigh wave (Sato et al., 1991; Tokimatsu and Miyadera, 1992). Higher frequency microtremor bears resemblance to Shear Wave characteristics (Nakamura, 1989; Wakamatsu and Yasui, 1995). On the other hand, microtremors can also be dominated by Love-wave (Tamura et al. 1993). Suzuki et al. (1995) has applied microtremor measurements to the estimation of earthquake ground motions based on a hypothesis that the amplitude ratio defined by Nakamura can be regarded identical with half of the amplification factor from bedrock to the ground surface. However, the real generation and nature of microtremors have not yet been established.

This chapter presents the past researches related to microtremor technique. The reliability of Horizontal to Vertical Spectral Ratio (H/V) has been discussed from different points of view. The relationship between microtremor analysis and seismic activity has also been included in this chapter. The characteristics of various types of microtremor waves have been illustrated using mathematical expressions. Finally, seismic damage assessment of Nakamura's Vulnerability Index for damage estimation of soil has been included. Microtremor observation and damage assessment as shown in Figure 2.1

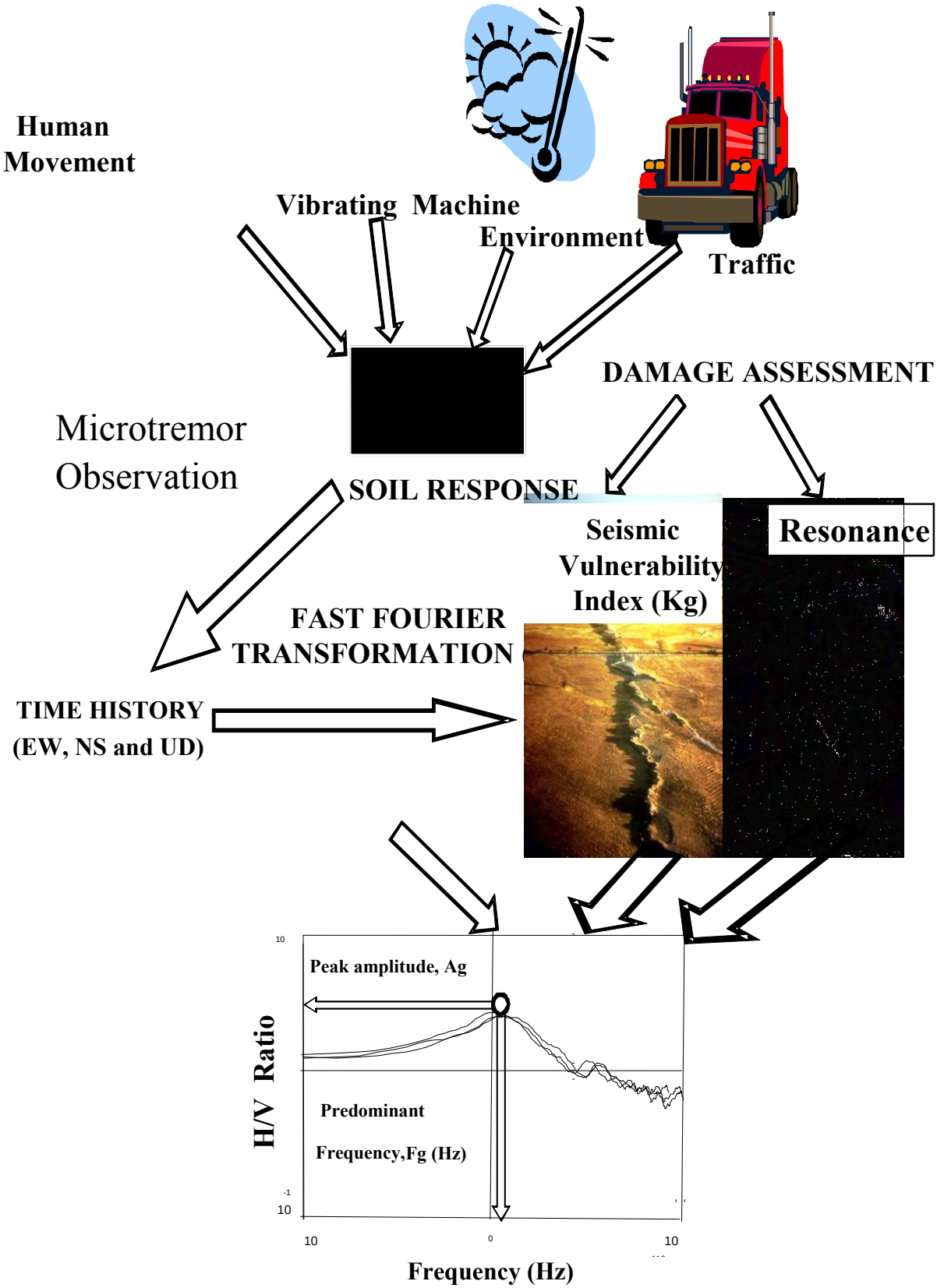

Figure 2.1 Microtremor observation and damage assessment

2.2 Regional Tectonics

Plate tectonics provide a physically simple mechanism for large-scale horizontal motions of separate portions of the earth's crust. One of the central concepts of plate tectonics is that a small number of large plates of high strength lithosphere, move rigidly with respect to one another at rates of 1 to 20 cm/year over the low-strength asthenosphere. According to Molnar and Tapponnier (1975), for the past 40 million years the Indian subcontinent has been pushing northward against the Eurasian plate at a rate of 5 cm/year, giving rise to the severest earthquakes and most diverse land forms known. Figure 2.2 Estimated slip potential along the Himalaya (after Bilham et al., 2001) and Figure 2.3 shows India's northward drift over the last 70 million years (after Molnar and Tapponnier, 1975)

The region of northeastern India, northern Burma and Southwestern China is tectonically and seismically one of the most interesting active plate boundaries. The region comprises the Himalayas, the Indo-Burma Ranges, the Tripura folded belt, the Bengal Basin, the Shillong Plateau and the Assam Valley. Figure 2.4 shows the Generalized tectonic map of Bangladesh and adjoining areas (After GSB, 1991). It is a rifted eastern marginal basin of Indian plate that is gradually shortening due to the subduction of the Indian plate and overriding of the Burmese plate from the east.

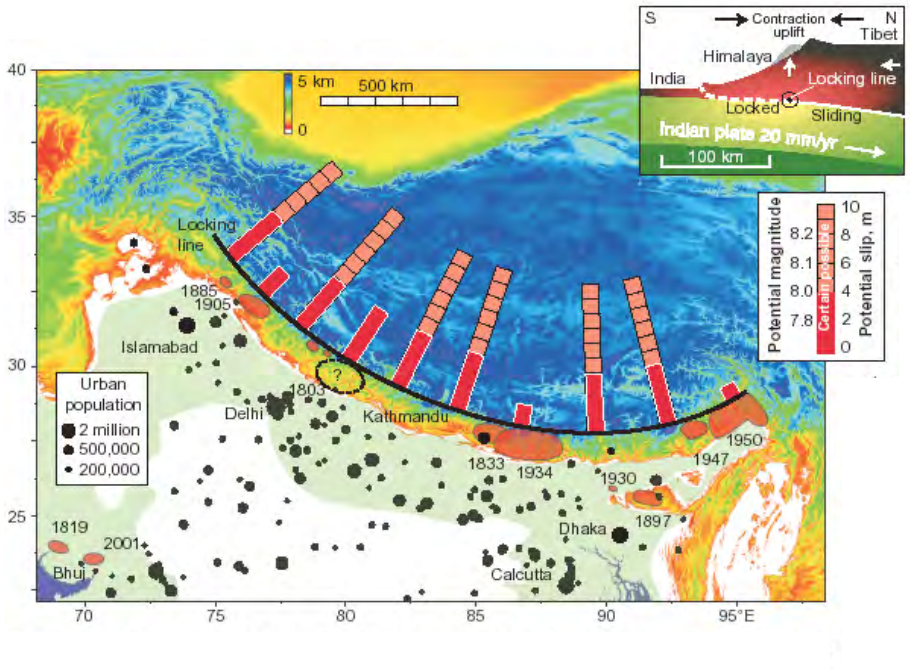

Figure 2.2 Estimated slip potential along the Himalaya (after Bilham et al., 2001)

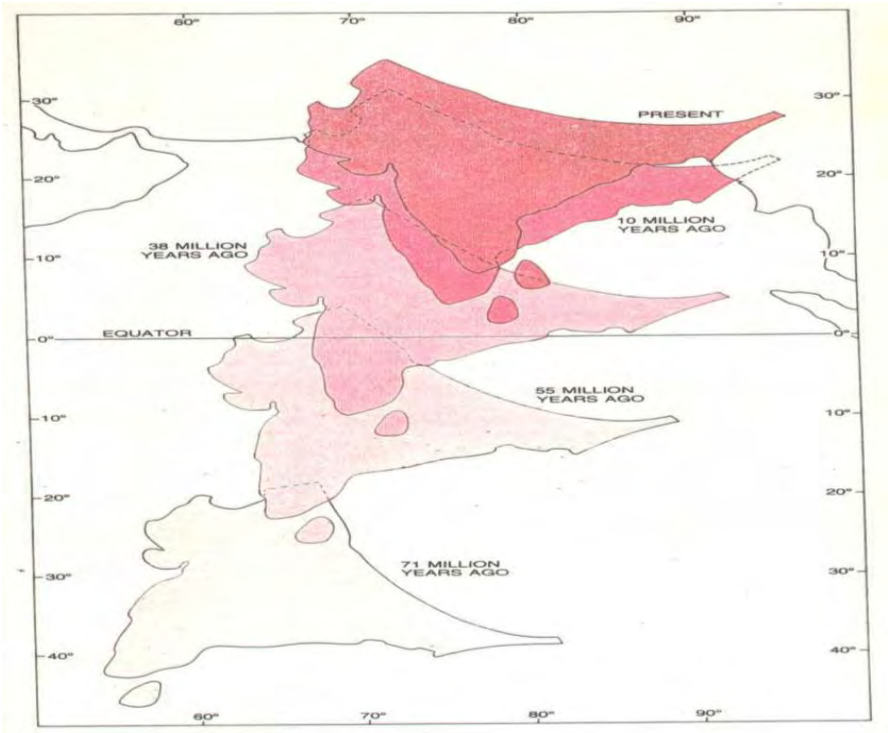

Figure 2.3 India's northward drift over the last 70 million years (after Molnar and Tapponnier,1975)

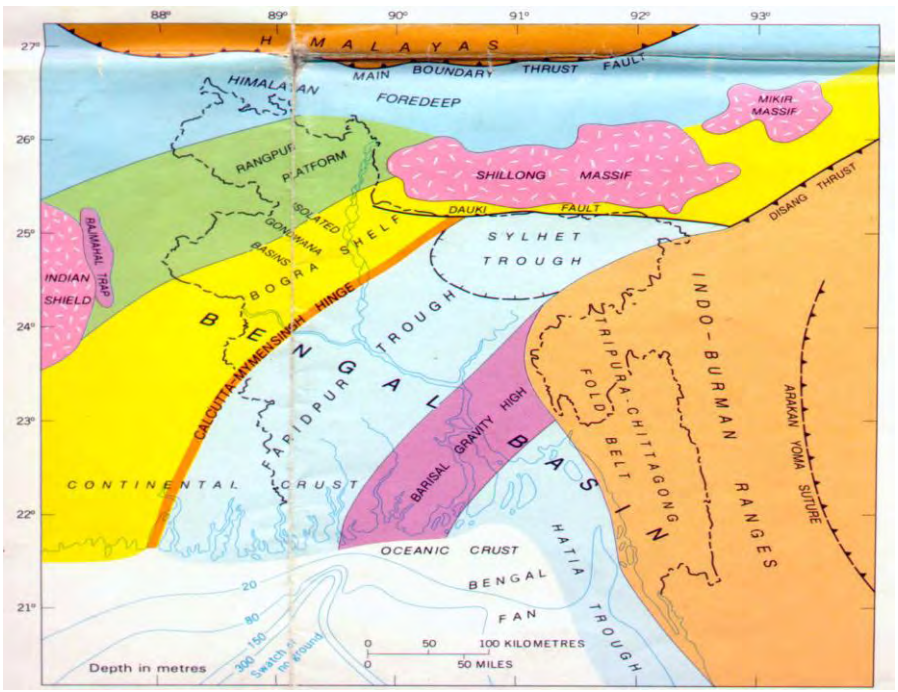

Figure. 2.4 Generalized tectonic map of Bangladesh and adjoining areas (After GSB, 1991)

2.3 Seismotectonic Setup

Khandaker (1989) has divided Bangladesh into three major tectonic zones:

(1) *The Shelf zone*: It consists of mainly the northwestern part of the country including the districts of Rangpur, Dinajpur and Bogra.

2) *The Hinge zone*: It passes through Calcutta, Pabna, Mymensingh and extend further NE across the Dauki fault.

(3) *The Bengal Foredeep zone*: It comprises of the rest of area of the country and occupies the area between the Shelf zone in the west and Arakan-Yoma Hill range in the east. The deep basin area of the foredeep is composed of the Surma Basin or Sylhet Trough, Faridpur Trough and the Hatia Trough.

The junction between the platform and the foredeep running southwest from Mymensingh to Calcutta (the Hinge line) is considered to be a zone of weakness. However, no association of the hinge with earthquakes has so far been established. The Foredeep is terminated in the northeast by a major fault, the Dauki fault at the southern margin of the Shillong Plateau. Some major earthquakes can be related to this fault. There are numerous faults particularly in the eastern part of the folded flank of the Foredeep. Here again there is no association with any major earthquake. Most recorded earthquakes had epicenter further east in Burma.

The eastern margin of the Indian plate is supposed to run through Myanmar, not far from the Bangladesh border, and northeast Assam (Arunachal Pradesh) is considered to be a corner of the northern and eastern margins of the plate.

The Himalayan arc can be regarded as one of the most intensely active seismic regions of the world. In northeast India, the Shillong plateau and adjacent syntaxis between the two arcuate structures is one of the most unstable regions in the Alpine-Himalayan belt and faced three major earthquakes of magnitude greater than 8.0 within the last two hundred years (1897, 1934, and 1950).

At present, the southernmost thrusting in the Himalaya-Shillong Plateau region could be taking place along the southern fringe of the plateau coinciding with the Dauki fault.

Currently, it is believed that the Shillong plateau has a thrust plane beneath it and is undergoing southward thrusting against a concept of vertical tectonism along the Dauki fault.

The Shillong plateau and its adjoining region including the northeastern part of Bangladesh have high seismic status. The seismic activity along the Dauki-Haflong fault zone is comparatively lower and a seismic gap has been postulated along this fault zone. The major earthquakes that have affected Bangladesh since the middle of the last century is presented in Table 2.1.

Table 2.1 Great historical earthquakes in and around Bangladesh

Date	Name	Epicentre	Magnitude (M)
10-01-1869	Cachar Earthquake	Jantia Hill, Assam	7.5
14-07-1885	Bengal Earthquake	Sirajgonj, Bangladesh	7.0
12-06-1897	Great Indian Earthquake	Shillong Plateau	8.7
18-07-1918	Srimangal Earthquake	Srimangal, Sylhet	7.6
02-07-1930	Dhubri Earthquake	Dhubri, Assam	7.1
15-01-1934	Bihar-Nepal Earthquake	Bihar, India	8.3

2.4 Major Seismic Sources

The seismic hazard is typically determined using a combination of seismological, morphological, geological and geotechnical investigations, combined with the history of earthquake in the region. Bolt (1987) analyzed different seismic sources in and around Bangladesh and arrived at conclusions related to maximum likely earthquake magnitude (Bolt, 1987). Bolt identified the following four major sources:

(i) *Assam fault zone*
(ii) *Tripura fault zone*
(iii) *Sub- Dauki fault zone*
(iv) *Bogra fault zone*

A brief description of geology, tectonics of the individual fault zone are given below:

(i) Assam fault zone: The east-west fault separates the Assam fault zone from sub-Dauki fault zone. This zone consists of Archaean Proterozoic basement complex and characterized by the maximum concentration earthquake events. The hypocenter beneath the Shillong plateau is shallow focus in origin and are scattered. Only a few epicenters appear on or close to Dauki fault indicate that this fault is relatively seismically inactive during the recent time. But it was active since the Jurassic and was the main architect for the evolution of Shillong plateau. The great earthquake of 1897 originated in the Assam fault zone. Number morphotectonic lineaments have been identified from the study of the satellite imagery. Most of the lineaments trend NE-SW with a few trending N-S. The N-S trending Brahmaputra fault is present along the course of Brahmaputra River. The fault dips steeply to the north. This zone is characterized by scattered shallow depth earthquake probably due to prevalent upward forces existing below the Shillong Plateau.

ii) Tripura fault zone: This zone is characterized by high concentration of earthquake events. A number of morphotectonic lineaments have been identified. Among these the Kopili lineament trending NW-SE is remarkable and is geologically recent in origin. Seismic section reveals that this lineament is the surface expression of deep-seated subvertical fault and termed as the Kopili fault, which belongs to the category of high angle reverse fault. At the north of this zone Halflong-Dissang thrust is present. Morphotectonic lineaments around the Halflong-Dissang thrust zone trend NE-SW, E-W and NW-SE. Mikir hill is present to the northeast corner of the Halflong-Dissang thrust, which separates the Shillong plateau by Kopili fault.

iii) Sub-Dauki fault zone: This zone covers the southern part of Dauki fault and eastern part of Bogra fault zone and bounded by longitude 90°E and 92°E. The morphotectonic lineaments trend NNW- SSE and NW-SE. The Sylhet plain covers the area and comprises the vast alluvial tract and the linear belts of folded Tertiary rocks trending N-S and NNE-SSW. Sylhet lineament of 180 km long trending NE-SW is the subsurface expression of deep seated high angle reverse fault having a dip of about 70° towards southeast and as named as Sylhet fault. A number of epicenteres fall on or close to this fault and some of them were of damaging character. Among them the earthquake of 1845 and Srimangal earthquake of 1918 are remarkable.

iv) Bogra fault zone: This is the westernmost area bounded by latitude 20°N and 28°N, and longitude 87°E and 90°E. The area is covered with thick deposits of alluvium. The main boundary fault of Himalayan ranges occurs in the north of this fault zone. A number of morphotectonic lineaments have been identified from the study of satellite imagery. These are mostly oriented NW/ NNW- SE/SSE. One such lineament is Teesta lineament. Gupta and Nandi seismic activity in the Garo-Rajmahal gap is related to the activity along the Jamuna fracture which is the surface

manifestation of apparently deep-seated sub-vertical fault. Most of the earthquakes along this fault are shallow in depth. But one earthquake had a depth of hypocentre of 100 km. The 1885 earthquake of magnitude 7.0 was originated in this fault.

The magnitudes of earthquake suggested by Bolt (Table 2.2) are the maximum magnitude generated in these blocks as recorded in the historical seismic catalogue. The historical seismic catalogue of the regions covers approximately 250 years of (starting 1762) recent seismicity of the region and such a meagre database does not provide true picture of seismicity of the tectonic provinces. For example, the Assam and Tripura fault zones contain significant faults capable of producing magnitude 8.6 and 8.0 earthquakes respectively in future. Similarly maximum magnitude of 7.5 in Sub- Dauki fault zone and Bogra fault zones are not unlikely event.

Table 2.2 Significant Seismic Sources and Maximum Likely Earthquake Magnitude in Bangladesh (After Bolt, 1987)

Location	Maximum likely earthquake magnitude
A. Assam fault zone	8.0
B. Tripura fault zone	7.0
C. Sub-Dauki fault zone	7.3
D. Bogra fault zone	7.0

After a thorough review of available data, Ali and Choudhury (1992) recommended magnitudes of Operational Basis Earthquakes and Maximum Credible Earthquakes inTable.2.3

Table 2.3 Operational Basis Earthquake, Maximum Credible Earthquake and Depth of Focus of Earthquakes for Different Seismic Sources (After Ali And Chowdhury, 1992)

Location	Operational basis earthquakes (Richter)	Maximum credible earthquakes	Depth of focus (km)
A. Assam fault zone	8.0	8.7	0-70
B. Tripura fault zone	7.0	8.0	0-75
C. Sub-Dauki fault zone	7.3	7.5	0-75
D. Bogra fault zone	7.0	7.5	0-70

Reliable historical data for seismic activity affecting Indian subcontinent is available only for the last 450 years (Gupta et al., 1982). Recently developed earthquake catalogue for Bangladesh and surrounding area (Sharfuddin, 2001) showed that 66 earthquakes with Ms ≥4.0 occurred from 1885 to 1995 within a 200 km radius of Dhaka City. The most prominent historical earthquakes affecting of Bangladesh was listed in Table 2.4

Table 2.4 Magnitude, EMS Intensities and distances of some major historical earthquakes around Dhaka (after Ansary, 2001)

Name of Earthquake	Magnitude	Intensity at Dhaka	Distance (km)
1869 Cachar Earthquake	7.5	V	250
1885 Bengal	7.0	VII	170
1897 Great Indian Earthquake	8.7	VIII+	230
1918 Srimangal Earthquake	7.6	VI	150
1930 Dhubri Earthquake	7.1	V+	250

2.5 SEISMIC ZONING MAP OF BANGLADESH

The seismicity zones and the zone coefficients may be determined from the earthquake magnitude for various return periods and the acceleration attention relationship. It is required that for design or ordinary structures, seismic ground motion having 10% probability of being exceeded in design life of a structure(50 years) is considered critical. An earthquake having 200 years return period originating in sub-Dauki zone have epicentral acceleration of more than 1.0g but at 50 kilometer the acceleration shall be reduced to as low as 0.3g.

Ali(1998) presented the earthquake base and seismic zoning map of Bangladesh. Tectonic frame work of Bangladesh adjoining areas indicate that Bangladesh is situated adjacent to the plate margins of India and Eurasia where devastating earthquake have occurred in the past. Non-availability of earthquake, geology and tectonic data posed great problem in earthquake hazard mapping of Bangladesh in the past. The first seismic map which was prepared in 1979 was developed considering only the epicentral location of past earthquake and isoseismic map of very few of them. During preparation of National Building Code of Bangladesh in 1993, substantial effort was given in revising the existing seismic zoning map using geophysical and tectonic data, earthquake data, ground motion attenuation data and strong motion data available from within as well as outside of the country. Geophysical and tectonic data were available from Geological survey of Bangladesh. Earthquake data were collected from NOAA data files and geodetic survey, US.Dept. of commerce.

Seismic zoning map for Bangladesh has been presented in Bangladesh National Building code (BNBC) published in 1993. The pattern of ground surface acceleration contours having 200 year return period from the basis of this seismic zoning map. There are three zones in the map- zone 1, zone2, zone3. The seismic coefficients of the zones are 0.075g, 0.15g and 0.25g for zone 1, zone2and zone 3 respectively. Bangladesh National building Code (1993) placed Dhaka city area in seismic zone 2 as shown in figure 2.5. however, the seismic zones in the code are not based on the analytical assessment of seismic hazard and are mainly based on the location of historical data.

The first seismic zoning map of the subcontinent was compiled by the Geological Survey of India in 1935. The Bangladesh Meteorological Department adopted a seismic zoning map in 1972. In 1977, the Government of Bangladesh constituted a Committee of Experts to

examine the seismic problem and make appropriate recommendations. The Committee proposed a zoning map of Bangladesh in the same year.

According to Bangladesh National Building Code (BNBC, 1993), Bangladesh is divided into 3 earthquake zones shown in Figure 2.5 and proposed updating seismic zoning Map of Bangladesh as shown in Figure 2.6

- **Zone-I** comprising the southwestern part of Bangladesh is seismically quiet, with an estimated basic seismic zoning co-efficient of 0.075.

- **Zone-II** comprising the central part of Bangladesh represents the regions of recent uplifted Pleistocene blocks of the Barind and Madhupur Tracts, and the western extension of the folded belt. The zone extends to the south covering Chittagong and Cox's Bazar. Seismic zoning coefficient for Zone II is 0.15.

- **Zone-III** comprising the northern and eastern regions of Bangladesh with the presence of the Dauki Fault system of eastern Sylhet and the deep seated Sylhet Fault, and proximity to the highly disturbed southeastern Assam region with the Jaflong thrust, Naga thrust and Disang thrust, is a zone of high seismic risk with a basic seismic zoning co-efficient of 0.25. Northern Bangladesh comprising greater Rangpur and Dinajpur districts is also a region of high seismicity because of the presence of the Jamuna Fault and the proximity to the active east-west running fault and the Main Boundary Fault to the north in India. The Chittagong-Tripura Folded Belt experiences frequent earthquakes, as just to its east is the Burmese Arc where a large number of shallow depth earthquakes originate.

Bangladesh National Building Code (1993) placed Dhaka (Latitude; 23.8°N, Longitude; 90.3°E) in Seismic zone 2. The seismic zones in the code are not based on the analytical assessment of seismic hazard and are mainly based on the location of historical data. An updated seismic map (Figure 2.6) based on analytical study was recently developed (Sharfafuddin, 2001). This zoning was based on consistent ground motion criterion such as equal peak ground acceleration levels. Based on the philosophy behind the seismic zoning and experience from recent earthquakes, it can reasonably be assumed that a major

earthquake event in Dhaka region is capable of higher damage than that assumed in the existing zoning map (BNBC 1983).

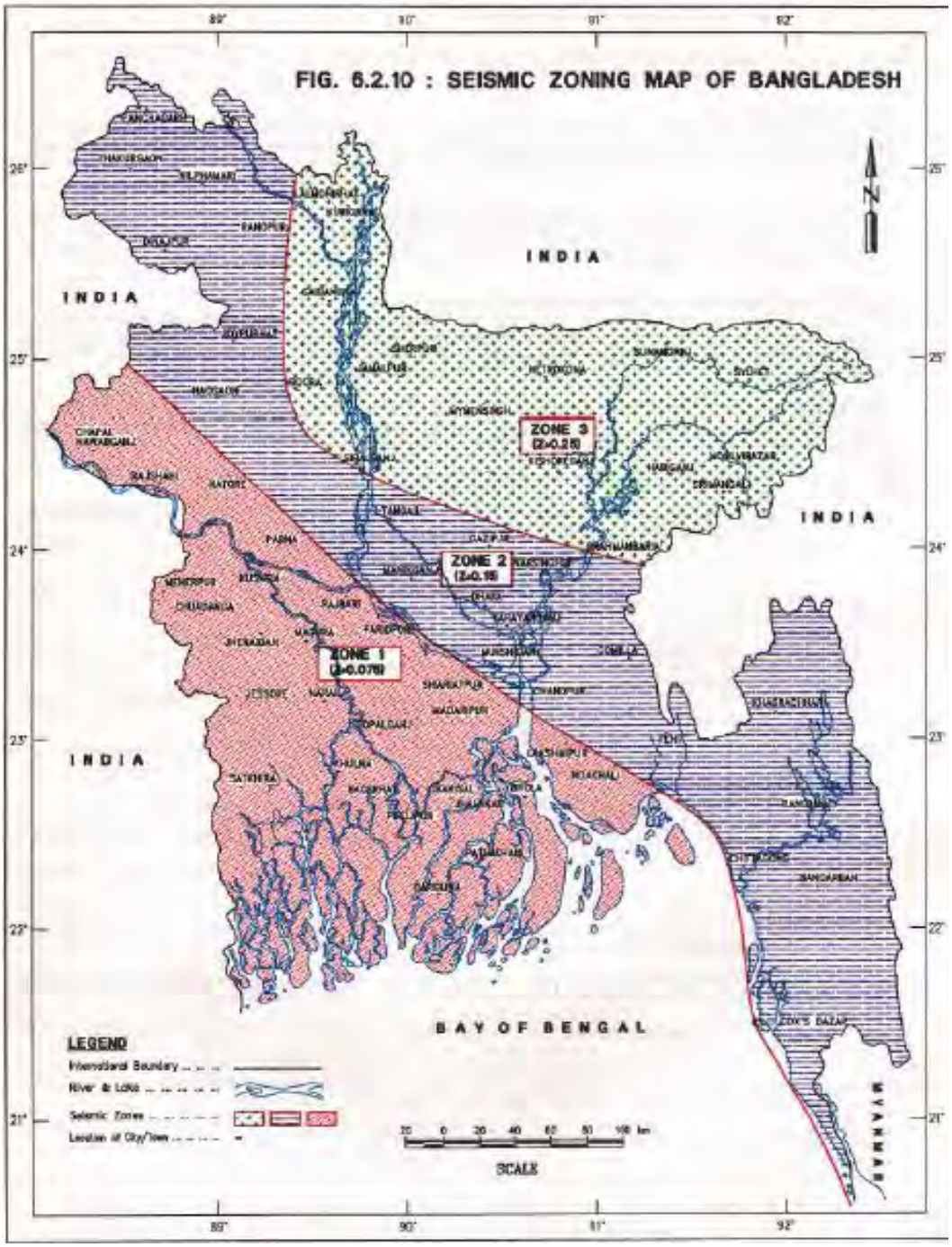

Figure 2.5 Seismic Zoning Map of Bangladesh (after BNBC, 1993)

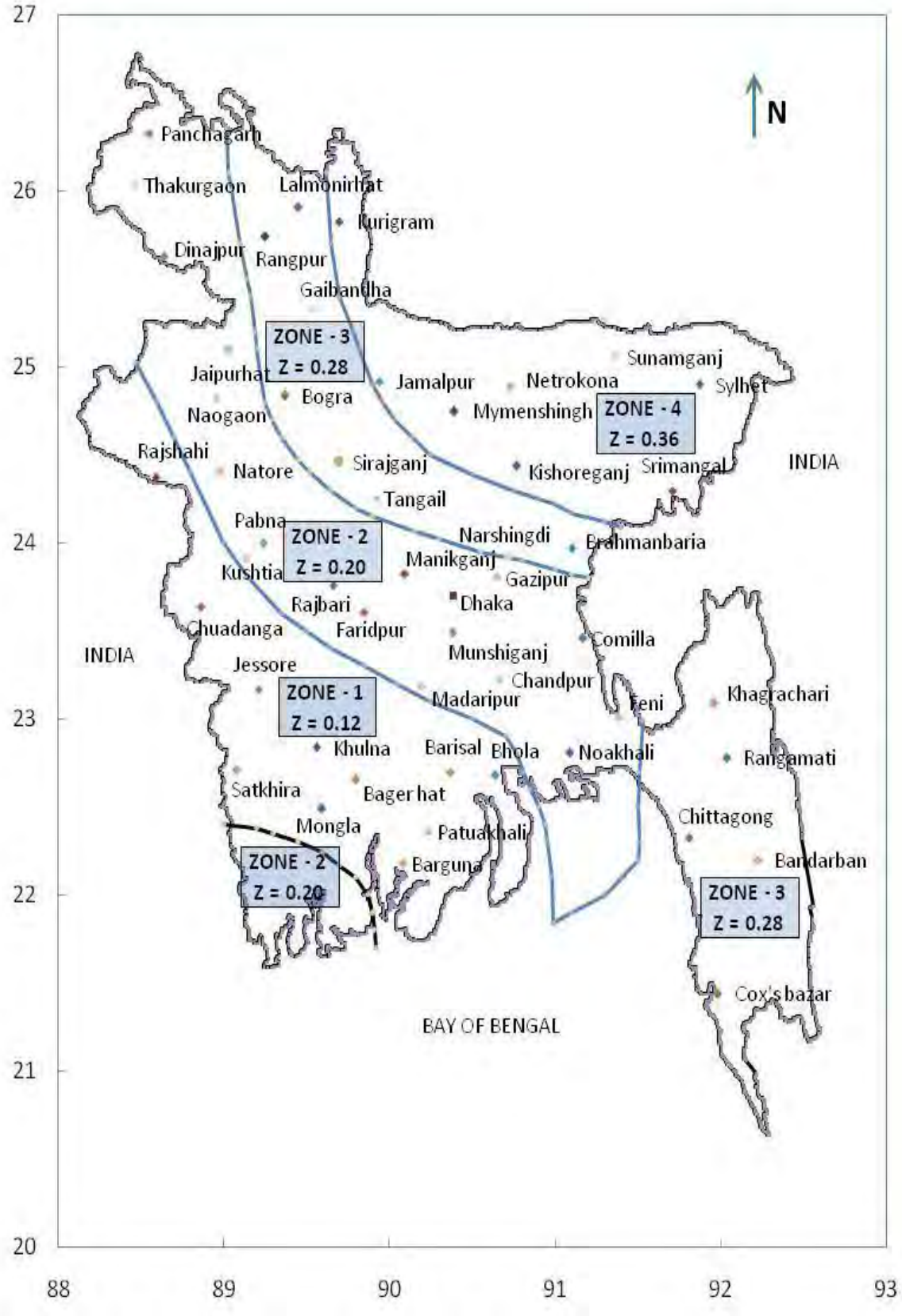

Figure 2.6 Proposed (Updating) Seismic Zoning Map of Bangladesh

2.6 PAST RESEARCHES ON MICROTREMOR

The infrequent occurrence of destructive earthquakes does not permit the compilation of enough data to support the estimation of the distribution of damages in the future. To overcome this lacking, different authors proposed the use of alternative sources of excitation, such as, distant earthquakes, small near earthquakes, explosions, aftershocks and microtremors. Wave propagation mechanism of microtremor and its relation with ground vibration characteristics have been studied from the beginning of microtremor studies (Aki, 1957; Kanai and Tanaka, 1961). Meanwhile, practical application of microtremor in the field of engineering has advanced tremendously. One of the powerful and simplest application of microtremor observation is in seismic micro-zoning.

The use of microtremors, an idea pioneered by Kanai et al. (1954) turns into one of the most appealing approaches in site effects studies, due to its relatively low economic cost and the possibility of recordings without strict spatial or time restrictions. The results obtained from the application of long period ambient noise measurements (Ohta et al., 1978; Yamanaka et al., 1993, 1994) allow the application microtremor for site effects. Short period ambient noise measurements have been applied to a wide range of seismic settings (Morales et al., 1991, 1993; Lermo and Chavez-García, 1993; Field and Jacob, 1993; Field et al., 1995; Seo, 1994). The H/V spectral ratio method (Nakamura 1989) has been discussed at great length and proven to be a suitable, quick and effective method (Konno and Ohmachi, 1998; Bard, 1999; Enomoto et al., 2002) for determining the predominant period of soil.

The H/V spectral ratio technique of microtremors gained popularity in the early nineties, after the publication of several papers (Nakamura, 1989; Field and Jacob, 1993; Lermo and Chavez- Garcia, 1994) claiming the ability of this technique to estimate the site response of soft sedimentary deposits satisfactorily. The mathematical expression of Microtremor H/V Technique is discussed in section 2.9 of this Chapter. The method is rather attractive in developing countries characterized by a moderate seismicity, where only very limited resources are available for seismic hazard studies.

Current researches show that Nakamura´s explanation, based on body waves, does not really demonstrate that spectral ratio is the soil response for horizontal oscillations neither around

predominant frequency (Bard, 1999). This assumption is supported on the presence of dispersion in seismic noise which is a typical characteristic of Rayleigh waves and Love waves. That evidence has been obtained from multiple experiments using arrays of sensors (Flores et al., 2003; Enomoto et al., 2002). The general agreement between ellipticity curves of Rayleigh waves and microtremor spectral ratio is established [Nogoshi and Igarashi (1971); Lachet and Bard (1994); Konno and Ohmachi, 1998). Ellipticity curves represent the horizontal to vertical ratio for the motion of a particle due to a plane Rayleigh wave.

The fundamental Rayleigh mode is used in the forward calculation and the method fails for some particular structures in which higher modes of surface waves and body waves should be considered. Arai and Tokimatsu (2004) improve that method taking all modes for surface waves and the relative contribution of Rayleigh and Love waves as 40% and 60% respectively for the entire considered frequency band. It has been used the scheme developed by Arai and Tokimatsu (2000, 2004) in order to check the reliability of this technique for a known soil profile which characteristics have been obtained from downhole and from S-wave refraction surveys.

Accordingly, a uniform layer upon a half space, is the model adopted for this work. In addition, it is useful to adopt likely values for the layer and half space properties. A typical soft site has a superficial layer of saturated soil, which has a high P-wave velocity and a low S-wave velocity (Poisson ratio n approaching 0.5). By contrast rock is closer to being a poisson solid.

The Nakamura technique (Nakamura, 1989), first proposed by Nogoshi and Igarashi (1970, 1971), is today one of the most commonly applied methods for microzonation studies of large areas (Parolai et al., 2001). A large number of studies using this rapid, economical and therefore attractive technique have been published (Field and Jacob, 1993; Mucciarelli, 1998; Bard, 1999; Fah et al., 2001). More recent studies (Fah et al., 2003; Scherbaum et al., 2003; Arai and Tokimatsu, 2004; Parolai et al., 2005; Picozzi et al., 2005; Parrolai et al., 2006) proposed and tested the possibility of inverting the Horizontal to Vertical (H/V) spectral ratio of noise (alone or in a joint inversion scheme) for investigating the S-wave subsoil structure. Moreover, attempts to provide standards for the analysis of seismic noise have only recently been carried out (Bard, 1999; SESAME, 2004; Picozzi et al., 2005). Most

authors disregarded the non-stationery noise from the analysis (Horike et al., 2001), while others (Mucciarelli et al., 2003) showed that the H/V ratio of non-stationery noise might be more similar, especially in amplitude, to the H/V ratio of non-stationery noise might be more similar, especially in amplitude, to the H/V spectral ratio determined for small-size earthquakes. These results (except for those from the stations located directly on the highway) seem to be in agreement with the pioneering study of Taniguchi and Sawada (1979) who made systematic noise measurements close to a highway under constructions and observed that (1) the frequency peak in the transient spectra has been stable independent of the mass of the source (a truck), hinting to the fact that the frequency of the traffic-induced vibration is mainly determined by ground soil conditions, and (2) traffic-generated vibrations have been dominated by Rayleigh waves. A recent investigation of seismic noise wave field induced by several source types can be found in Kim and Lee (2007).

Additional evidence of the role played by transients has been reported by Mucciarelli (1998) who showed that when generating transients with a sledge hammer near the recording sensor, the H/V peak becomes more clear. This result, probably too often overlooked, stimulates many intriguing questions. Since the energy released by the blow of sledge hammer peaks at frequencies much higher (50-70 Hz) than the fundamental resonance frequency of the site (1 Hz). Similarly, human generated seismic noise mainly affects frequencies higher than 1-2 Hz, with cars generating signals with frequencies mainly between 10-20 Hz (Toniguchi and Sawada. 1979; McNamara and Buland, 2004).

2.6.1 Earthquake and Microtremor Spectral Ratio

Worldwide, microtremor studies have shown that the peak amplitude of the microtremor H/V ratio tends to underestimate the peak amplitude of earthquake spectral ratios with respect to a reference (bedrock) site (Bard, 1999). The H/V spectral ratio determined from microtremors has shown a clear peak that is well correlated with the fundamental resonance frequency at “soft” soil sites (Bard, 2004; Horike et al., 2001; Lachet et al., 1996; Field and Jacob, 1995; Lachet and Bard, 1994; Lermo and Chavez-Garcia 1994a, 1994b). Numerical analysis suggests that microtremor site response can only be generated when the impedance contrast is greater than 3.5 (Malischewsky and Scherbaum, 2004), thus the good correlation at “soft” soil sites. Only a few studies claim rough agreement between the peak amplitude of

the microtremor H/V ratio and earthquake site-to-reference spectral ratios (Molnar and Cassidy, 2006; Mucciarelli et al., 2003; Horike et al., 2001; Lermo and Chavez-Garcia, 1994a, 1994b). In general, the site response shown by the earthquake site-to-reference spectral ratio method is regarded as the best approximation for engineering use, whereas H/V spectral ratios from earthquakes and/or microtremors are regarded as providing the fundamental peak and lower bound estimate of amplification for a soil site.

Figure 2.7 shown demonstrates the remarkable similarity between the earthquake site-to-reference and H/V ratio response, with the microtremor H/V ratio response at three strong-motion earthquake recording sites in greater Victoria. Traditionally strong-motion instrument has been used for earthquake recordings, rather than recordings from weak-motion sensors, as these instruments are designed to record the largest ground motions, and are generally present at sites of geologic interest (i.e. not bedrock). There are six BC Hydro substations in greater Victoria with a permanent strong-motion instrument. Since 1996, up to seven weak motion (peak ground acceleration $\leq$ 5.5 % g) earthquakes, ranging in magnitude from M_L 3.6 to M_W 6.8, have been recorded at these sites.

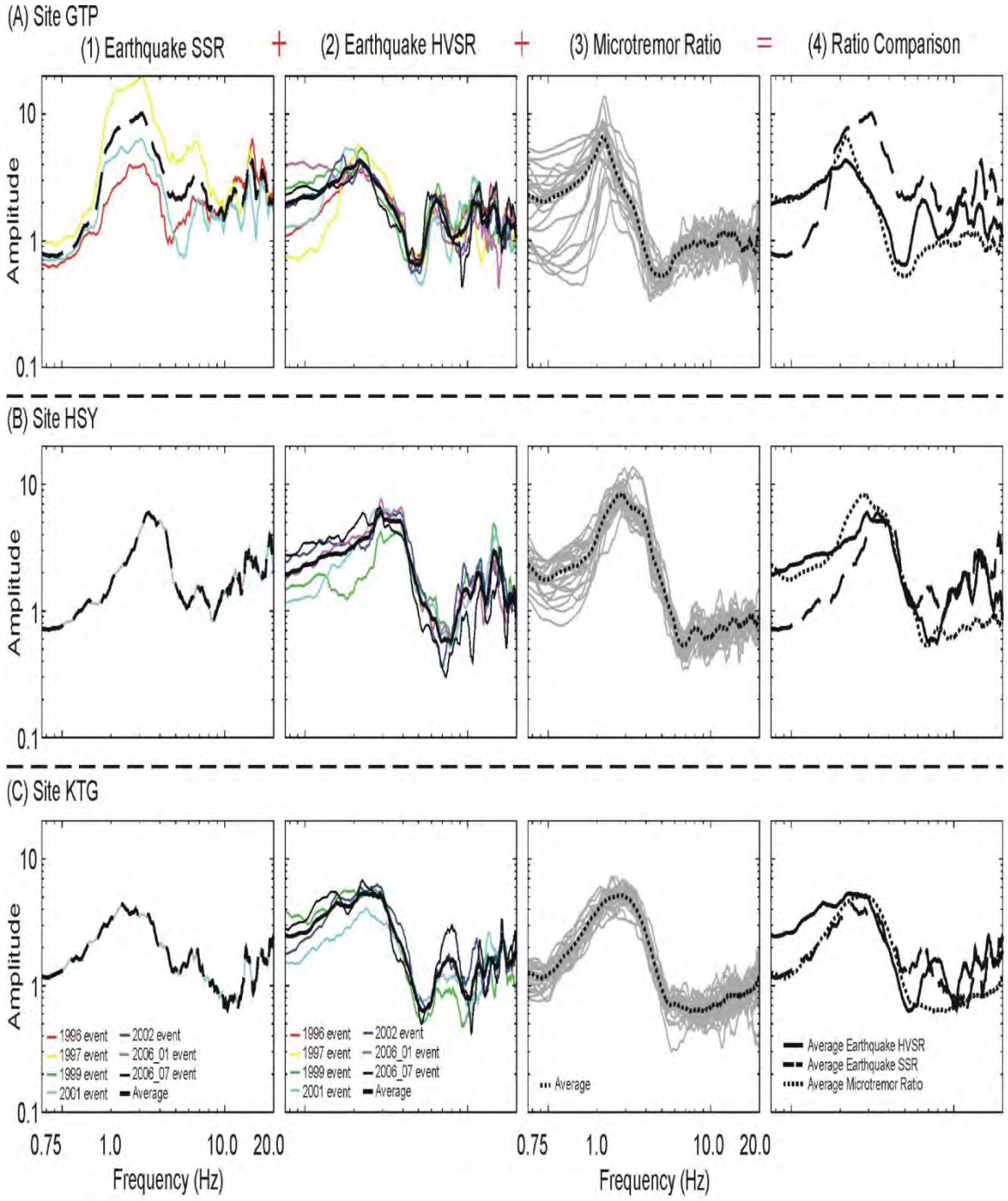

Figure 2.7 Comparision of (1) the average earthquake site-to-reference spectral ratios SSR) with (2) the average earthquake H/V spectral ratios (HVSR) of up to seven earthquakes, and (3) the average microtremor H/V spectral ratio at three strong-motion nstrument sites in greater Victoria (After Molnar et al., 2007)

All six BC Hydro instrument sites show similar response regardless of excitation source (weak-motion earthquakes or microtremors) and spectral ratio method (Molnar and Cassidy, 2006). This suggests that microtremor recordings are valid for estimation of linear earthquake response at sites in greater Victoria. Figure 2.8 shown comparision of the H/V spectral ratio from up to four weak-motion in microtremors at four sites across SW British Columbia (After Molnar et al, 2007)

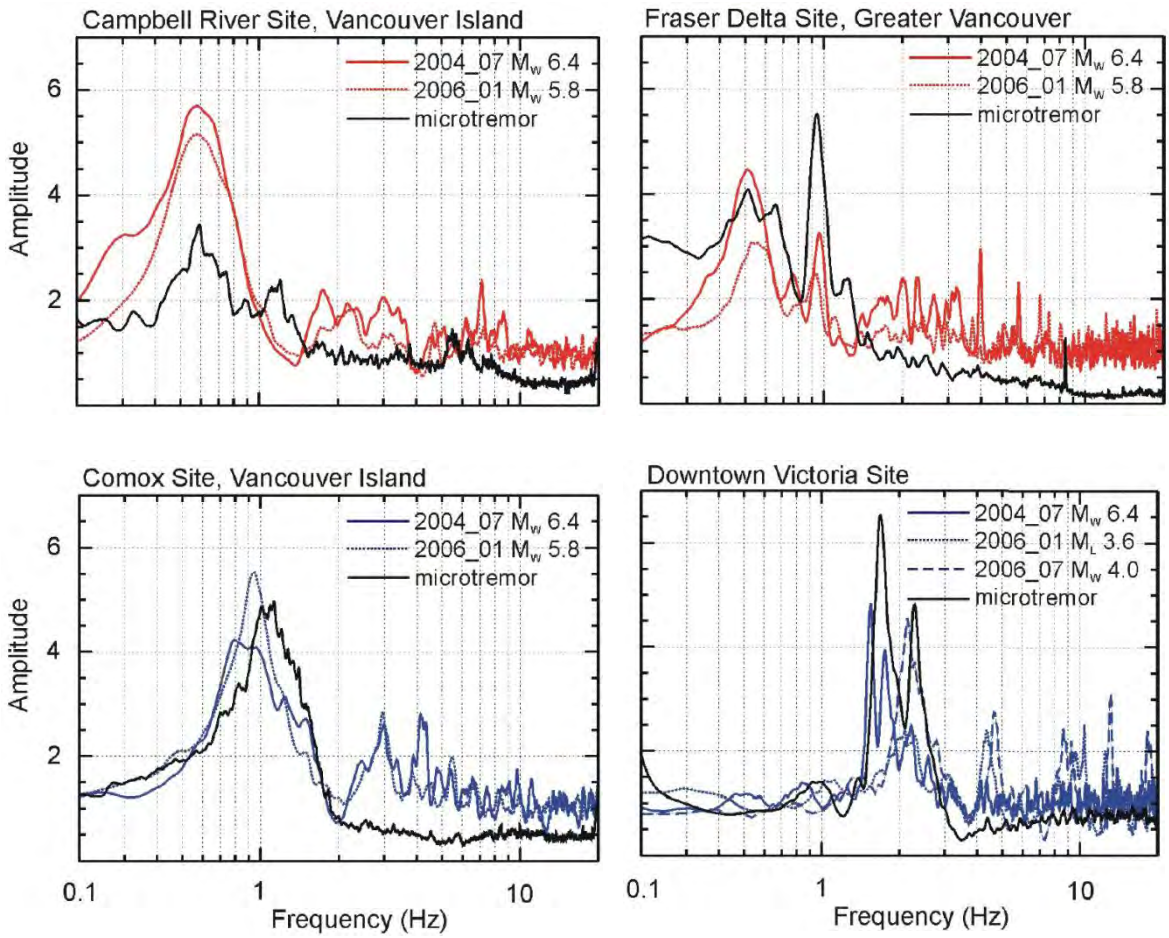

Figure 2.8 Comparision of the H/V spectral ratio from up to four weak-motion earthquakes and microtremors at four sites across SW British Columbia (After Molnar et al, 2007)

Another source of strong-motion earthquake recordings comes from the Geological Survey of Canada. In 2002, they began to operate strong-motion instruments that continuously record and communicate in near real-time over the Internet (Molnar et al. 2004, Molnar et al., 2006 Rosenberger et al., 2007). These new instrumentation features have provided

around 500 earthquake acceleration recordings across SW British Columbia (Cassidy et al., 2007) from only four earthquakes ranging in magnitude from M_W 4.0 to M_W 6.4. However, the recordings are all relatively low-level, varying in peak ground accelerations between 0.6 and 3.9 % g. Figure 2.8 shown good similarity of the fundamental period of the H/V spectral ratio response from these earthquake recordings with the microtremor response at four strong-motion instrument sites across SW British Columbia (Molnar et al., 2006).

Overall, for SW British Columbia excellent agreement has been observed in the fundamental period of a site 413 between earthquake and microtremor spectral ratio responses, and good agreement in the level of amplification, especially at sites in greater Victoria. The microtremor response at higher modes is always lower than that of the earthquake response. The microtremor underestimates earthquake response amplitude at frequencies greater than 2 to 3 Hz.

2.6.2 Observed and Amplitude Ratio

A microtremor research has been carried out at thirteen locations in Japan (Ansary et al, 1996). Soil model has been developed for theoretical analysis using the existing boreholes and PS loggings. The transfer function of the shear wave (The surface motion versus the incidental motion at some depth) and the amplitude ratio for the fundamental mode of Rayleigh wave have been calculated at the sites using those soil models. For the calculation of transfer function of shear wave, a damping ratio of 2 % has been used, assuming input motion at the outcrop.

Figure 2.9 shows the transfer function of shear wave, amplitude ratios of Rayleigh wave and microtremor for six locations in Japan. During the comparision of theoretical curves, the amplitude ratio, AR (T), of microtremor used have been expressed by the following equation:

$$\text{AR (T)} = \frac{\sqrt{F_{NS}(T)F_{EW}(T)}}{F_{UD}(T)} \qquad (2.1)$$

Where F_{NS}, $F_{EW}(T)$ and $F_{UD}(T)$ are average Fourier spectra of six time instants.

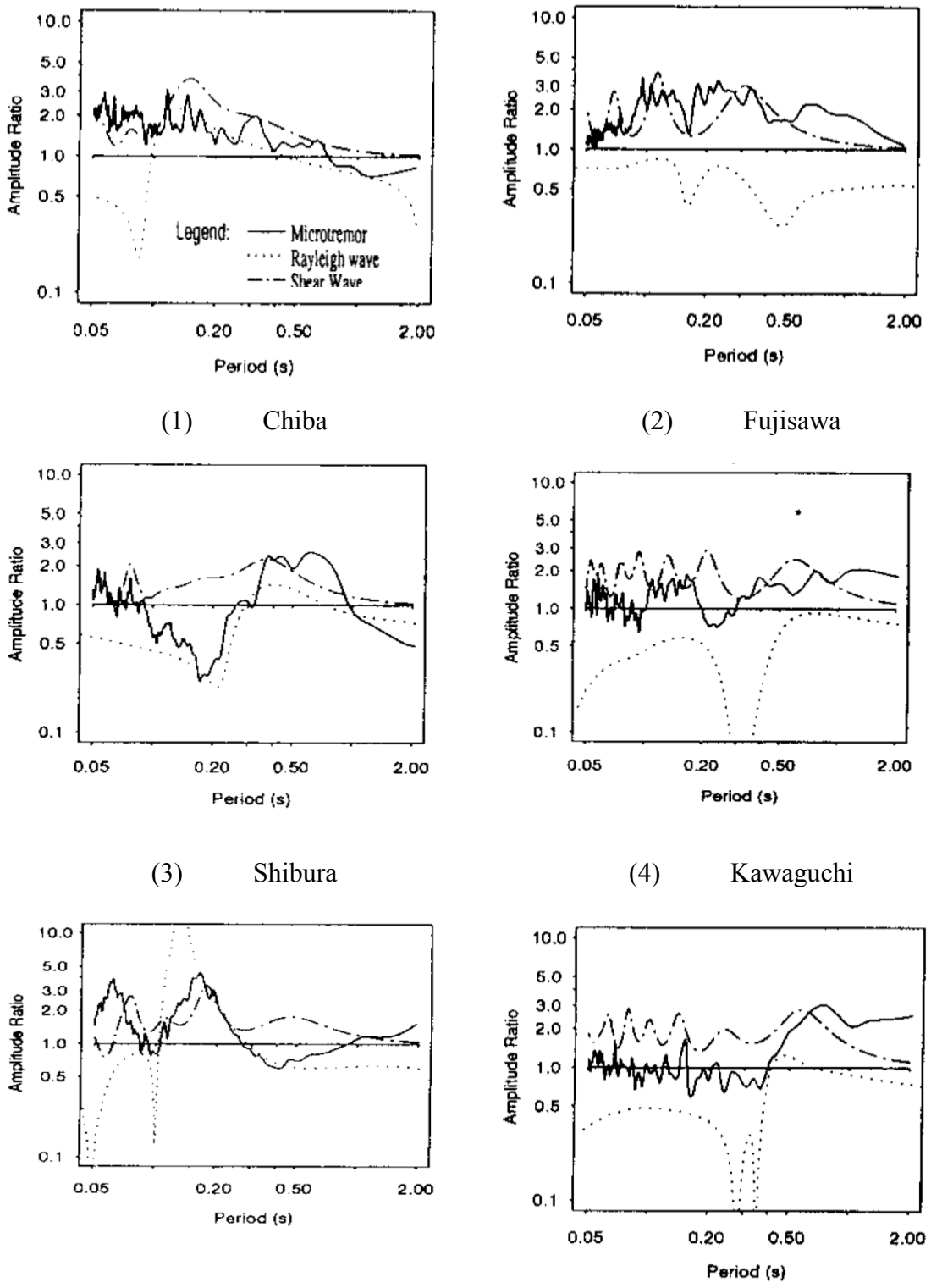

(1) Chiba (2) Fujisawa

(3) Shibura (4) Kawaguchi

(5) Kodaira (6) sasamegawa

Figure 2.9 Amplitude ratios of microtremor and theoretical Rayleigh-wave plotted with transfer function of shear wave (After Ansary et al., 1996)

The trend of three curves, i.e., two theoretical and one observed, somewhat resembles each other for these sites. Ansary et al. (1996) found that the period at which the Rayleigh wave amplitude ratio either suddenly drops or peaks, microtremor amplitude ratio closely resembles it. In a general sense, amplitude ratio for pure Rayleigh wave is always lower than the amplitude ratio of microtremor. The reason is that microtremor may contain some shear wave and Love wave contents as well as Rayleigh wave. Ansary et al. (1996) concluded that the characteristics of the microtremor's amplitude ratio are similar to that of Rayleigh wave and the period corresponding to the peak amplitude ratio corresponds to the peak periods of Rayleigh wave amplitude ratio and Shear wave transfer function. In also applicability of H/V microtremor technic for site response analysis at Dhaka City as shows in Figure 2.10 Amplitude ratios of microtremor and theoretical transfer function of shear wave at National University Tongi, Gazipur (after Rahman, 2011).

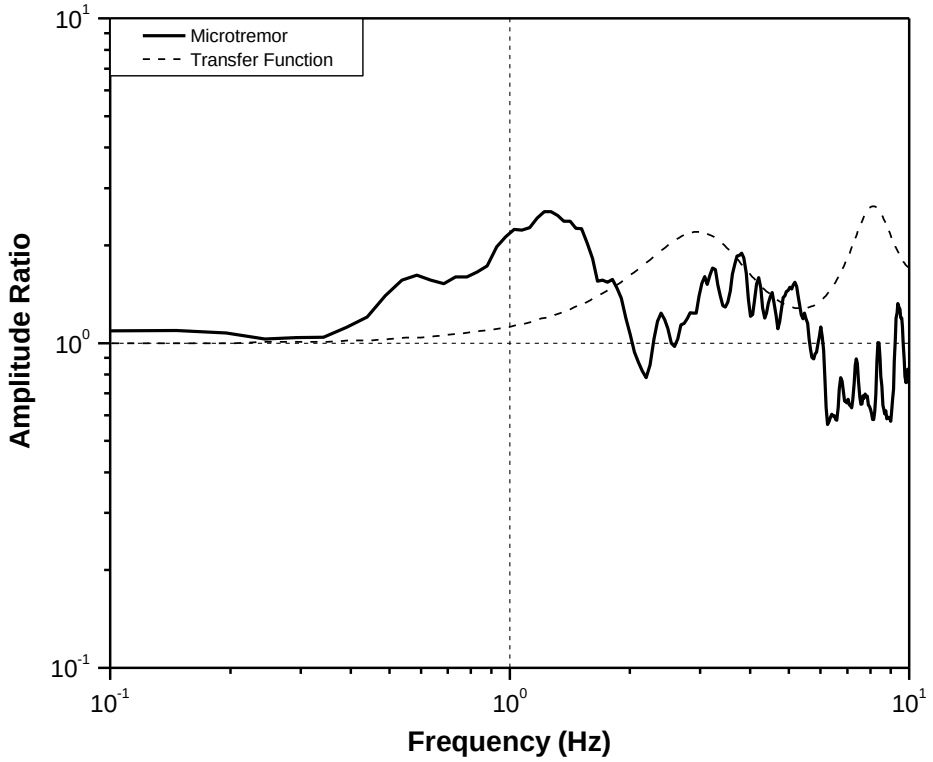

Figure 2.10 Amplitude ratios of microtremor and theoretical transfer function of shear wave at National University Tongi, Gazipur (after Rahman, 2011)

Figure 2.11 shown demonstrates that the peak amplitude ratio of transfer function has been moved toward right side of microtremor at Bashundhara River view Project. But, the peak

value of transfer function is lower amplified than microtremor H/V ratio. The predominant frequency of microtremor H/V ratio is 1.05 Hz where as transfer function shows this value is 1.85 Hz. On the other hand, peak H/V ratio of microtremor is 3.51 wheras transfer function shows this value 3.03.

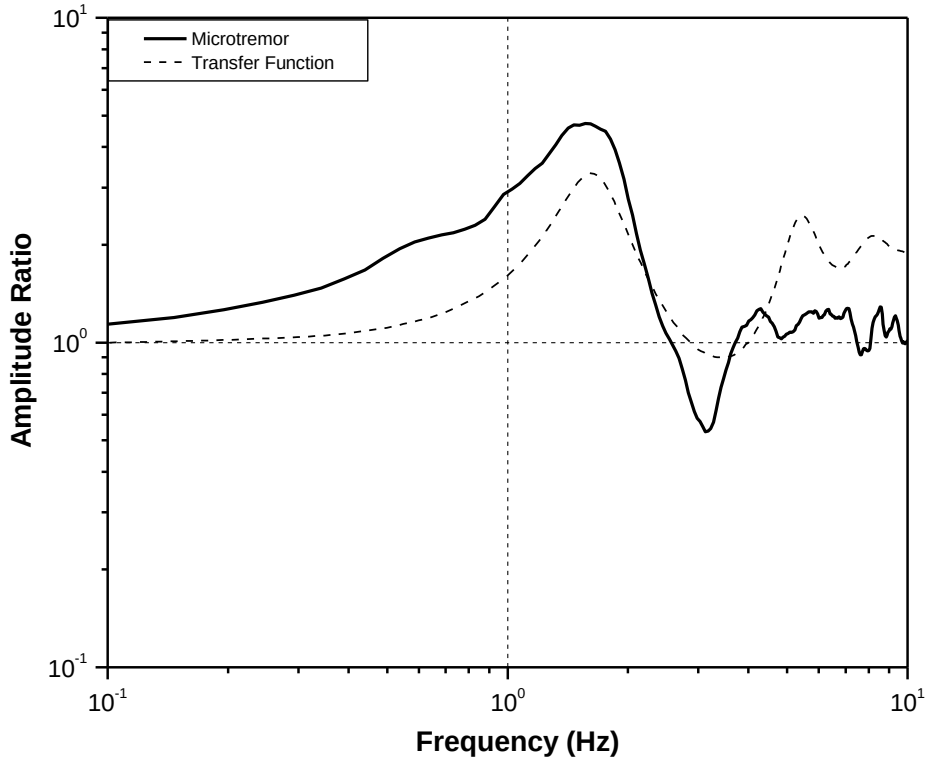

Figure 2.11 Amplitude ratios of microtremor and theoretical transfer function of shear wave at Block-D, Bashundhara (after Rahman, 2011)

2.7 MICROTREMOR AND EARTHQUAKE GROUND MOTION OF H/V TECHNIQUE

Damages caused by the recent earthquakes are concluded as a direct result of local geological conditions affecting the ground motion. Best approach for understanding ground conditions is through direct observation of seismic ground motion, but such studies are restricted to areas with relatively high rates of seismicity. Because of these restrictions in other methods, such as high rates of seismicity and the availability of an adequate reference site, non-reference site methods have been applied to site response studies. Microtremor is a very convenient tool to estimate the effect of surface geology on seismic motion without

needing other geological information. H/V technique fits very well to this description and it has received great attention from all over the world with its simplicity together with quick information about dynamic characteristics of ground and structures. Although several researchers claimed that theoretical background of this technique is not clear, there have been many successful experimental studies performed. Method is attractive since it gives the ease of data collection and it can be applied in areas of low or even no seismicity.

2.7.1 Method of Microtremor and Earthquake Ground Motion with H/V ratio Technique

Techniques for analyzing microtremors are generally divided into two main categories: non-reference site (H/V) and reference site (Hs/Hr) techniques. In Hs/Hr method, assumptions are that at nearby sites, source and path effects are believed to be identical and reference site is free of any site effect. Therefore, motion recorded at the reference station is representative of the excitation arriving at the interface sediments under the soft soil site and spectral ratio, Hs/Hr, constitute a reliable estimate of site response. This technique, introduced first by Borcherdt (1970), is still widely used and is very popular for the analysis of weak or strong motion records. It has been applied to microtremor measurements by Kagami et al. (1986) with good results. In the traditional spectral ratio method, Hs/Hr, site and source effects are estimated from observations at a reference site. In practice, adequate reference site are not always available especially in flat areas. Therefore, methods have been developed that do not need reference sites (Bard, 2004).

A technique using horizontal to vertical spectral ratios (H/V) of the microtremors, which was first applied by Nogoshi and Igarashi (1970, 1971) and popularized by Nakamura (1989), has been widely used to estimate the site effects. Several recent applications of this technique have proved to be effective in estimating fundamental periods as well as relatively amplification factors. Several methods have been proposed for spectral calculation of ground motions including microtremors. Fourier spectrum is the most convenient one that is used widely. Some investigations showed that different methods give similar results (Dimitriu et al., 1998). However some researchers declare that a suitable spectral method gives more reliable results. Ghayamghamian and Kawakami (1997) introduced segmental cross-spectrum (SCS), as an effective tool for compensating unknown effects like source

effects and noise in input and output measurements. They evaluated the performance of SCS in contrast with the conventional methods, i.e. Fourier or power spectra through the mathematical modeling and numerical simulations. Results of their studies indicated that SCS gives more reliable results for both amplification factor and predominant resonance frequency of the site than the conventional methods.

2.7.2 Theory of Microtremor and Earthquake H/V Technique

The typical geological structure of sedimentary basin has been shown in Figure 2.12. Definition of ground motions and their spectra at different places are defined in following lines. Here microtremor is divided into two parts considering it contains Rayleigh wave and other waves. Then, horizontal and vertical spectra on the surface ground of the sedimentary basin (H_f, V_f) can be written as follows.

$$H_f = A_h * H_b + H_s \quad V_f = A_v * V_b + V_s \tag{2.2}$$

$$T_h = \frac{H_f}{H_b} \quad T_v = \frac{V_f}{V_b} \tag{2.3}$$

Where $A_h$and A_v are amplification factor of horizontal and vertical motions of vertically incident body wave. H_b and V_b are spectra of horizontal and vertical motion in the basement under the basin (outcropped basin).

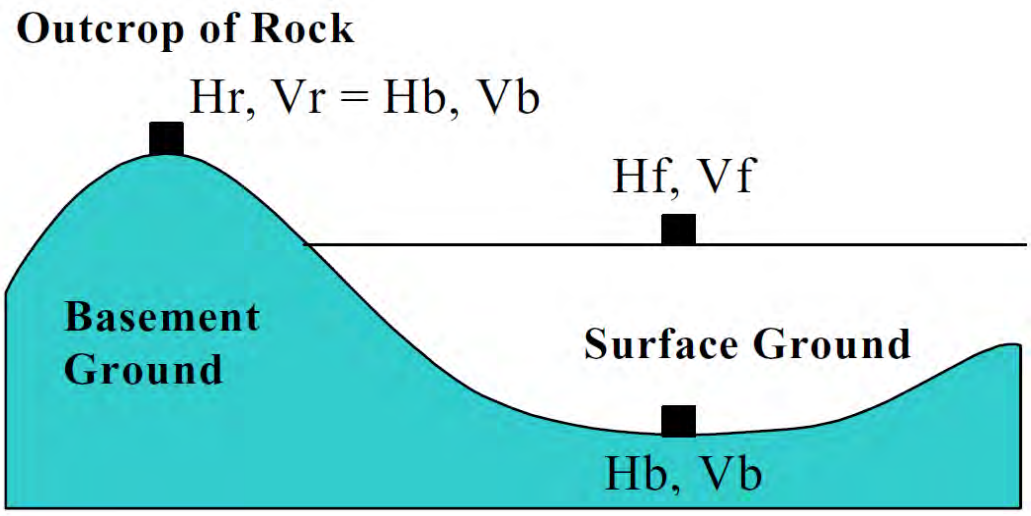

Figure 2.12 Typical geological structure of sedimentary basin

H_s and V_s are spectra of horizontal and vertical directions of Rayleigh waves. T_h and T_v are amplification factor of horizontal and vertical motion of surface sedimentary ground based on seismic motion on the exposed rock ground near the basin. In general, P wave velocity is more than three-four times of S wave velocity. In such sedimentary layer, vertical component cannot be amplified (A_v=1) around the frequency range where horizontal component receives large amplification. If there is no effect of Rayleigh waves, $V_f \approx V_b$. On the other hand, if V_f is larger thanV_b, it is considered as the effect of surface waves. Then estimating the effect of Rayleigh waves by V_f/V_b (= T_v), horizontal amplification can be written as,

$$T_h^* = \frac{T_h}{T_v} = \frac{\frac{H_f}{V_f}}{\frac{H_b}{V_b}} = \frac{QTS}{\frac{H_b}{V_b}} = \frac{\left[A_h + \frac{H_s}{H_b}\right]}{\left[A_v + \frac{V_s}{V_b}\right]} \tag{2.4}$$

$$\text{QTS} = \frac{H_f}{V_f} = \frac{A_h * H_b + H_s}{A_v * V_b + V_s} = \frac{H_b}{V_b} \cdot \frac{\left[A_h + \frac{H_s}{H_b}\right]}{\left[A_v + \frac{V_s}{V_b}\right]} \tag{2.5}$$

In equation (2.5), $\frac{H_b}{V_b} \approx 1$. $\frac{H_s}{H_b}$ and $\frac{V_s}{V_b}$ are related with the route of energy of Rayleigh waves. If there is no influence of Rayleigh wave, QTS = A_h/A_v. If amount of Rayleigh wave is high, then second term in above formulation gets dominant and QTS = H_s/V_s and the lowest peak frequency of H_s/V_s is nearly equal to the lowest proper frequency F_o of A_h in (Figure 2.13).

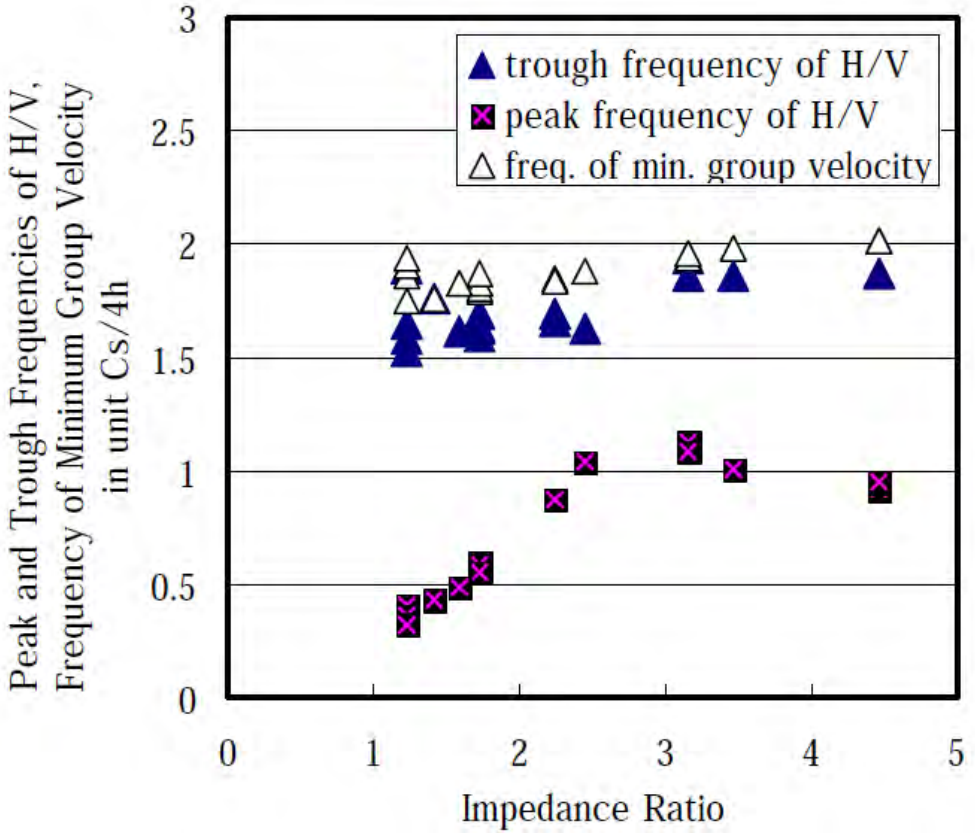

Figure 2.13 Relationship between charactersistics of Rayleigh Wave and Impedance Ratio (After Nakamura, 2000)

In the range of, A_v= 1. QTS shows stable peak at frequency, F_0. Even when influence of Rayleigh wave is large, V_s becomes small (which results in a peak of H_s/V_s) around the first order proper frequency due to the multiple reflection of horizontal motions. And QTS = A_h, if microtremors of the basement V_b is relatively large comparing to the Rayleigh wave.

Figure 2.14 shows a schematic comparison of Horizontal (H_f), Vertical (V_f), H_f/H_b (spectral ratio of sediment site to the reference site) and H_f/V_f (H/V technique). As it can be followed QTS is smaller than the theoretical transfer function. Since H_f includes the effects of Rayleigh waves, H_f/H_b is bigger than the theoretical transfer function. If influence of Rayleigh wave becomes larger, QTS < 1 in the wide range of frequency and if influence is small, QTS locally expected to be smaller than one, in the narrow frequency range at frequency several times higher than F_o, because of the influence of vertical motion. Main

waves consisting of microtremors are either body waves or Rayleigh waves, or depending on the location and other conditions can be mixture of both waves.

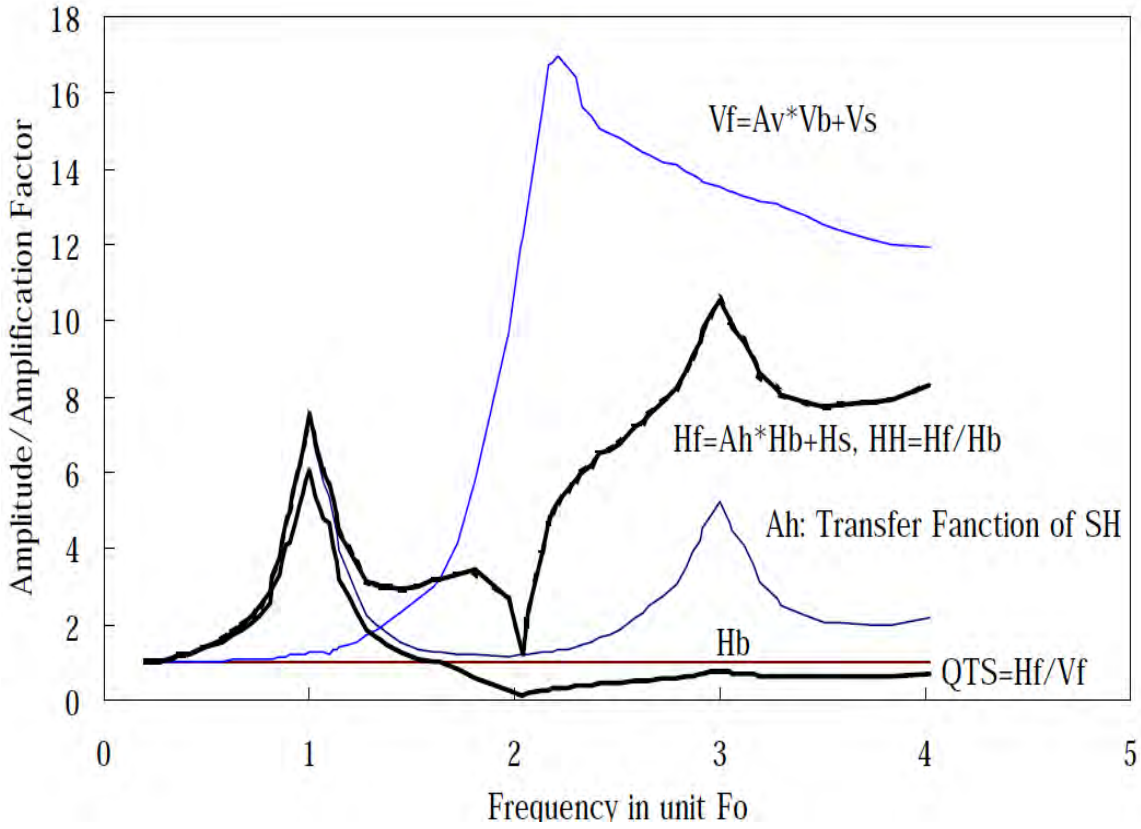

Figure 2.14 Schematic comparison of Horizontal (H_f), Vertical (V_f), H_f/H_b (spectral ratio of sediment site to the reference site) (After Nakamura, 2000)

2.8 Relationship Between Shear Wave Velocity (V_s) and SPT (N) Value

There are several empirical relations correlating the SPT-N value and Shear Wave Velocity (Vs) as shown in Table 2.5. The overburden correction of SPT-N value is demonstrated in Figure 2.15. The Standard Penetration Test (SPT) has been widely used to investigate soil deposit for identifying subsurface soil profiles. The empirical relationships presented here can be used to convert SPT-N value into Shear Wave Velocities

This is the first time shear-wave velocity for any locations are estimated using PS logging in Bangladesh. The Small scale microtremor measurement has been carried out at two locations in our study area of Jamuna Bridge in order to determine shear wave velocity (Hossain, 2009) and PS logging for site response analysis in Dhaka city (after Fahad 2015)

and also Estimation of earthquake induced liquefaction potential of selected areas of Dhaka city based on shear wave velocity (after Tanvir 2009).

These SPT data has been used to estimate the SWV using different empirical SPT N-value and Shear wave velocity (Table 2.5). Figure 2.16 shows correlations of Shear Wave Velocity and SPT N-value for clay and sand for those locations (Ansary et al., 2010). These correlations have been used to SPT N-value and estimation of Shear Wave Velocity. The SWV of other empirical methods have been calculated to compare SWV. These results of converted SWV have been shown in this Chapter 3

Table 2.5 Empirical correlation between SPT N-value and Shear Wave Velocity
(After TC4, ISSMFE, 1993)

Researchers	**Equation**
Imai and Yoshimura (1970)	$Vs = 76\ N^{0.33}$
Ohba and Toriumi (1970)	$Vs = 84\ N^{0.31}$
Ohta and Goto (1978)	$Vs = 69\ N^{0.17}\ D^{0.2}\ F_1\ F_2$ Where F_1 = 1.0 (H); F_2 = 1.00 (clay) = 1.3 (P); = 1.09 (f. Sand) = 1.07 (m. Sand) = 1.14 (c. Sand) = 1.15 (g. Sand) = 1.45 (gravel)
Imai (1977)	$Vs = a\ N^b$ Where a = 102; b = 0.29 (H. Clay) = 81; = 0.33 (H. Sand) = 114 = 0.29 (P. Clay) = 97 = 0.32 (P. Sand)

Okamoto et al. (1989)	$Vs = 125\ N^{0.3}$ (P. Clay)
Tamura and Yamazaki (2002)	$Vs = 105\ N^{0.187}\ D^{0.179}$
Ansary et al. (2010)	$Vs = 109.92\ N^{0.28}$ (Clay) $Vs = 84.16\ N^{0.34}$ (Sand)

Here, Vs = Shear Wave Velocity (m/s); N = Corrected SPT blow count

D = Depth (m); H = Holocene; P = Pleistocene

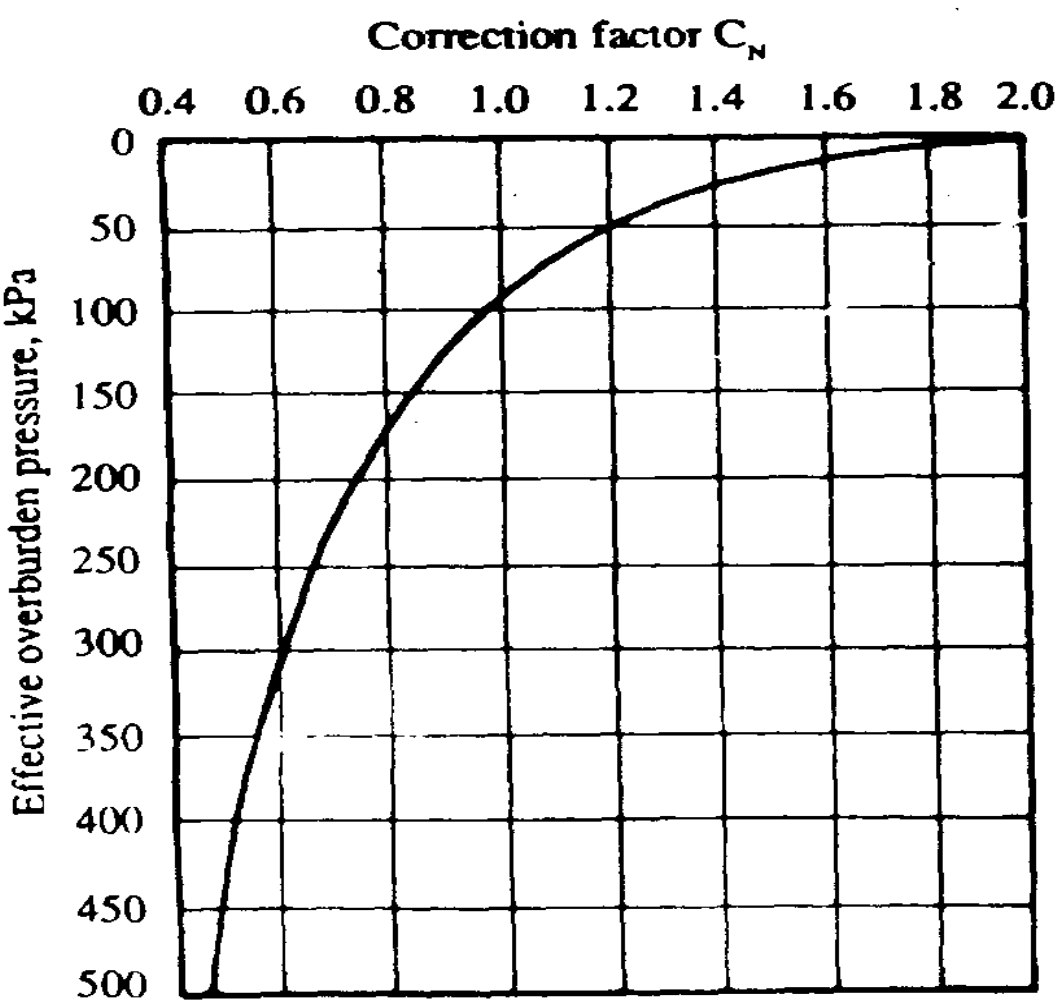

f = Fine; m = Medium; c = Coarse; g = Gravel

Figure 2.15 Recommended Curves for Correction Factor from Effective Overburden Pressure (After Murthy, 1991)

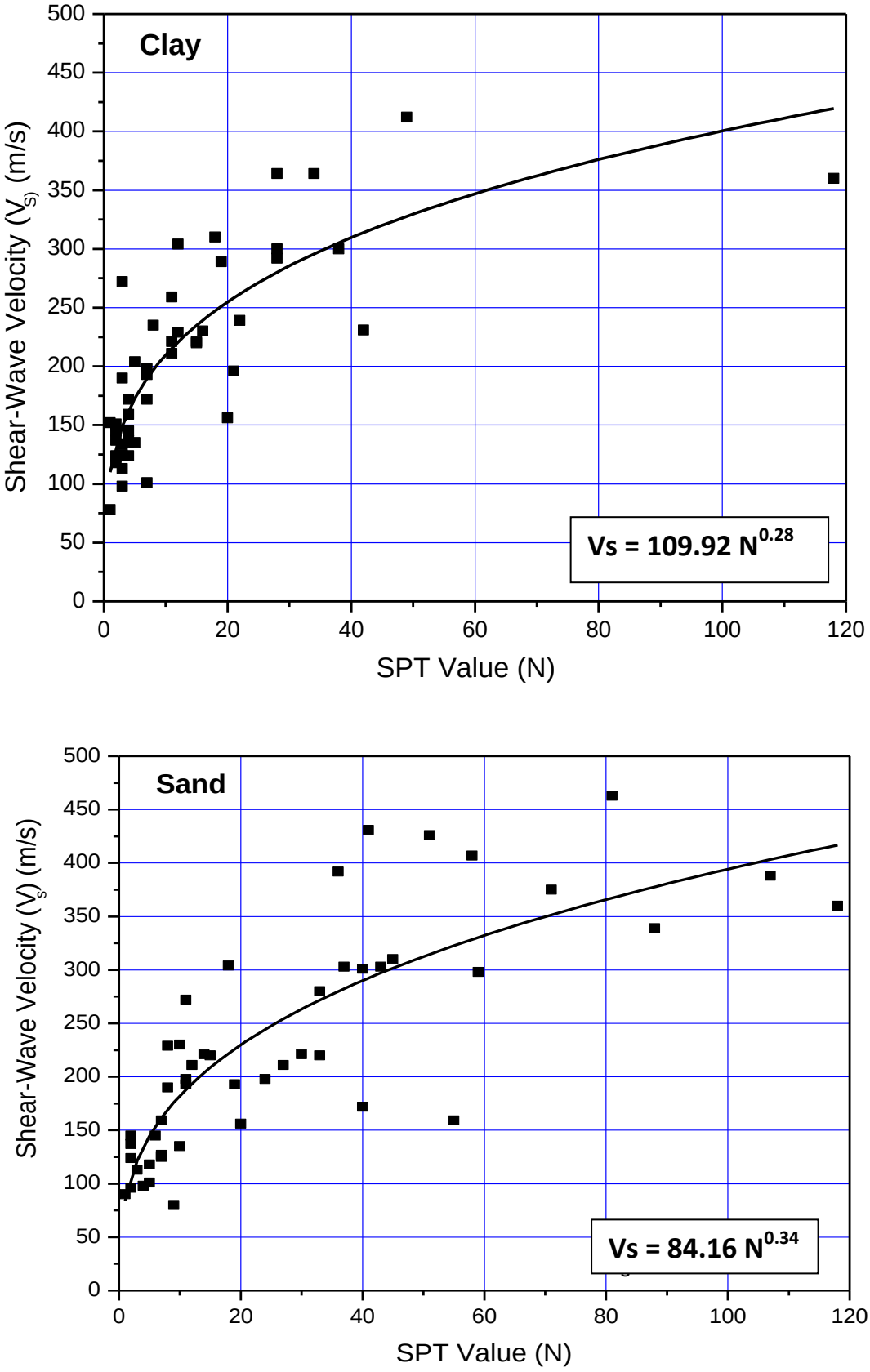

Figure 2.16 Proposed Shear Wave Velocity and SPT N-value correlations for clay and sand (After Ansary et al., 2010)

2.9 DAMAGE ASSESSMENT

Soil conditions are often variable even inside of a relatively small area as a town. So it is necessary to find a low-cost method to obtain a detailed dynamic characterization of soil. Microtremor is the most convenient, reliable and low-cost technique to assess the damage of any site and building. Damage assessment of any building and site can be done in two ways. First one is Resonance Criteria, which is assessed from the analysis microtremor data in both building and site. Second one is Nakamura's Seismic Vulnerability Index (K_g). These two techniques have been discussed in this section.

2.9.1 Seismic Vulnerability Index (Kg) for soil

Kg values have been proposed by Nakamura (1996) for accurately estimating earthquake damage of surface ground and structures. Here in this study, only the formulation of K_g, have been given an example of application of outputs from QTS method. For calculating K_g, shear strain of the ground is consider

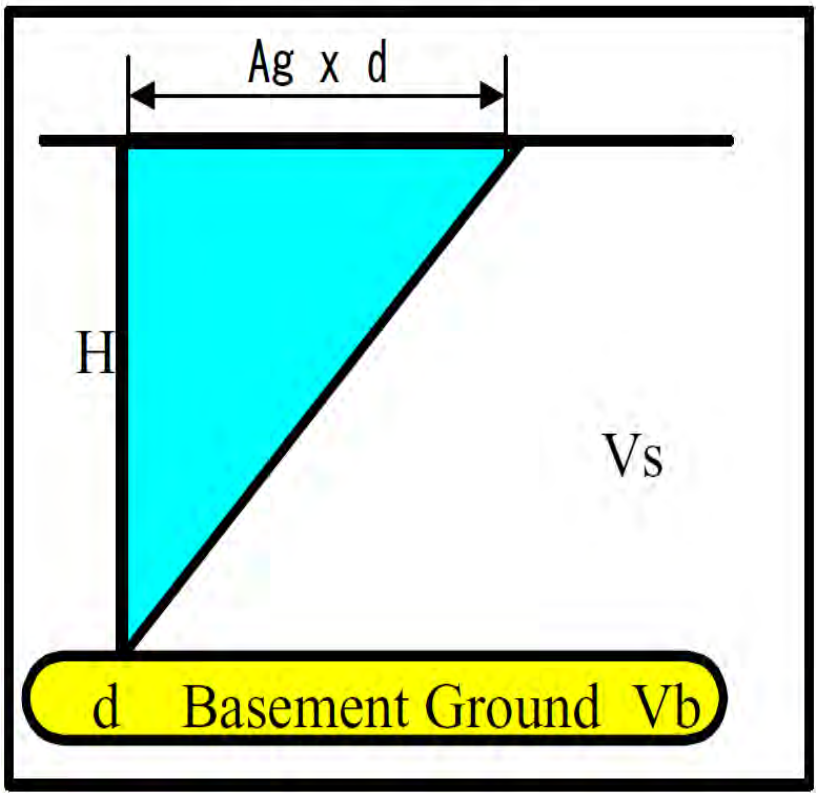

Figure 2.17 Surface ground deformation

Putting the S wave velocities of the basement and surface layer (C_b and C_f) natural frequency Fg of the surface layer can be expressed as,

$$F_g = \frac{V_b}{4A_g.h} \tag{2.9}$$

Acceleration α in the basement can be written as

$$\gamma = \frac{A_g.\alpha_b}{(2\Pi\ F_g)^2} \cdot 4A_g.\frac{F_g}{C_b} \tag{2.10}$$

$$= \frac{A_g^2}{F_g}.\frac{\alpha_b}{\Pi^2 C_b}$$

$$= \mathrm{c}.K_g\alpha$$

$\alpha_b = (2\Pi\ F_g)^2 \mathrm{d}$ and shear strain γ is expressed as follows,

Where,

$$\mathrm{c} = \frac{1}{\Pi^2.v_b}; \qquad K_g = \frac{A_g^2}{F_g} \tag{2.11}$$

C is expected to be almost constant for various sites. Effective shear strain defined by e % of equation (2.11) becomes to nearly equal to the product of K_g and α_b, under the assumptions of e = 60 % and C_b = 600 m/s. K_g is a value corresponding to the site and can be considered as a vulnerability index of the site, which might be useful to select weak points of ground. Figure 2.18 shown in $K_g$values calculated for Loma Prieta Earthquake. Figure 2.18 shown in $K_g$values calculated for Loma Prieta Earthquake. (After Nakamura et al., 1990)

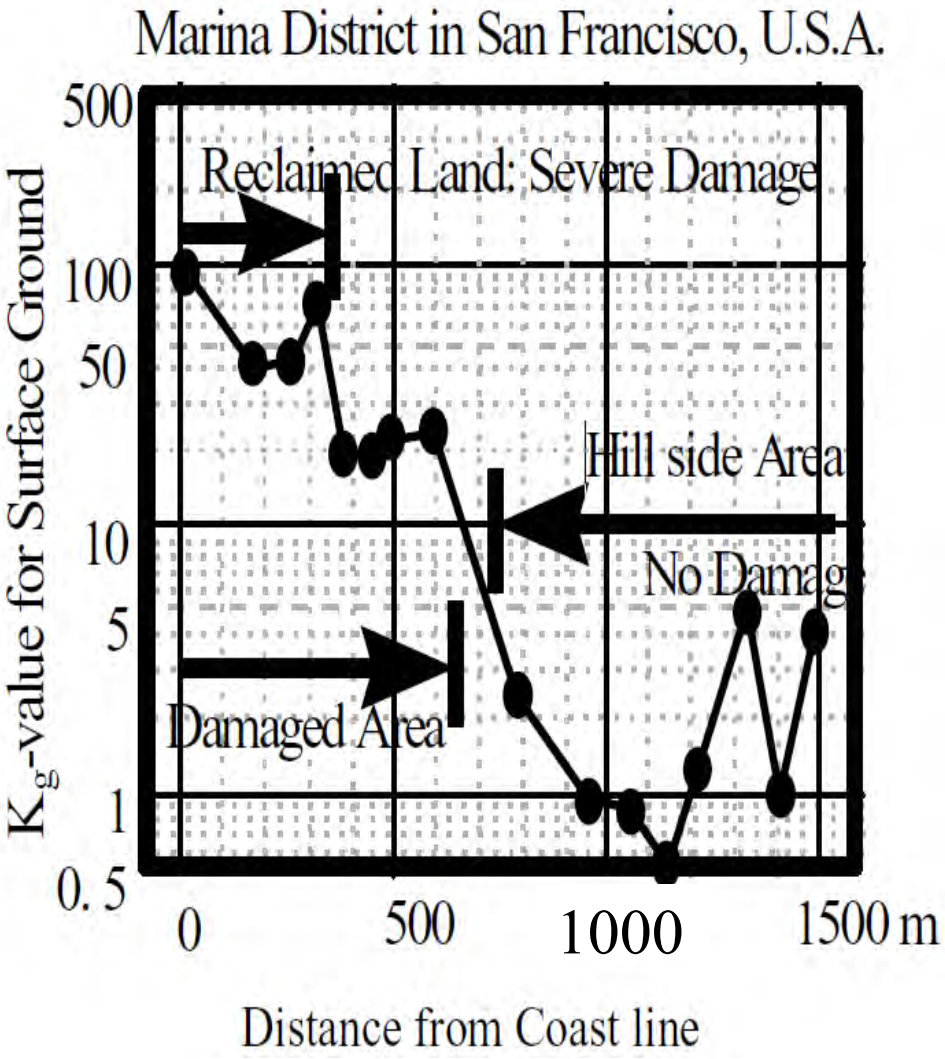

Figure 2.18 K_g values calculated for Loma Prieta Earthquake (After Nakamura et al., 1990)

The damage assessment using Nakamura's (2000) Vulnerability Index (Kg) for Loma Prieta Earthquake has been shown in Figure 2.18. The result shows the similarity between actual damage and theoretical damage assessment using Kg value.

2.10 SUMMARY

In this chapter definition of microtremor and earthquake, its sources and relevant literatures such as relationship between microtremor and earthquake, relationship between microtremor and earthquake H/V ratio and theoretical transfer function of shear wave etc. have been reviewed.

Microtremor and earthquake studies have been showed that the peak amplitude of the microtremor H/V ratio tends to underestimate the peak amplitude of earthquake spectral ratios with respect to a reference site soil. The H/V spectral ratio determined from microtremors has shown a clear peak that is well correlated with the fundamental frequency. Plate tectonics movement and major seismic sources and also different types of soil correlations have been described in this chapter.

Finally, the literature related to damage assessment using H/V technique has been described in this chapter. These are the practical application of H/V technique. The theory and methodology of the vulnerability of site soil according to Nakamura's (2000) Vulnerability Index (Kg) has been illustrated. The application of seismic Vulnerability in various places also included.

CHAPTER THREE

DATA COLLECTION AND ANALYSIS

3.1 GENERAL

Damage in recent earthquakes showed that local site conditions have a significant effect on ground motion. Site response studies play an important role in seismic microzonation studies. The application of microtremor is to determine dynamic characteristics (predominant frequency and amplification factor). Microtremor measurements are usually used in site characterization due to their simplicity, low cost and minimal disturbance to other activities.

In the traditional spectral ratio method, H_S/H_r, site and source effects are estimated from observation at a reference site. In practice, adequate reference site are not always available especially in flat areas where exposed rock is not available. Therefore, methods have been developed that do not need reference sites (Bard 1994). Several recent applications of this technique have proved to be effective in estimating predominant frequency (Field and Jacob 1993; Ohmachi et al. 1994) and amplification factors (Lermo and Chavez-Garcia 1994; Konno and Ohmachi 1995). The use of microtremor and earthquake H/V technique for site response analysis has been discussed in Chapter 2.

Several methods have been proposed for spectral calculation of ground motions including microtremor. Fourier spectrum is the most convenient one that is used widely. Some investigations showed that different methods give similar results (Dimitriu et al. 1998). However some researchers declare that a suitable spectral method gives more reliable results (Ghayamghamian and Kawakami 1997). That's why five segments of spectra have been selected to compute the mean segmental cross spectra. Standard deviation of mean has also been calculated to show the deviation of mean value from Fourier spectra in East-West and North-South direction. Among these locations, empirical soil correlations developed by Ansary et al. (2010) and other empirical correlations (After TC4, ISSMFE, 1993) have been used to convert SPT-N value to shear-wave velocity.

3.2 STUDY LOCATIONS

29 SMAs have been deployed by BUET from 2003 to 2005 and all these digital seismic measuring device are located at free-field stations in and around of Bangladesh as shown Figure 3.1. Out of these 29 SMAs locations, 6 are selected for this research and Microtremor Array data of those six points have been collected.

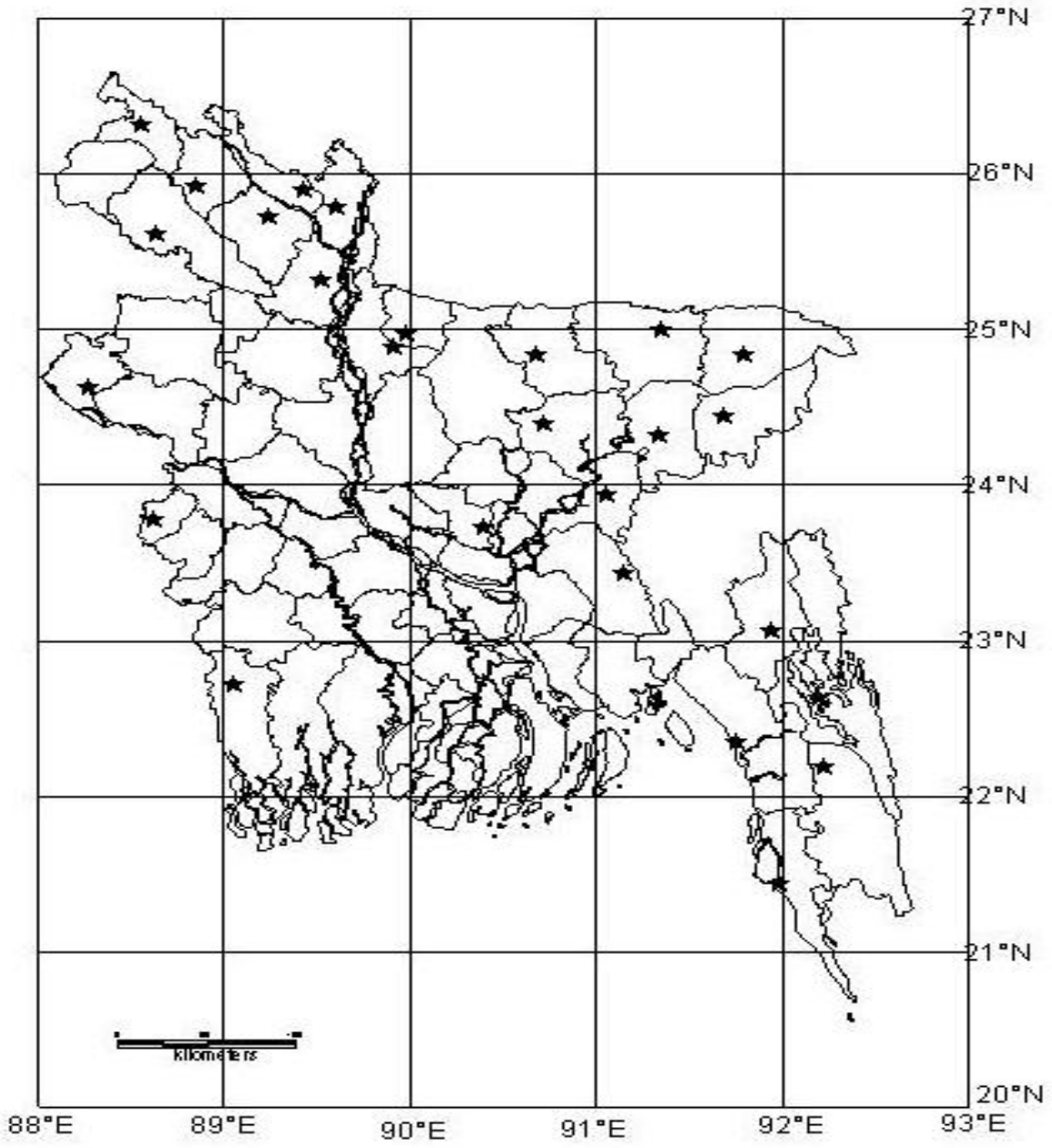

Location of Digital Seismic Measuring Device at free-field Station (ETNA) as shown Table 3.1

Table 3.1 Location of Digital Seismic Measuring Device Station (ETNA)

SL.No	Model	Location	Latitude	Longitude
*1	ETNA (BUET)	LGED, Bogra	23.32^0N	88.45^0E *
*2	ETNA (BUET)	LGED, Natore	23.22^0N	88.35^0E *
3	ETNA (BUET)	Jamuna Bridge West-End	23.28^0N	88.25^0E
*4	ETNA (BUET)	Jamuna Bridge East-End	23.25^0N	88.20^0E *
5	ETNA (BUET)	LGED, Mymensingh	25.43^0N	90.65^0E
*6	ETNA (BUET)	BUET-Dhaka	23.92^0N	90.25^0E *
7	ETNA (GSB)	PWD Office, Satkhira	23.85^0N	88.52^0E *
*8	ETNA (GSB)	PWD, Ashkona-Hajji camp	23.71^0N	90.38^0E *
*9	ETNA (GSB)	Pollice Staff College	23.72^0N	90.25^0E
10	ETNA (GSB)	GSB-Dhaka	23.75^0N	90.35^0E
11	ETNA (GSB)	GSB-Chittagong	22.15^0N	91.80^0E
12	ETNA (GSB)	PWD, Cox's-bazar	21.42^0N	91.89^0E
13	ETNA (GSB)	PWD, Bandarban	22.25^0N	92.32^0E
14	ETNA(JIDPUS)	PWD, Rangamati	22.72^0N	92.38^0E
15	ETNA (GSB)	PWD, Sunamganj	25.07^0N	91.32^0E
16	ETNA (GSB)	PWD, Sylhet	25.15^0N	91.25^0E
17	ETNA (GSB)	PWD, Moulvibazar	24.35^0N	91.72^0E
18	ETNA(JIDPUS)	PWD, Comilla	23.22^0N	91.35^0E
19	ETNA (GSB)	PWD, B.Baria	23.92^0N	91.25^0E
20	ETNA (GSB)	PWD, Kishoreganj	24.35^0N	90.92^0E
21	ETNA (GSB)	PWD, Netokona	24.72^0N	90.65^0E
22	ETNA(JIDPUS)	Haluaghat, Mymensingh	25.05^0N	90.25^0E
23	ETNA(GSB)	PWD, Jamalpur	25.15^0N	90.12^0E
24	ETNA(GSB)	PWD, Rangpur	25.80^0N	89.20^0E
25	ETNA (GSB)	PWD, Lalmonirhat	25.90^0N	89.35^0E

26	ETNA(JIDPUS)	PWD, Kurigram	25.60^0N	89.80^0E
27	ETNA (GSB)	PWD, Panchagarh	26.15^0N	88.25^0E
28	ETNA(GSB)	PWD, Meherpur	23.75^0N	88.62^0E
29	ETNA(JIDPUS)	Ruppur, Pabna	23.42^0N	88.75^0E

*Microtremor observations have been made

3.3 MAJOR EARTHQUAKES WHICH ARE AFFECTED IN BANGLADESH ON THE LAST DECAY

On May 25, 2015 the major "Nepal earthquake" occurred in Pokhara province, Nepal. Its Magnitute is 7.8 and distance 741 km from Dhaka, Bangladesh. This earthquake been recorded by the free-field stations at Kurigram, Bogra, Natore, Sylhet, Ruppur at Pabna, Jamuna Bridge at Sirajganj, Police Staff College, at Mirpur, and BUET-Dhaka at 12:15:45 hrs BST (06:15:45 hrs GMT, May 25, 2015). The maximum acceleration of this earthquake recorded in Bogra with a values of 23.56 cm/sec.^{2} in East-west direction. Some major earthquakes that have affected Bangladesh recently is shown in Table 3.2

Table 3.2 Some earthquakes that have affected in and around Bangladesh

Date	Name	Epicentre	Magnitude (M)
14-02-2006	Sikim Earthquake	Bihar, India	5.9
16-11-2006	Bengal Earthquake	Jessore, Bangladesh	5.5
11-09-2010	Assam Earthquake	Shillong Plateau	5.1
18-03-2012	Sikim Earthquake	Jantia Hill, Assam	7.1
25-04-2015	Nepal Earthquake	Pokhara, Nepal	7.8

3.4 METODOLOGY OF EARTHQUAKE AND MICROTREMOR DATA ANALYSIS

At first, site is selected for data collection. There are six selected locations Bogra, Natore, Jamuna Bridge at Sirajganj, Haji-Camp at Ashkona, Police Staff College at Mirpur and BUET. Microtremore and earthquakes collected data along in three directions (x, y and z directions). Fast Fourier Transformation (FFT) along x, y, and z directions and their H/V Ratio analysis with frequency are conducted. Ultimate target is to etimation of predominant frequency of these site from HVR of Microtremor and Earthquakes analysis. The following flow chart (Figure 3.2) shows the outline of the Metholodogy.

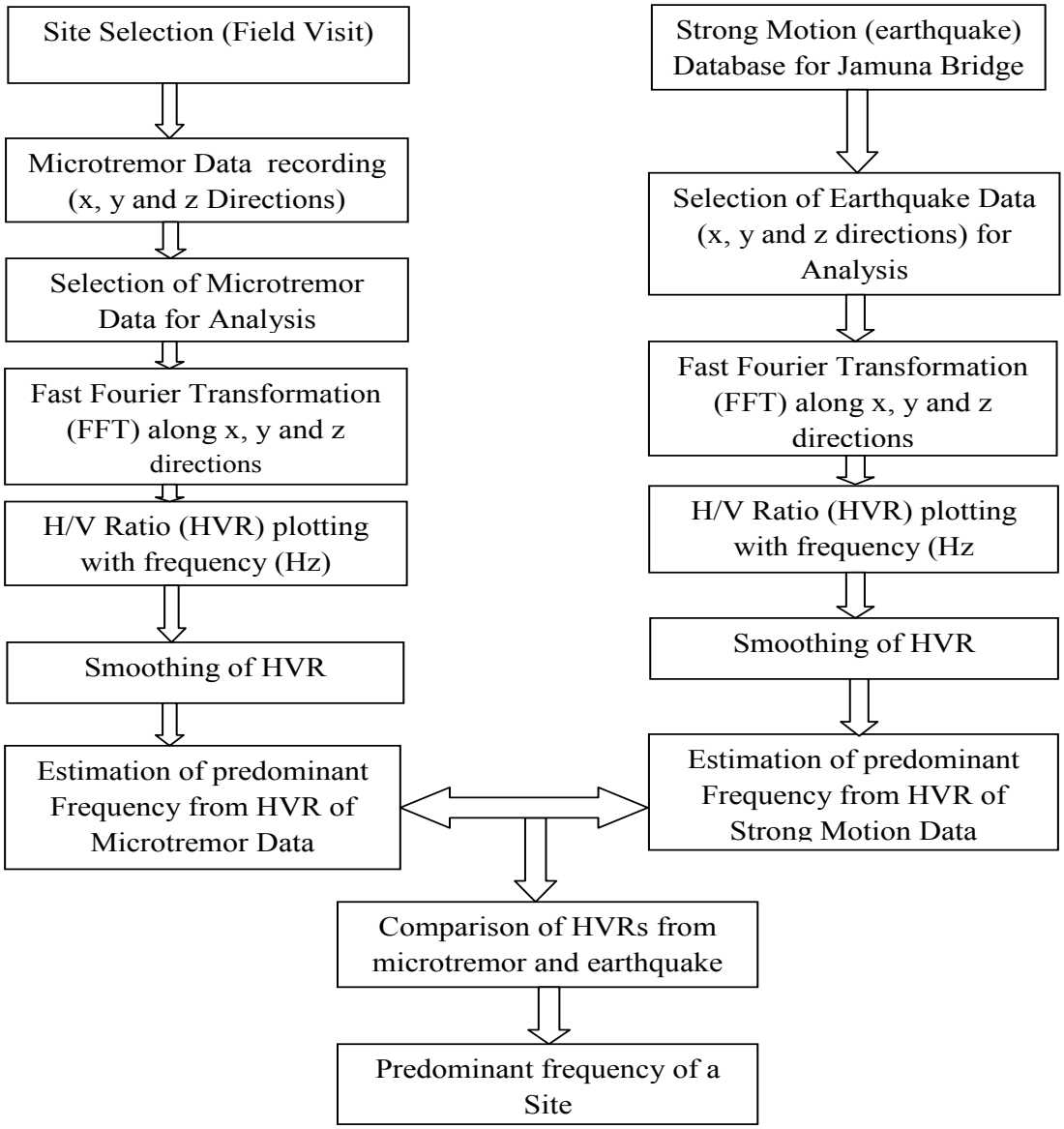

Figure 3.2 Flow Chart for Microtremor and Strong Motion Data Analysis

3.5 Sub-Soil Characteristics from SPT-N Values and Microtremor Array Analysis

Sub-soil investigation is necessary for the analysis of dynamic characteristics of soil. Shear wave velocity (SWV) is used to develop soil model. For this study Standard Penetration Test (SPT) has been carried out three locations at Bogra, Natore and Jamuna Bridge east side. Shear wave velocity as well as SPT data has been collected from other sources and SWV from Small Scale Microtremor Measurement (SSMM) as well as SPT data has been collected at the six microtremor test locations (MT Array). Finally, SWV has been estimated using SPT and SWV correlation (Ansary et al., 2010) where there is no SWV test result. The other three soil correlations (Ohta and Goto 1978; Imai and Yoshimura 1970; Ohba and Toriumi 1970) have been used to compare SWV. We have been used the equation (Ohta and Goto 1978) Article 2.10 Chapter 2. Soil profile and shear wave velocity LGED office at Bogra as shown Figure 3.3 and Figure 3.4. Similarly, Soil profile and shear wave velocity at Natore, Jamuna Bridge East side, at Sirajganj, Haji-Camp at Ashkona, Police Staff College at Mirpur and BUET-Campus, Dhaka are shown in Figures 3.5 to 3.8.

Time period has been estimated at selected locations using the following equation

$$T_{soil} = (4H/Vs) \text{ sec} \quad (3.1)$$

Where, H=Depth of soil (m) and Vs=Shear wave-velocity (m/s)

and shear wave velocity are estimated from SPT-N using the following equation

$$Vs = 69\, N^{0.17}\, D^{0.2}\, F_1\, F_2 \quad (3.2)$$

(a) Sub-Soil Characteristics of LGED office at Bogra

SPT Results

Depth, SPT-N Values and Soil Profile at Bogra LGED office as shown in Figure 3.3. It has been observed from the disturbed soil sample, the borehole consists of five soil layers. The Light grey silt with some trace clay and sand varies from 0 to 3.0 m from EGL. Second layer is Reddish brown to brown clayey silt and its varies from 3.0 to 4.5 m. Next layer is Brown medium dense sandy with trace clay and its veries from 7.5 to 9.0 m. On the other hand, Light grey dense to very dense silty sand to sand with some silt layer, exists from 10.5 to 30 m from EGL. The uncorrected SPT N-value of this site varies from 5 to 45. The SPT-N value of Light grey silt with some trace clay and sand varies from 5 to 16. The SPT N-value

of Reddish brown to brown clayey silt and Brown medium dense sandy with trace clay layer varies between 16 to 25 and last on Light grey dense to very dense silty sand to sand with some silt layer varies from 25 to 65.

LGED office at Bogra		
Depth (m)	SPT-N (Values)	Soil Type
1.5	5	Light grey silt with some trace clay and sand.
3.0	13	
4.5	15	Radish brown to brown clayey silt
6.0	16	Brown medium dense sandy with trace clay.
7.5	25	Brown medium dense silty sand
9.0	15	
10.5	34	Light grey dense to very dense silty sand to sand with some silt
12.0	37	
13.5	62	
15.0	65	
16.5	45	
18.0	64	
19.5	25	
21.0	30	
22.5	36	
24.0	40	
25.5	45	
27.0	43	
28.5	49	
30.0	47	

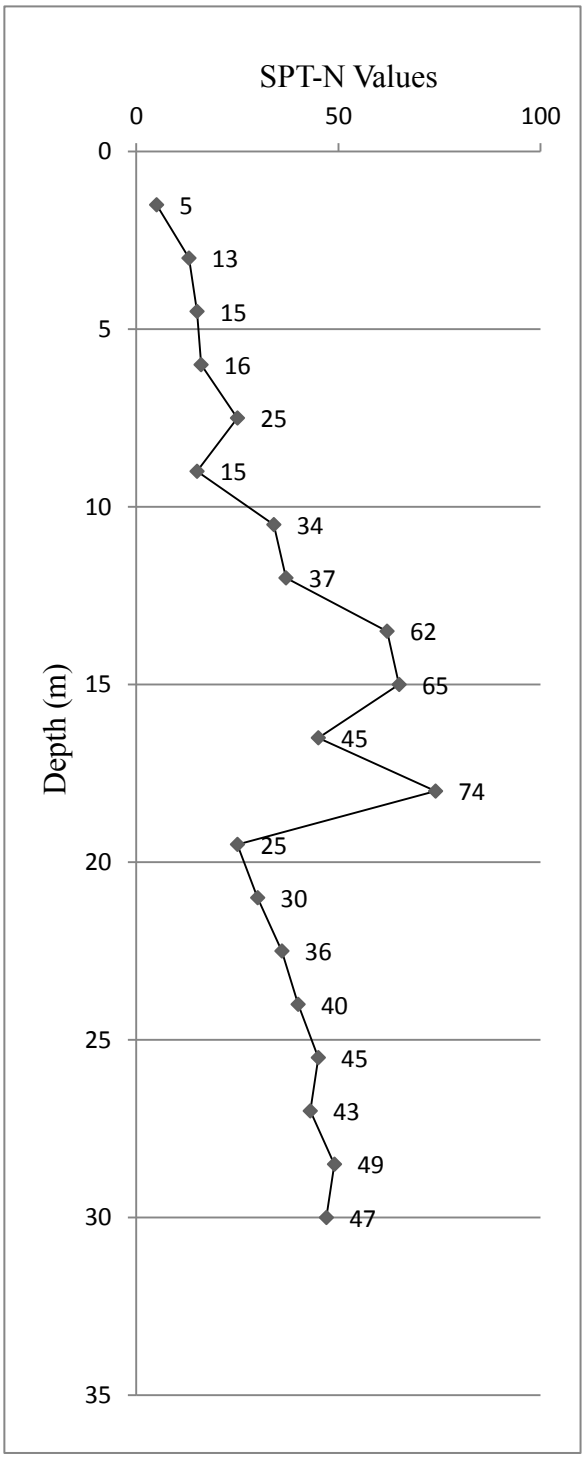

Figure 3.3 Depth, SPT-N Values and Soil Profile at Bogra LGED office

Shear Wave Velocity Results in the LGED office at Bogra

Shear wave velocity has been estimated at Bogra LGED office using soil correlation as shown Figure 3.4 and equation 3.2. According to soil correlation proposed by Ansary et al. (2010), the shear wave velocity varies from 142 to 261 m/sec. On the other hand, SWV of Ohba and Toriumi (1970), which varies from 127 to 231 m/sec, shows slightly higher value than Imai and Yoshimura (1970), which shows ranging between 138 and 242 m/sec. The average shear-wave velocity over a 30m (V_{s30}) depth has been estimated to be 210 m/s, using the correlations of soil by Ohta and Goto (1978). Time period has been estimated from equation (3.1) to be 0.40 sec.

Depth (m)	Velocity (m/sec)
1.5	98
3.0	133
4.5	148
6.0	158
7.5	178
9.0	170
10.5	201
12.0	209
13.5	234
15.0	241
16.5	231
18.0	256
19.5	216
21.0	226
22.5	235
24.0	244
25.5	250
27.0	253
28.5	261
30.0	262
Avg (V_{s30}) =	210

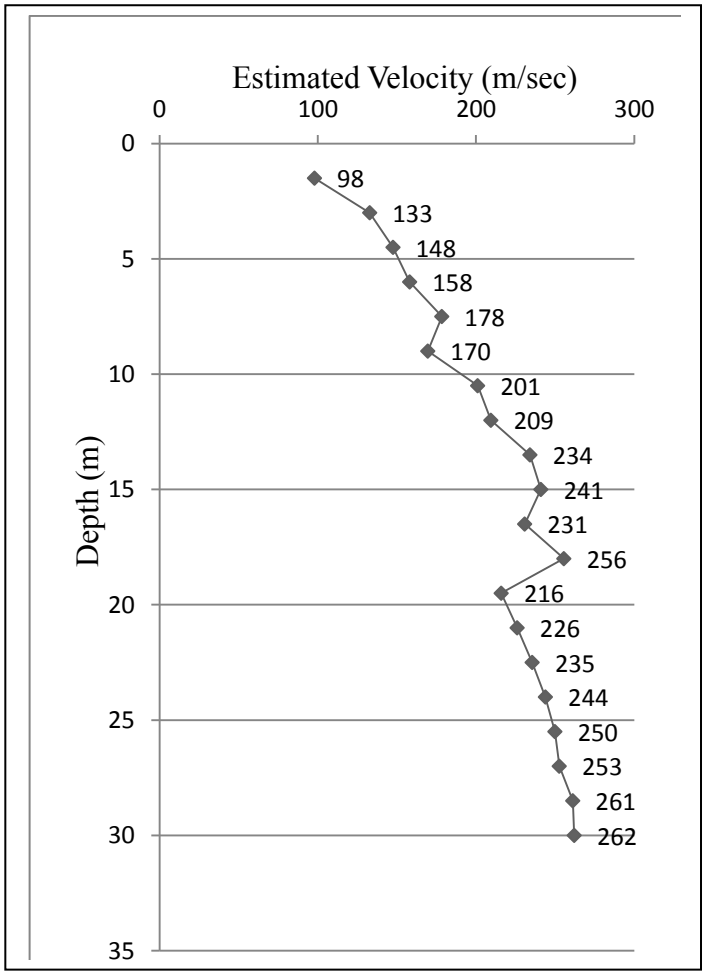

Figure 3.4 Depth and Shear Wave Velocity at Bogra LGED office

(b) Sub-Soil Characteristics of Natore LGED office

SPT Results

From the disturbed soil sample, the borehole consists of four soil layers. Light brown sand and silt with some sand. The Light grey sand silt with some medium to dense sand varies from 0 to 4.5 m from EGL. On the other hand, medium to very dense silty sand to sand with some silt from 9 to 28.5 m from EGL. The uncorrected SPT N-value of this site varies from 5 to 12. The SPT-N value of Light brown sand and silt with some sand varies from 8 to 27. The SPT N-value of medium to very dense silty sand to sand with some silty layer varies between 7 and 42. Depth, SPT-N Values and Soil Profile at Natore LGED office as shown in Figure 3.5

LGED office at Natore		
Depth (m)	SPT-N (Values)	Soil Type
1.5	8	Light brown sand and silt with some sand.
3.0	7	
4.5	6	Light grey sand silt with some medium to dense sand.
6.0	3	Light grey with some dense sand and silt with clay to clayey silt.
7.5	5	Light grey medium to very dense silty sand to sand with some silt
9.0	7	
10.5	10	
12.0	6	
13.5	20	
15.0	16	
16.5	28	
18.0	42	
19.5	74	
21.0	46	
22.5	38	
24.0	47	
25.5	37	
27.0	45	
28.5	42	
30.0	44	

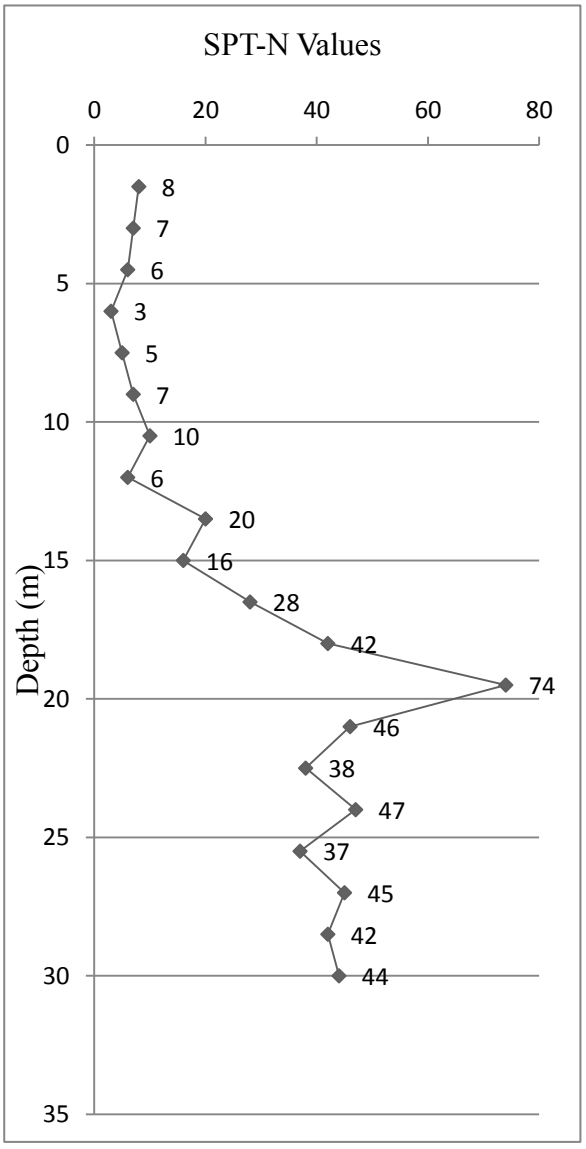

Figure 3.5 Depth, SPT-N Values and Soil Profile at Natore LGED office

Shear Wave Velocity Results

Shear wave velocity has been estimated at Natore LGED office using soil correlation as shows in Figure 3.6 and equation 3.2. According to soil correlation proposed by Ansary et al. (2010), the shear wave velocity varies from 136 to 259 m/sec. On the other hand, SWV of Ohba and Toriumi (1970), which varies from 142 to 246 m/sec, shows slightly higher value than Imai and Yoshimura (1970), which shows ranging between 138 and 246 m/sec. The average shear-wave velocity over a 30m (V_{s30}) depth has been estimated to be 292 m/s, using the correlations of soil by Ohta and Goto (1978). Time period has been estimated from equation (3.1) to be 0.41 sec.

Depth (m)	Velocity (m/sec)
1.5	107
3.0	120
4.5	126
6.0	119
7.5	136
9.0	149
10.5	163
12.0	154
13.5	193
15.0	190
16.5	213
18.0	232
19.5	260
21.0	243
22.5	238
24.0	251
25.5	244
27.0	255
28.5	254
30.0	259
Avg (V_{s30})=	195

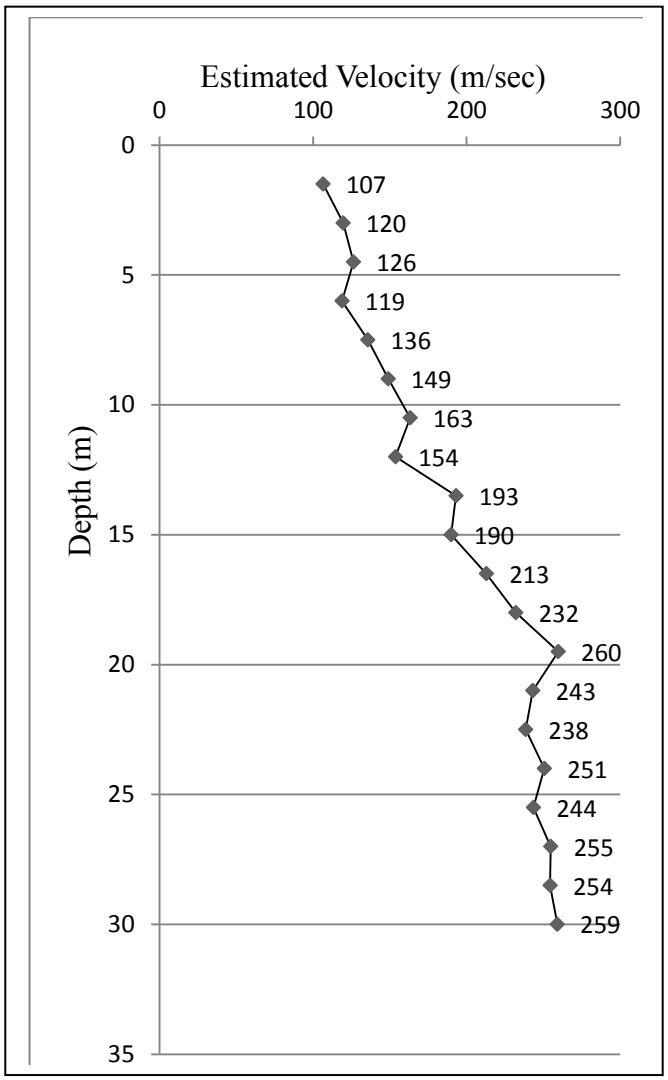

Figure 3.6 Depth and Shear Wave Velocity at Bogra LGED office

(c) Sub-Soil Characteristics of Jamuna Bridge East side, Sirajganj

Depth, SPT-N Values and Soil Profile at Jamuna Bridge East Side, Serajgnj as shown in Figure 3.7. From the disturbed soil sample, the borehole consists of four soil layers. Light brown to Light dense Sand with some trace silt and Light gray loose Sand with some some silt varies from 0 to 4.5 m from EGL. On the other hand, Light grey medium dense silt with some sand veries from 6 to 12 m and last on Light grey medium to very dense silty sand to sand with some silt exists from 13.5 to 30 m from EGL. The uncorrected SPT N-value of this site varies from 3 to 37. The SPT-N value of silt and Light gray loose Sand with some some silt veries from 8 to 27. The SPT N-value of Light Light grey medium tovery dense silty sand to sand with some silt layer varies between 28 and 82

Jamuna Bridge East Side at Sirajganj.		
Depth (m)	SPT-N (Values)	Soil Type
1.5	37	Light brown to light grey dense sand with some to trace silt.
3.0	27	
4.5	10	Light grey loose sand with some to silt.
6.0	8	Light grey medium dense silt with some Sand.
7.5	18	
9.0	9	
10.5	7	
12.0	14	
13.5	27	
15.0	28	Light grey medium to very dense silty sand to Sand with some Silt.
16.5	29	
18.0	41	
19.5	66	
21.0	82	
22.5	85	
24.0	54	
25.5	55	
27.0	59	
28.5	49	
30.0	56	

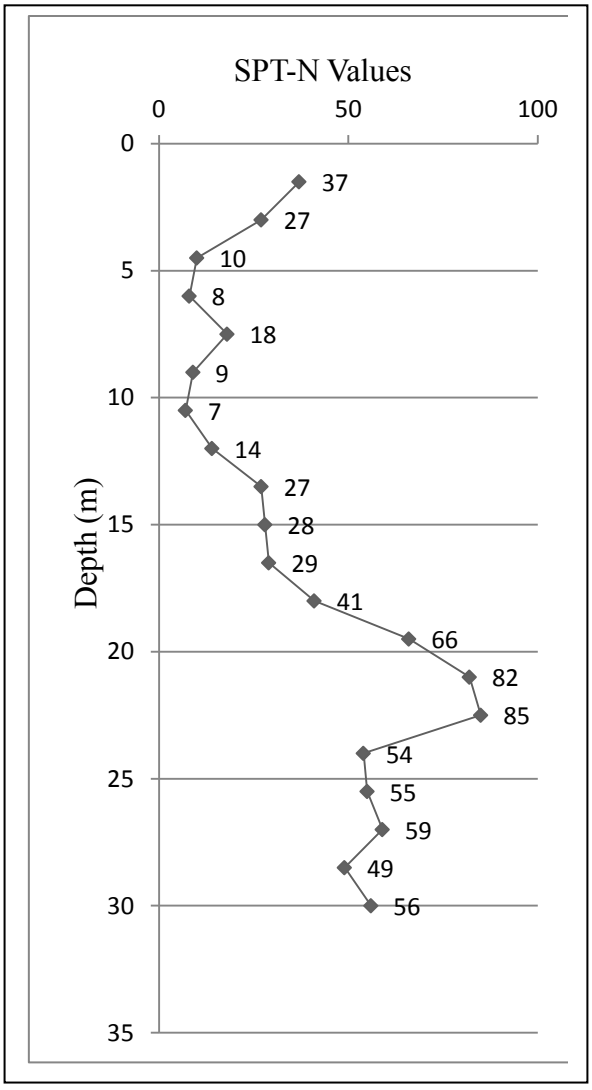

Figure 3.7 Depth, SPT-N Values and Soil Profile at Jamuna Bridge East Side, Sirajganj

Shear Wave Velocity Results

Shear wave velocity has been estimated at Jamuna Bridge east side using soil correlation as shown Figure 3.8 and equation 3.2. According to soil correlation proposed by Ansary et al. (2010), the shear wave velocity varies from 147 to 273 m/sec. On the other hand, SWV of Ohba and Toriumi (1970), which varies from 137 to 247 m/sec, shows slightly higher value than Imai and Yoshimura (1970), which shows ranging between 142 and 253 m/sec. The average shear-wave velocity over a 30m (V_{s30}) depth has been estimated to be 207 m/s, using the correlations of soil by Ohta and Goto (1978). Time period has been estimated from equation (3.1) to be 0.45 sec.

Depth (m)	Velocity (m/sec)
1.5	138
3.0	150
4.5	138
6.0	141
7.5	169
9.0	155
10.5	154
12.0	178
13.5	203
15.0	209
16.5	175
18.0	231
19.5	255
21.0	268
22.5	274
24.0	257
25.5	261
27.0	267
28.5	261
30.0	270
Avg (Vs_{30}) =	207

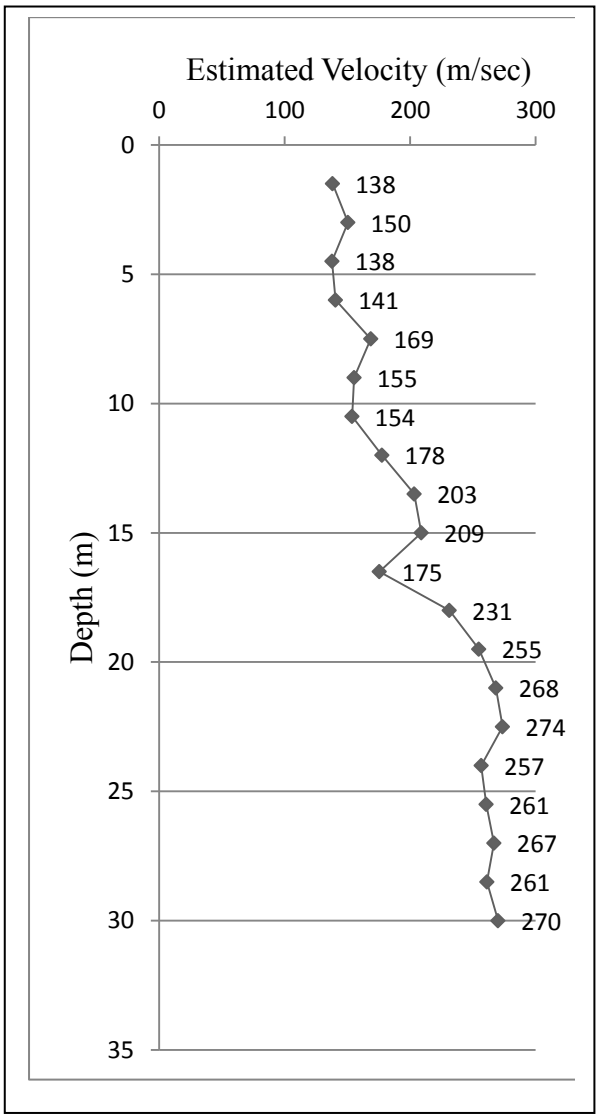

Figure 3.8 Depth and Shear Wave Velocity at Jamuna Bridge East Side, Sirajganj

3.6 MICROTREMOR DATA COLLECTION

The ground is always vibrating at amplitudes. Microtremors are ambient vibrations of the ground caused by natural or artificial disturbances such as wind, sea waves, traffic, human activities and industial machinery. Microtremor data has been collected in consideration of noise in different geological and geomorphological unit. Microtremor observation at six locations Bogra, Natore, Jamuna Bridge east side at Serajganj, Police staff college at Mirpur, Haji camp at Ashkona and BUET campus have been selected. Traffic movement, human activities, any power plant and noise from other sources have been considered during data recording as well. Most of the microtremor observation has been executed in consideration of recent filling. However, some non recent filling areas have also been selected for observation.

Figure 3.9 demonstrates microtremor measurement apparatus for data recording. This includes Geodas 15-HS equipment (Data logger and Laptop), Sensor, Cable, Battery and GPS. Mtobs.exe software is used to record microtremor data. Although there are five sensors in this observation system, two or five sensors have been used for data recording. Sensor has been used in consideration of surface condition, weather, time and geology of sites. CR4.5-1S velocity type sensor with sensitivity coefficient 0.0882μm/sec/digit has been used in observation system. Sensors comprise three components, which can record the horizontal motion (in Latitude and Longitude directions) and the vertical motions (up and down). Microtremor sensor sensitivity was 295900μm/sec/V. The converting speed was 50 kHz. The sampling frequency was 100 Hz. The amplification factor was used 20 db in observation system. Figure 3.10 shows some pictures of microtremor measurement Bogra, Natore, Jamuna Bridge East, Jamuna Bridge West, Ashkona Haji-Camp, Police Staff college, at Mirpur, and BUET, Dhaka. These pictures are taken at different time during microtremor data recording.

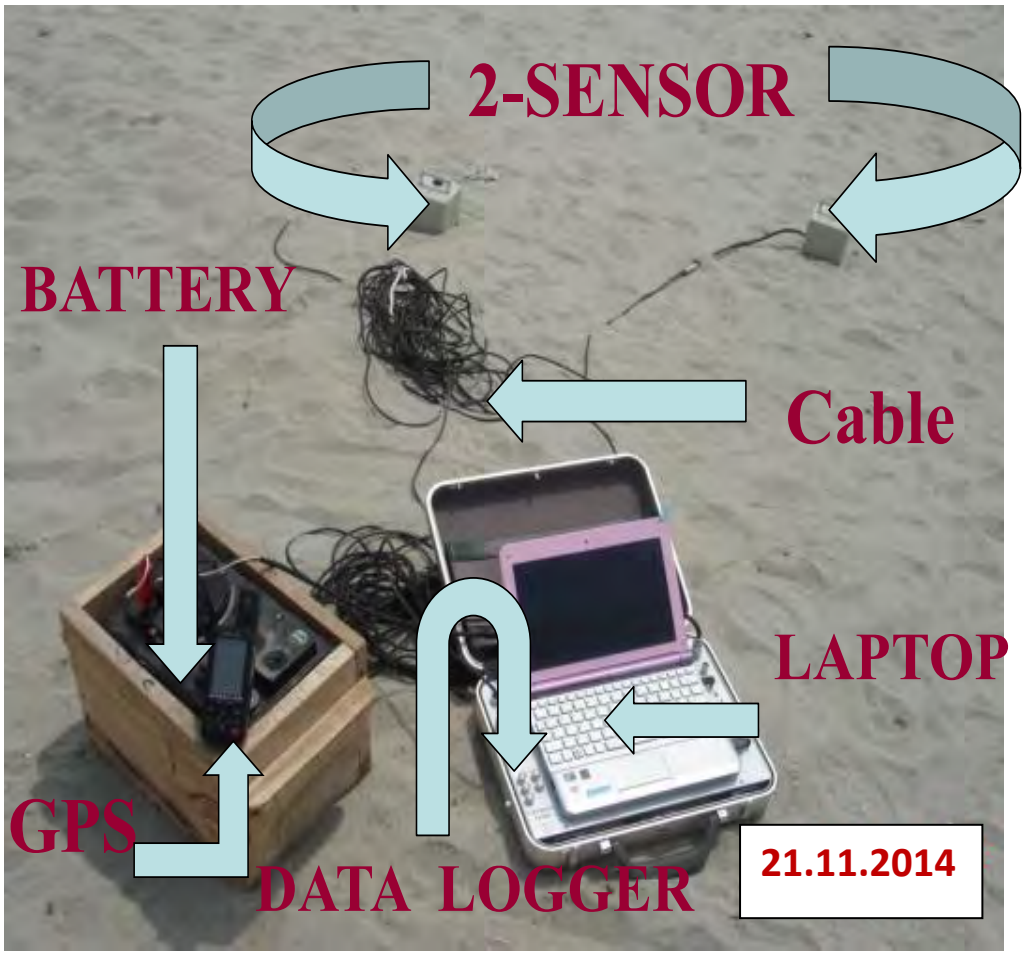

Figure 3.9 Microtremor measurement apparatus

Figure 3.10 Field data collection Process for Microtremor and Seismic measuring devices

3.7 MICROTREMOR DATA ANALYSIS

For six locations LGED office at Bogra and Natore, Jamuna Bridge east side at Serajganj, Police staff college at Mirpur, Haji camp at Ashkona and BUET campus have been selected. This accelerometer and microtremor gives data in North-South, East-West and Up-Down direction. Then Fourier spectrum ratio (Horizontal to Vertical) for various free field stations are studied and compared. In Strong motion acceleration data, The main steps of the process to estimate the distributions of the ground shaking intensity and of the corresponding damage to structures.

Velocity time history field microtremor data has been recorded in Mtobs.exe software with suitable number of observation channels, observation length, observation frequency, specific low or high pass filter code, amplification ratio, observation latitude and longitude, observation time and observation channel mode. Figure 3.11 as shown a typical time history field data recording of LGED office at Bogra (North side) at 2:30 PM on 21 November, 2014. The content of all input data are 2 CR4.5-1S velocity type sensors, 24000 observation data length, 100Hz sampling frequency, 0.05 Hz Low-pass filter, 20db amplification ratio, Latitude-23˚32′22″and Longitude-88˚55′40″.

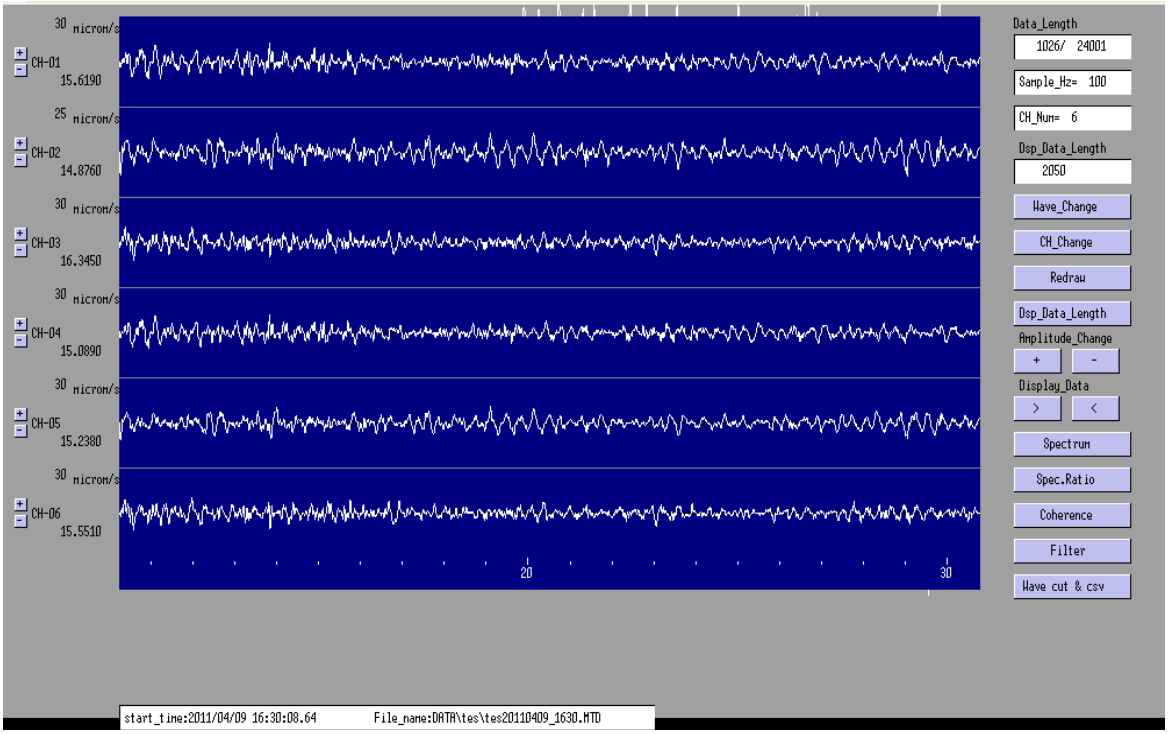

Figure 3.11 Time history of Microtremor obseravation LGED office at Bogra

3.7.1 Time history and Fourier spectrum Microtremor data analysis at six selected locations of Bangladesh

Time history and Fourier spectrum of microtremor data analysis at Bogra as shpown in Figure 3.12 [(a), (c) and (e)] in the segment 1, 2, 3, 4, 5 with 180000 observed data length. Segment 1, illustrates time history data of (0-41)sec. Segment 2 demonstrates time history data of (41-82)s Segment 3 demonstrates time history data of (82-123)sec, Segment 4 demonstrates time history data of (123-164)sec and Segment 5 demonstrates time history data of (164-205)sec.

Time history data is not suitable to estimate the dynamic properties (predominant frequency and amplification ratio). So, transformation of time domain data to frequency domain data is required with Fourier Transformation. Therefore, Fast Fourier Transformation (FFT) has been used to transfer time domain data to frequency domain data presents. Fast Fourier Transformation data at segment 1, 2, 3, 4 and 5 in EW, NS and UD directions as shown in Figure 3.12 [(b), (d) and (f)] respectively at Bogra. Similarly Natore, Jamuna Bridge East side at Sirajganj, Haji-Camp at Ashkona, Police Staff College at Mirpur and BUET-Campus, Dhaka as shown in Figures 3.13 to 3.17.

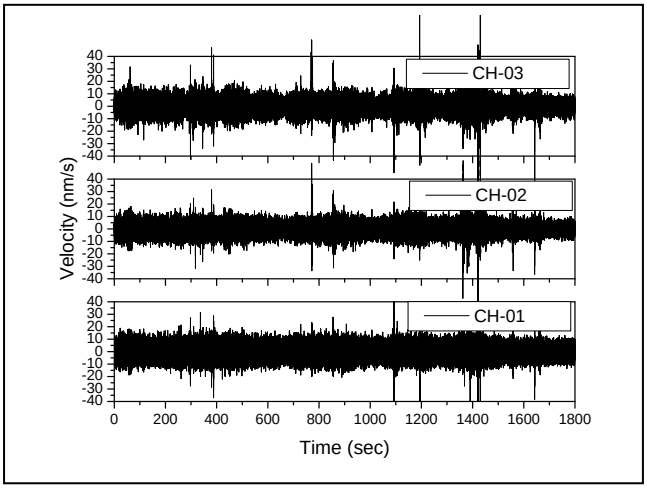

(a)

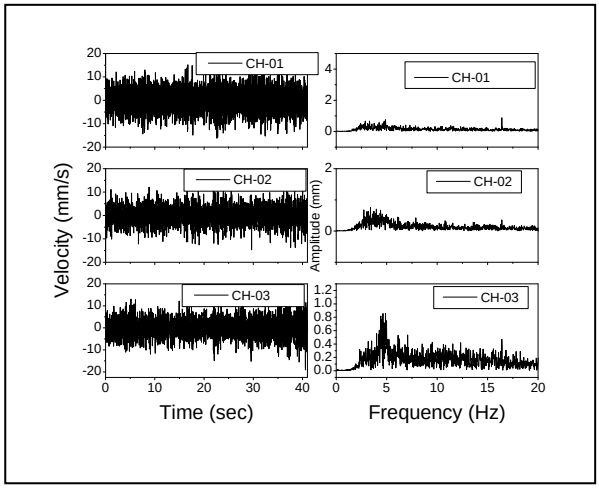

(b)

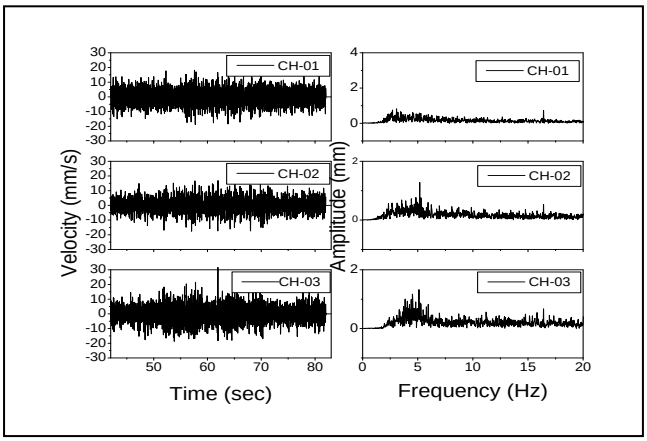

(c)

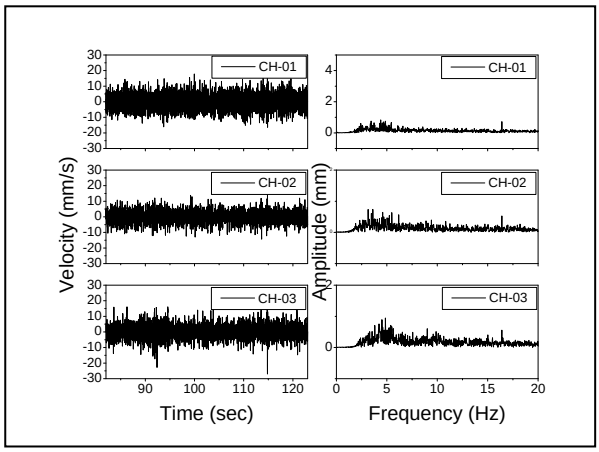

(d)

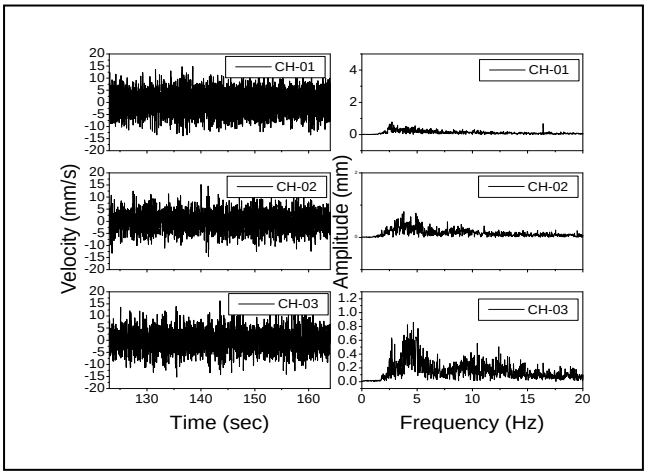

(e)

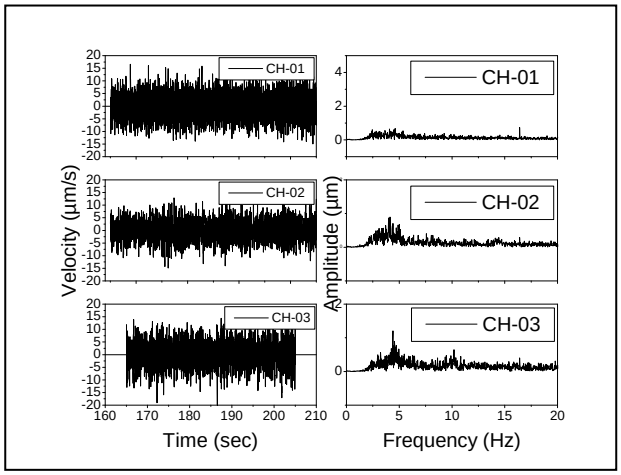

(f)

Figure 3.12 (a) Total time history (0-1800) sec (b)Segment-1 (0-41) sec (C) Segment-2 (41-82) sec (d) Segment-3 (82-123) sec (e) Segment-4(123-164) sec and (f) Segment-5 (164-205) sec for Time History and FFT of Microtremor analysis at LGED office Bogra.

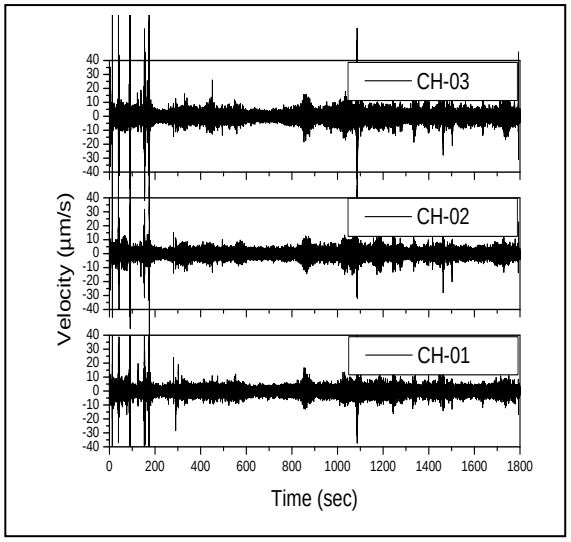

(a)

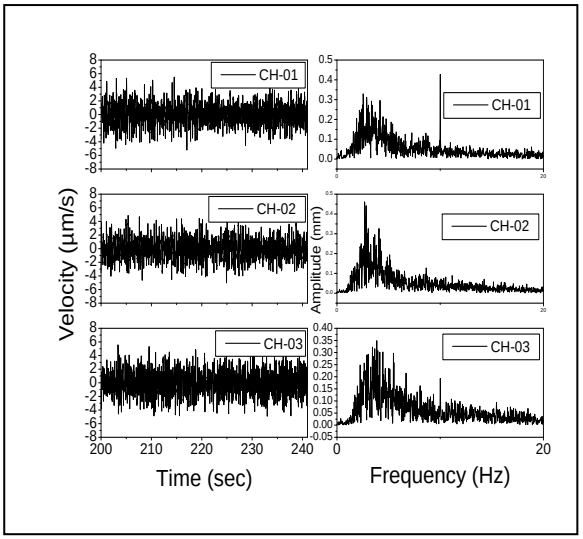

(b)

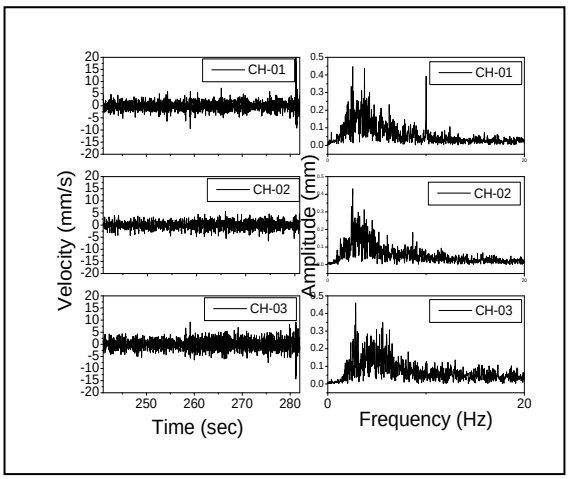

(c)

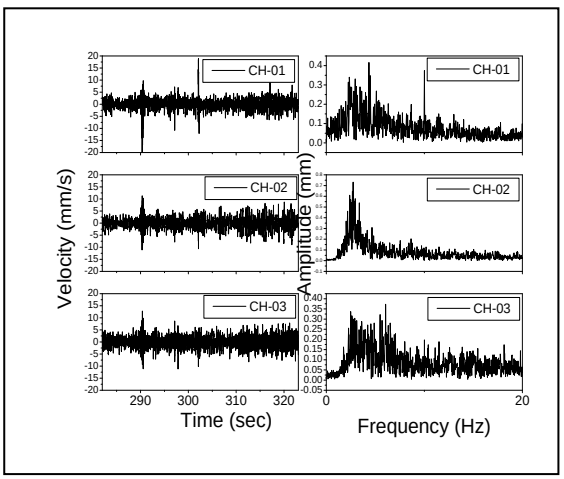

(d)

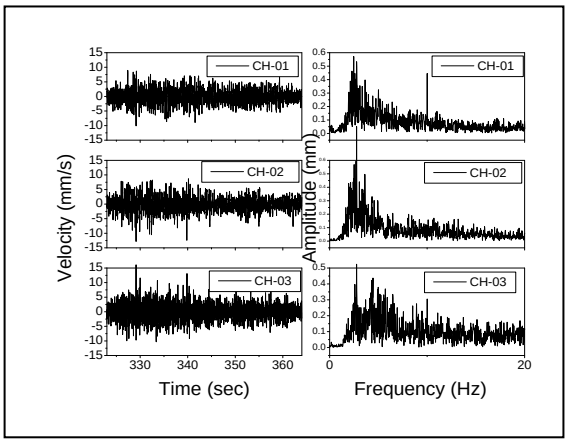

(e)

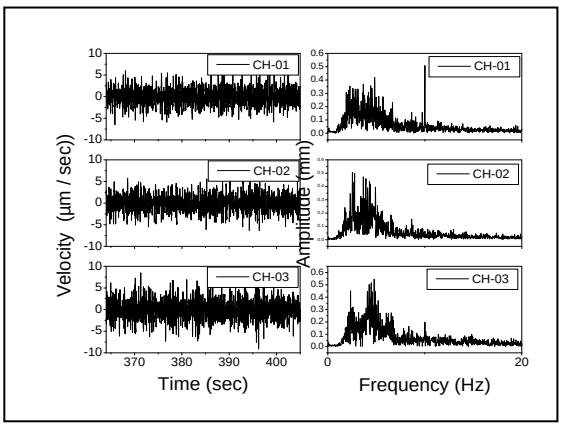

(f)

Figure 3.13 (a) Total time history.(0-1800)sec (b)Segment-1 (200-241)sec (C) Segment-2 (241-282)sec (d) Segment-3 (282-323)sec (e) Segment-4 (323-364) sec and (f) Segment-5 (364-405)sec for Time History and FFT of Microtremor analysis at LGED office Natore

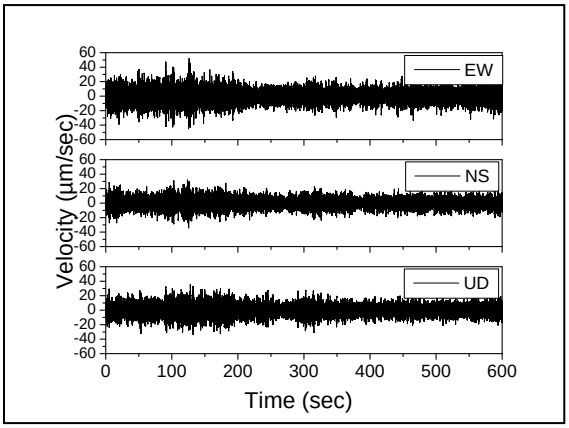

(a)

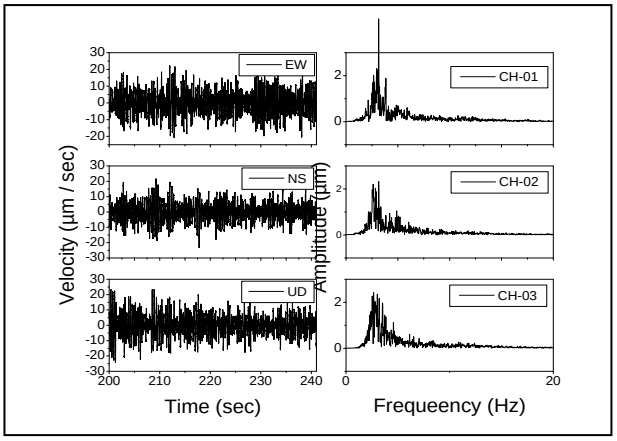

(b)

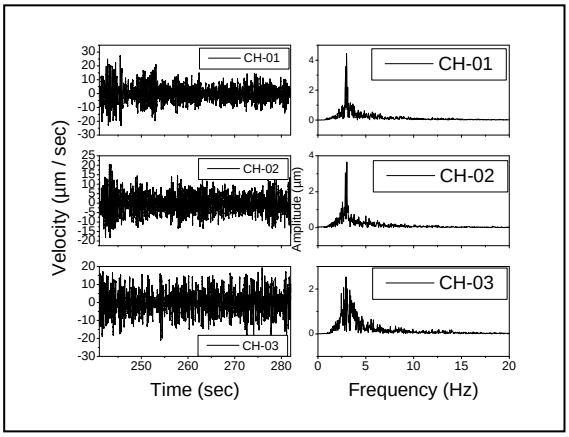

(c)

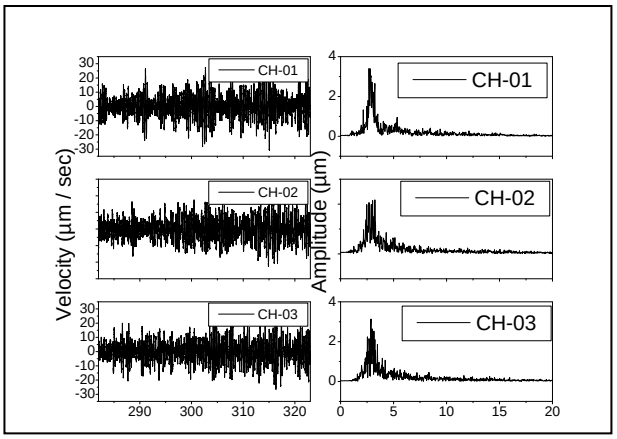

(d)

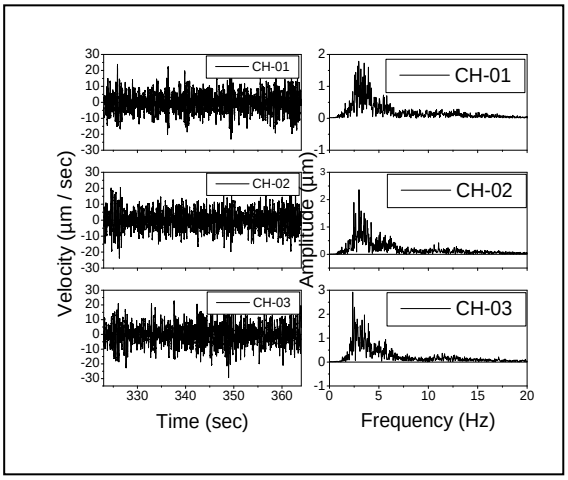

(e)

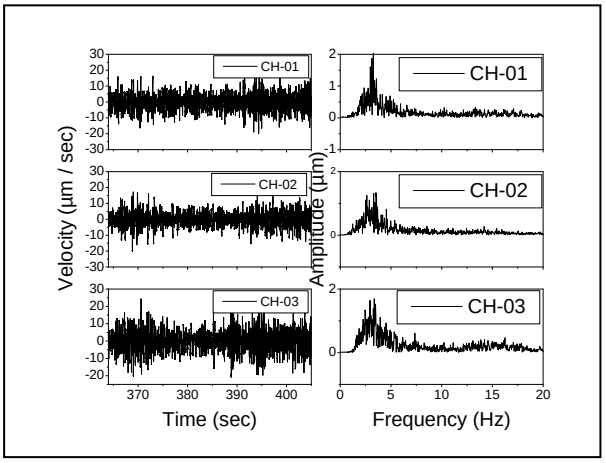

(g)

Figure 3.14 (a) Total time history (0-600) sec (b) Segment-1 (200-241) sec (C) Segment-2 (241-282) sec (d) Segment-3 (282-323) sec (e) Segment-4 (323-364) sec and (f) Segment-5 (364-405) sec for Time History and FFT of Microtremor analysis at Jamuna Bridge East Side

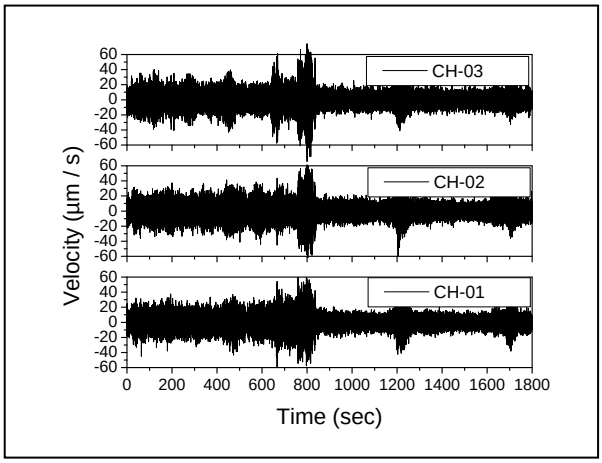

(a)

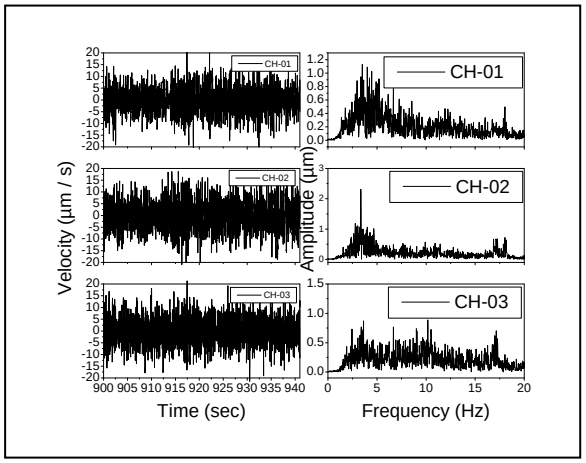

(b)

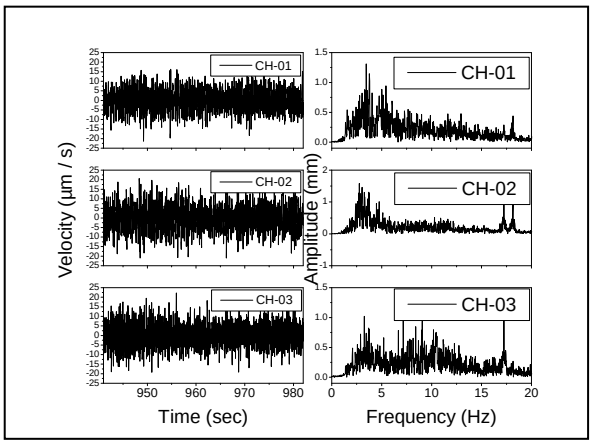

(c)

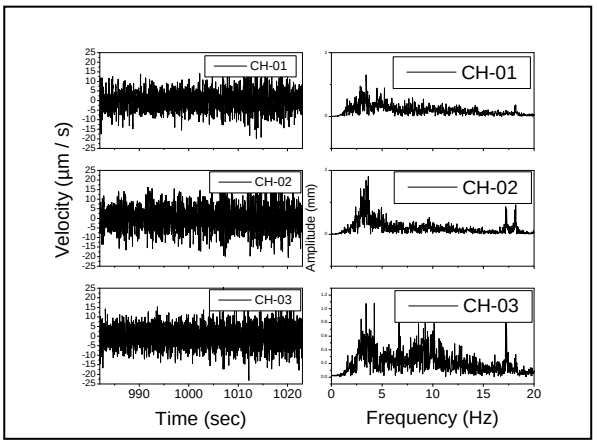

(d)

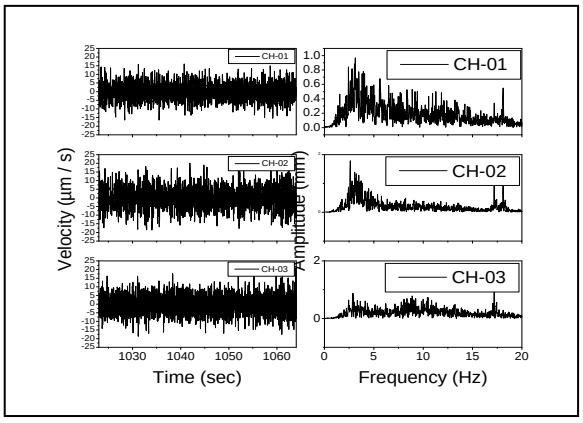

(e)

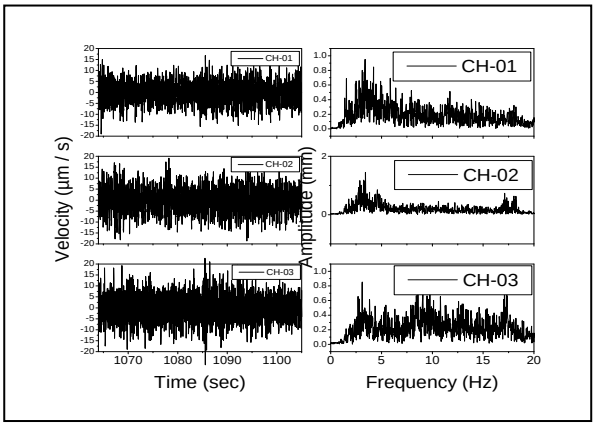

(f)

Figure 3.15 (a) Total time history.(0-1800) sec (b) Segment-1 (900-941) sec (C) Segment-2(941-982) sec (d) Segment-3 (982-1023) sec (e) Segment-4(1023-1064) sec and (f) Segment-5 (1064-1105)sec for Time History and FFT of Microtremor analysis at Airport, Ashkona Haji-Camp,Dhaka

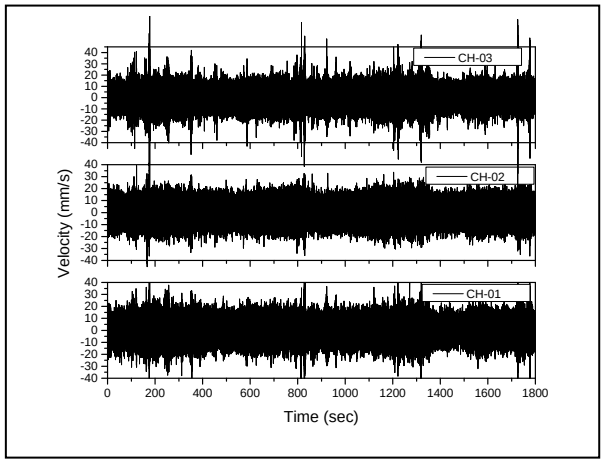

(a)

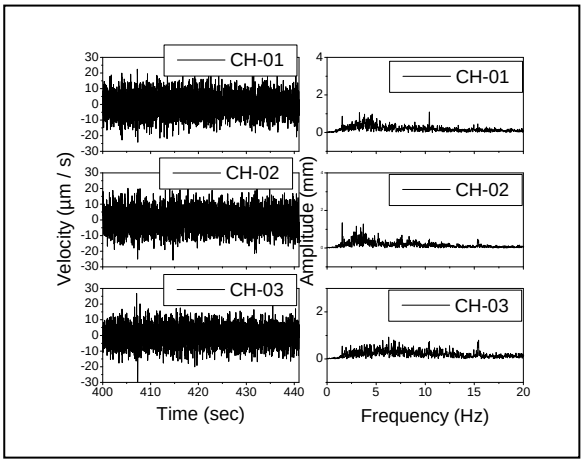

(b)

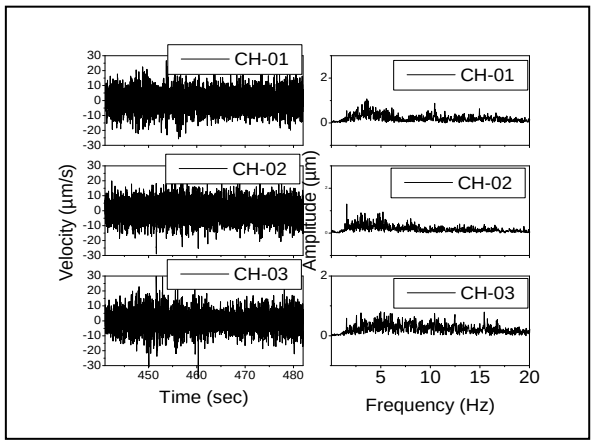

(c)

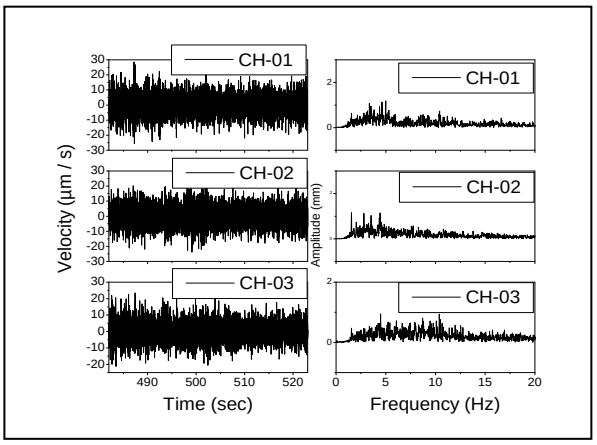

(d)

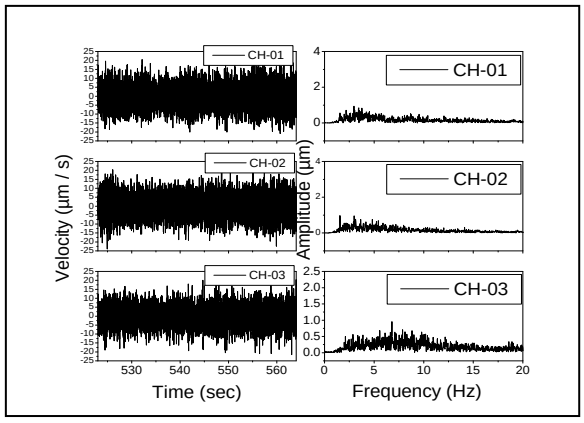

(e)

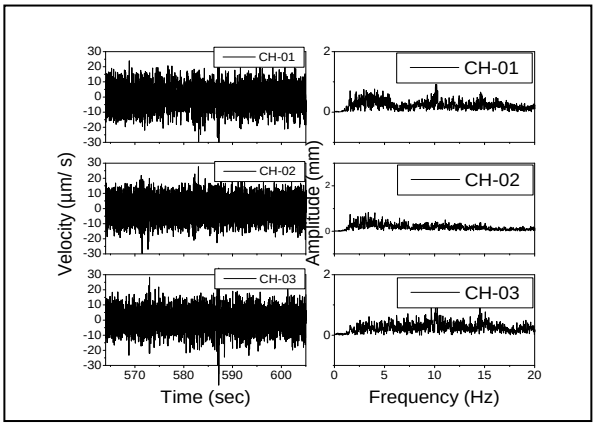

(f)

Figure 3.16 (a) Total time history.(0-1800)sec (b) Segment-1 (400-441)sec (C) Segment-2 (441-482) sec (d) Segment-3 (482-523) sec (e) Segment-4 (523-564) sec and (f) Segment-5 (564-605) sec for Time History and FFT of Microtremor analysis at Police Staff College, Mirpur-Dhaka

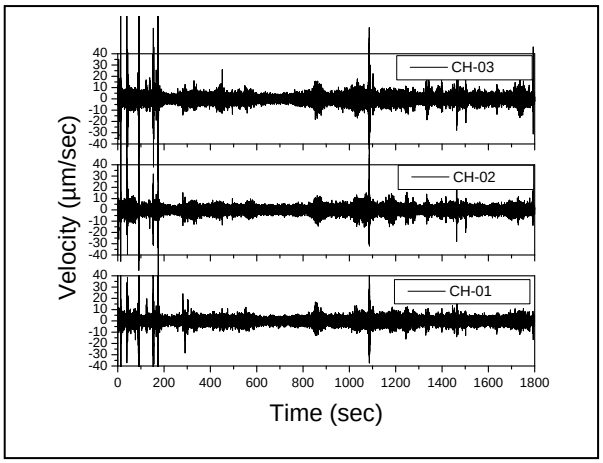

(a)

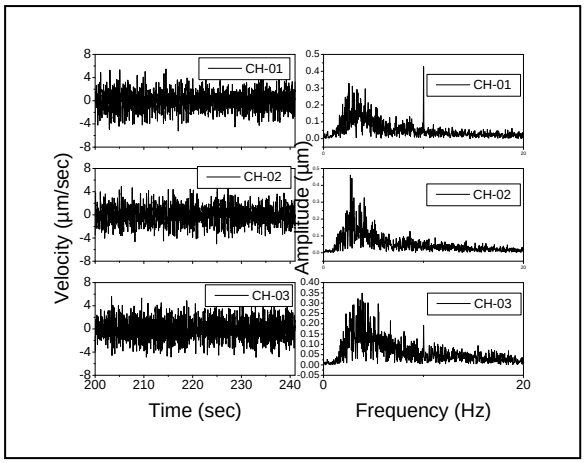

(b)

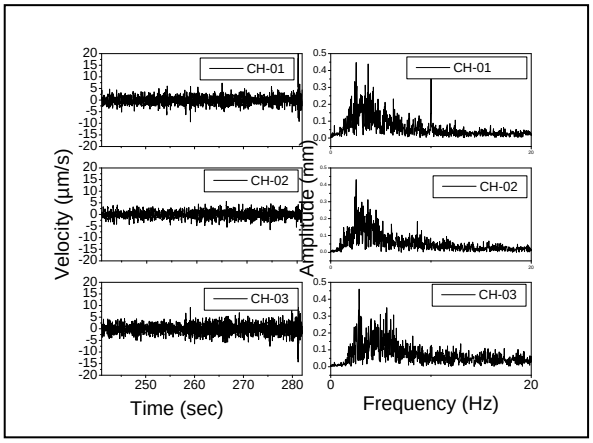

(c)

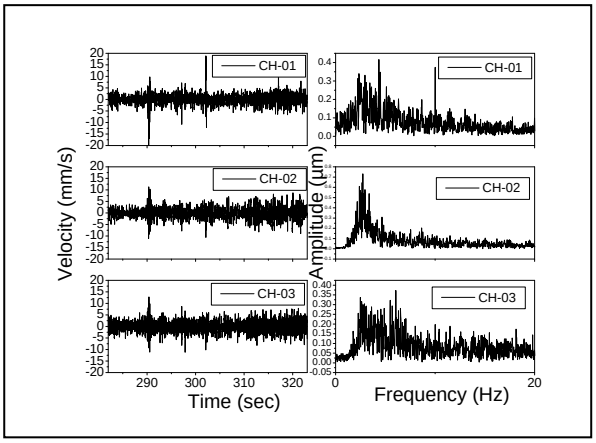

(d)

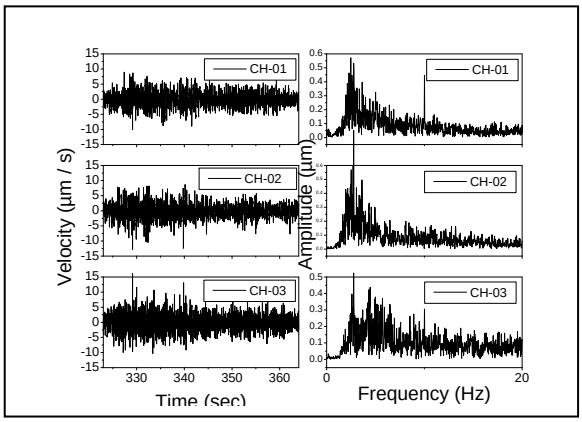

(e)

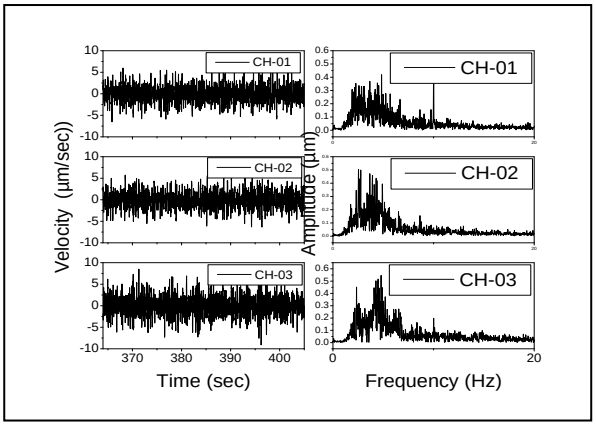

(f)

Figure 3.17 (a) Total time history.(0-1800) sec (b) Segment-1 (200-241) sec (c) Segment-2(241-282) sec (d) Segment-3 (282-323) sec (e) Segment-4 (323-364) sec and (f) Segment-5 (364-405) sec for Time History and FFT of Microtremor analysis at BUET-Campus-Dhaka

3.8 EARTHQUAK DATA ANALYSIS

There are some custom-made softwares that came with the instruments to operate and monitor the whole system. One can also interact with the instruments (i.e., K2s) using the software called Quick Talk and change the settings. Quick Talk and Quick Look may be also used for downloading or viewing the incoming data without any processing. After the sensors were connected, they had to go through the Functionality Test done with the operating software. Then they had to be corrected for any offsets in the readings. Once all of these are done for each of the sensors, the system was ready. It was tested to see if data from all the channels are reaching the recorders, if they are set at real time through GPS. The GPS are set at UTC time as stated in the original documents. The system is such that each of the sensors can be configured separately, but they were kept the same at the beginning. Each sensor can be set to trigger the whole system. The trigger value for the twenty two free-field ground accelerometers was set at 0.5% of g (5 cm/sec^2). Whenever the acceleration exceeds the trigger value, automatic data recording will take place. To process, analyze and interpret the data, the software called Strong Motion Analyzer (SMA) is used. One can perform necessary filtering, corrections and plotting of the signals received from the sensor. Microtremor observation at six locations Bogra, Natore, Jamuna Bridge east side at Serajganj, Police staff college at Mirpur, Haji camp at Ashkona and BUET campus have been selected. This accelerometer gives data in North-South, East-West and Up-Down direction. Then Fourier spectrum ratio (Horizontal to Vertical) for various free field stations are studied and compared.

3.8.1 Time History and Fourier Spectrum analysis of different Earthquake at Selected Locations

Time history and Fourier spectrum in EW, NS and UD direction at different earthquakes analysis at Bogra as shown in Figure 3.18. Similarly analysis at Natore , Jamuna Bridge east side at Sirajganj, Haji-Camp at Ashkona, Police Staff College at Mirpur and BUET-Campus, Dhaka as shown in Figures 3.19 to 3.20

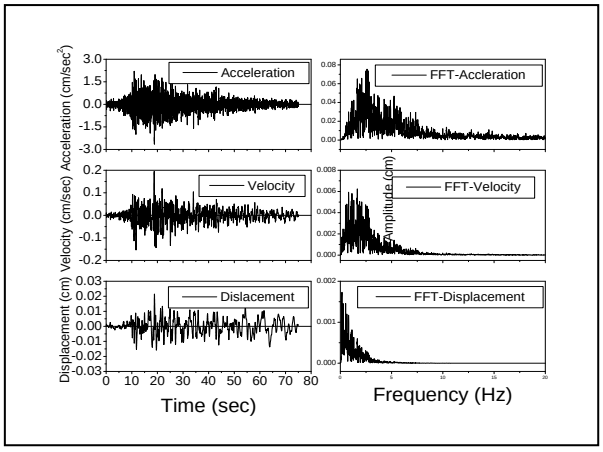

(a) Sikim EQ in Acceleration, Velocity, Displacement and FFT at Bogra.

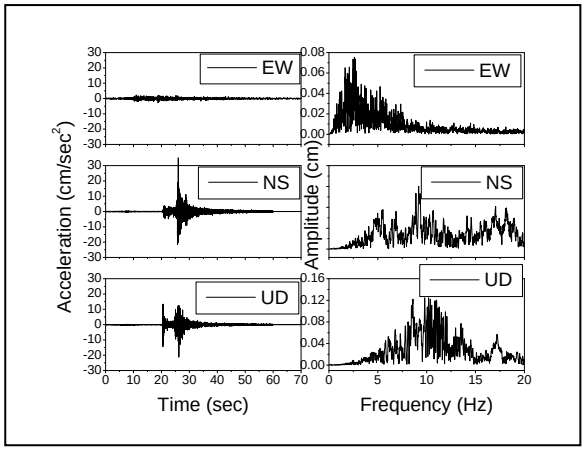

(b) Time history and FFT in the Sikim Earthquake at Bogra LGED office.

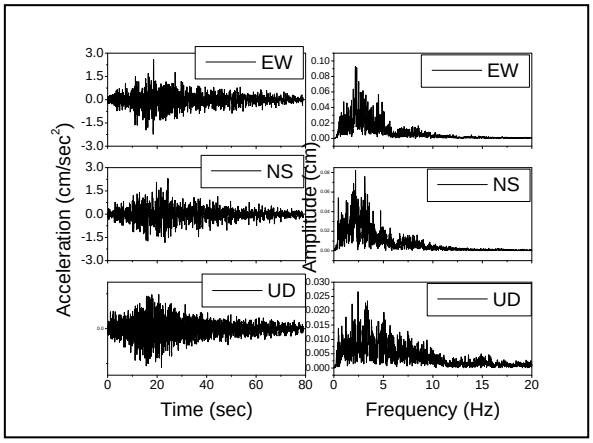

(c) Sikim EQ Natore

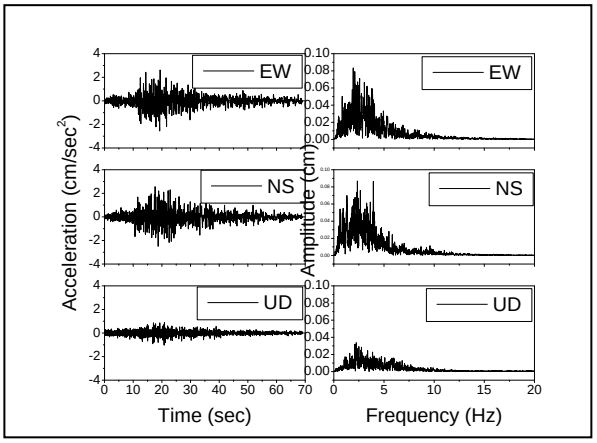

(d) Sikim EQ J.B.East

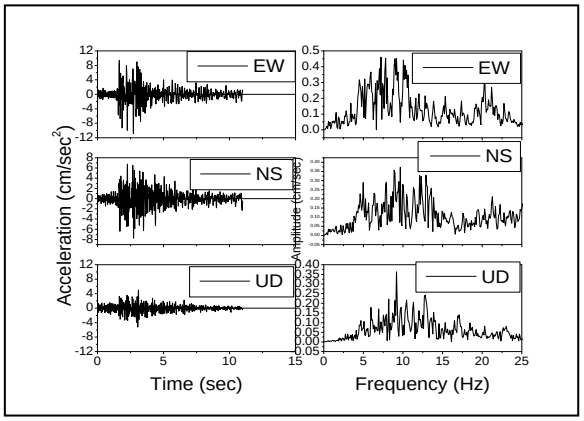

(e) Assam EQ Haji-Camp, Dhaka

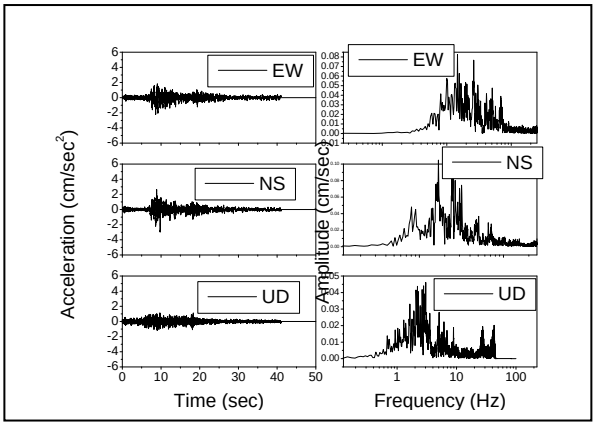

(f) Monipur EQ -BUET, Dhaka

Figure 3.18 Time history and FFT at (a) Sikim EQ in Acceleration, Velocity, Displacement and FFT at Bogra (b) Time history and FFT in the Sikim Earthquake at Bogra LGED office (c) Sikim EQ Natore (d) Sikim EQ Jamuna Bridge East (e) Assam EQ Haji-Camp, Dhaka and (f) Monipur Earthquake at BUET-Campus, Dhaka

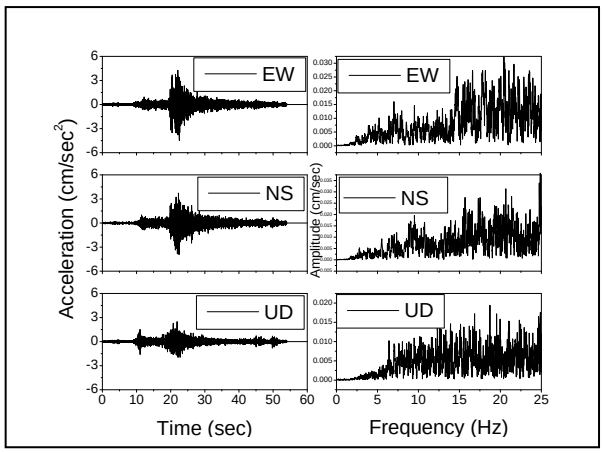

(a) Time history and FFT in the Jessore Earthquake at Bogra LGED office

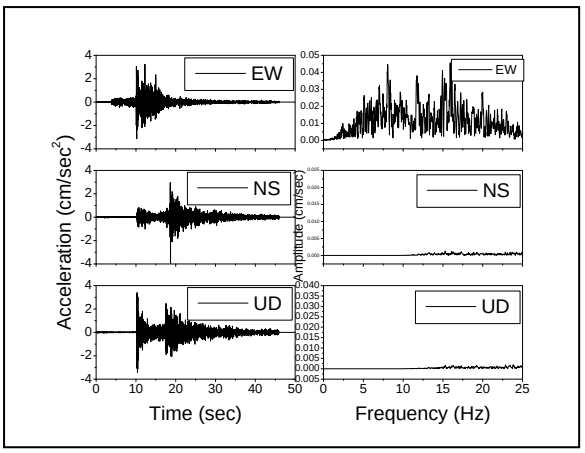

(b) Time history and FFT in the Jessore Earthquake at Natore LGED

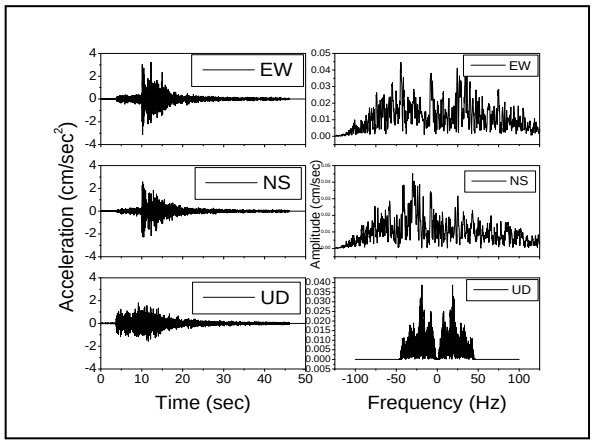

(c) Time history and FFT in the Jessore Earthquake at J.B.East side.

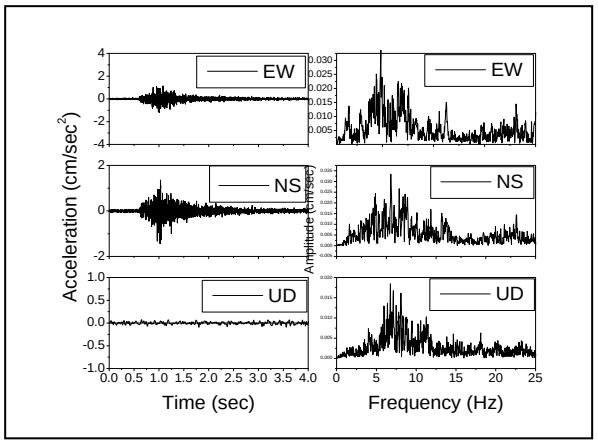

(d) Time history and FFT in the BI-Earthquake at Bogra LGED

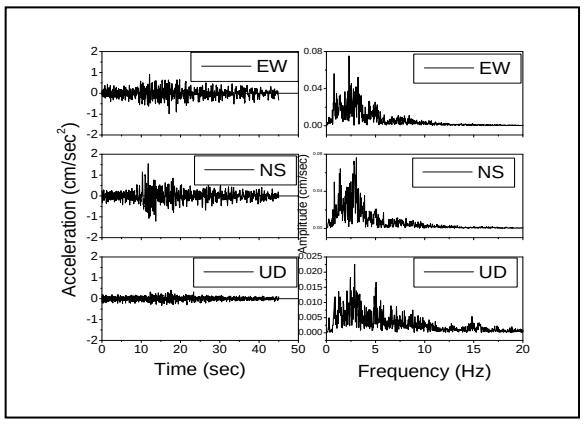

(e) BI- EQ at Natore LGED office

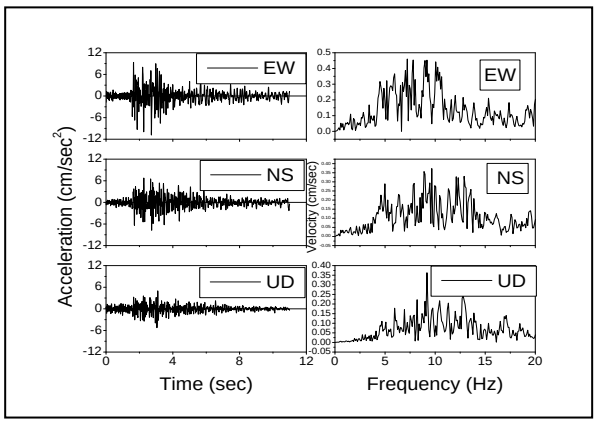

(f) MA-Assam EQ,PSC- Dhaka.

Figure 3.19 Time history and FFT at (a) Jessore Earthquake at Bogra LGED office (b) Jessore Earthquake at Natore LGED office (c) Jessore EQ J.B.East (d) Bhutan-India Earthquake at Bogra LGED office (e) Bhutan-India Earthquake at Natore LGED office and (f) Mynmar-Assam Earthquake at PSC, Dhaka

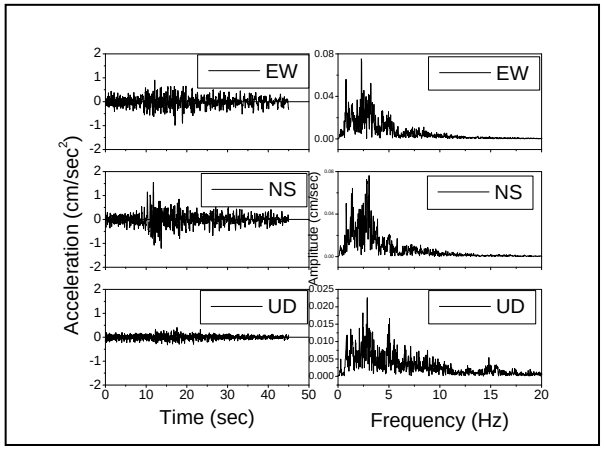

(a) Bhutan-India EQ at Natore LGED office, Natore.

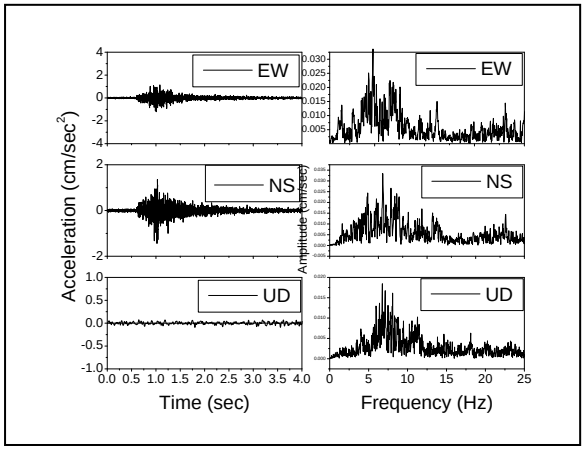

(b) Bhutan-India EQ at Bogra LGED office, Bogra.

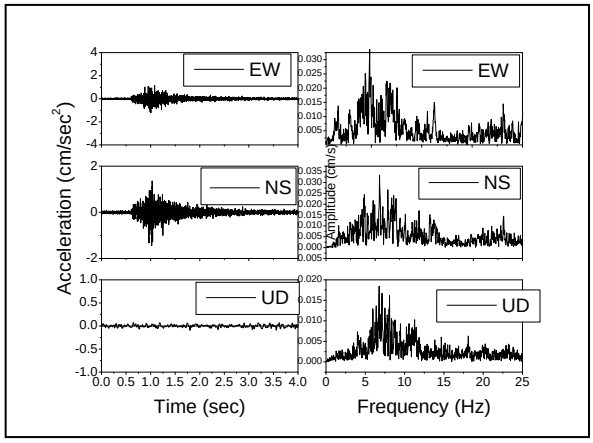

(c) Bhutan-India EQ at police Staff College,Mirpur-Dhaka

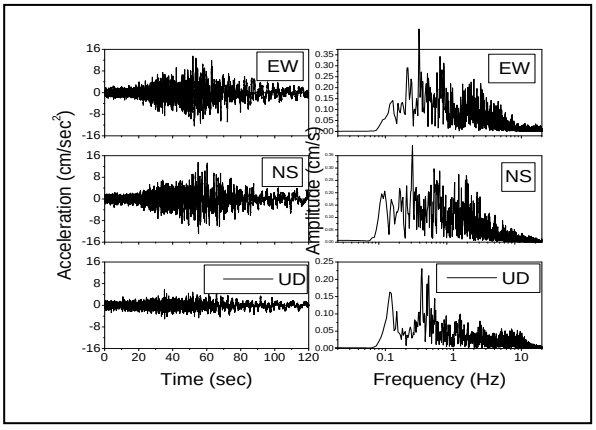

(d) Nepal EQ at Bogra LGED office, Bogra.

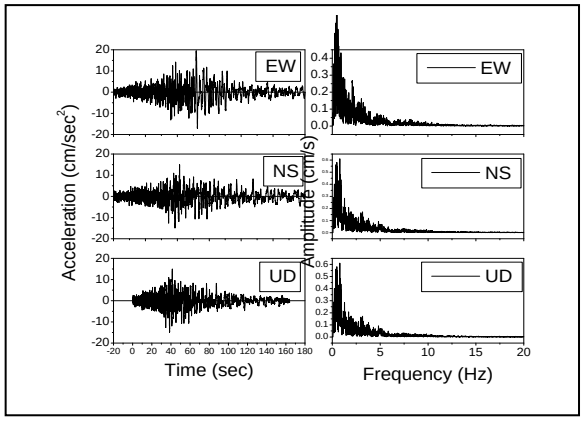

(e) Nepal EQ at Natore LGED office.

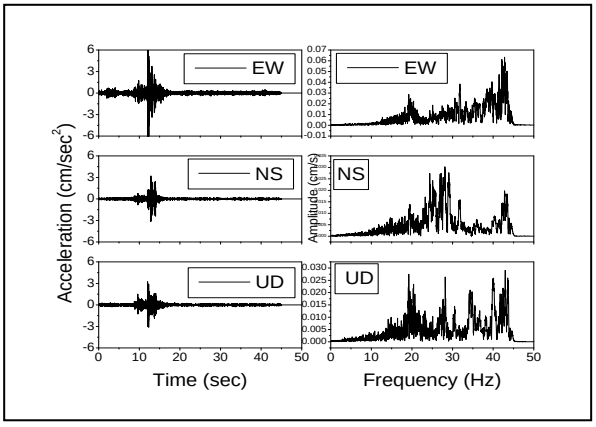

(f) Nepal EQ at BUET, Dhaka.

Figure 3.20 Time history and FFT at (a) Bhutan-India EQ T at Natore LGED office, Natore (b) Bhutan-India EQ at Bogra LGED office, Bogra LGED office (c)) Bhutan-India EQ T at police Staff College,Mirpur-Dhaka (d) Nepal EQ at LGED, Bogra (e) Nepal EQ Natore LGED office and (f) Nepal Earthquake at BUET-Campus, Dhaka

3.9 Stability Check of Microtremor and Earthquake Data

Microtremor is the combination of shear wave, Rayleigh wave and Love wave. The effect of different waves on microtremor data is significant. Therefore, stability check of microtremor data is important to estimate dynamic properties of any site soil. To carry out this research velocity and time history data have been recorded time ranging 30 minutes of six locations. The observation microtremor data recording varies from 0 to 30 minutes. There are five segments each window of 41.0s time domain data has been used to transform frequency domain spectrum. In order to get low noise data these Fourier spectra have been filtered using rectangular windows. The mean of these five segments of time domain data converted to frequency domain data have been calculated using smoothing function with average smoothing point 15 to 60. Mean Fourier spectrum along EW, NS and UD directions have been plotted in logarithmic windows from 0.1 Hz to 20 Hz along predominant frequency and from 0.001μm to 1μm along Fourier amplitude spectrum, respectively. From these observations, stability of microtremor data has been compared from Fourier spectrum. The horizontal to vertical spectral ratio has also been calculated in these locations to analyze the stability of H/V ratio with Fourier spectrum. Both Fourier spectrum and H/V ratio of six selected locations have been included in this section.

3.10 Smoothing Effects of Microtremor and Earthquake

Smoothing of microtremor data has significant effect to estimate predominant frequency and H/V ratio of any particular site. In some microtremor measurement locations, it is difficult to estimate dynamic properties. In that case, smoothing of data with suitable smoothing point gives accurate data. Therefore, almost all the microtremor locations data has been smoothed with suitable smoothing point. Generally, H/V ratio decreases and predominant frequency changes with the increase of smoothing point. So, proper justification is required before applying smoothing point on microtremor logarithmic window. Figure 3.21 to 3.26 show for microtremor and Figure 3.27 to 3.31 show for earthquake data with smoothing effect. Different smoothing points have been applied to determine predominant frequency and H/V ratio. Figure 3.21 shows that the peak H/V becomes decreases due to applying different smoothing point. Figure 3.21, 3.22 and 3.26 illustrate the application of suitable smoothing point to determine Predominant frequency and H/V ratio of soil. It is difficult to determine Predominant frequency of Horizontal Vs Vertical Ratio of Microtremor and Earthquake data analysis at different locations.

3.11 Horizontal versus Vertical Spectral Ratio (HVSR) and Smoothed HVSR analysis of Microtremor and Earthquake at Selected Locations of Bangladesh

This data is shown in logarithmic window in frequency from 0.1 Hz to 20 Hz and in Fourier Spectrum from 0.1 μm to 20 μm. Only the Fourier Spectrum along three subsequent directions is not appropriate to estimate the predominant frequency and amplification. So, Horizontal to Vertical spectral ratio (H/V) is required to determine the dynamic properties of soil. Horizontal to Vertical Spectral Ratio (HVSR) is determined dividing by Fourier Spectrum of UD direction to the Fourier Spectrum of EW or NS direction. H/V ratio analysis at Bogra as shown in Figure 3.21. Similarly at Natore, Jamuna Bridge Seast side at Sirajganj, Haji-Camp at Ashkona, Police Staff College at Mirpur and BUET-Campus, Dhaka as shown in Figures 3.22 to 3.26

On other hand, average HVSR and smoothed HVSR analysis of microtremor and earthquake analysis as shown in Figure 3.27 at Bogra. Similarly Similarly at Natore, Jamuna Bridge Seast side at Sirajganj, Haji-Camp at Ashkona, Police Staff College at Mirpur and BUET-Campus, Dhaka as shown in Figures 3.28 to 3.31

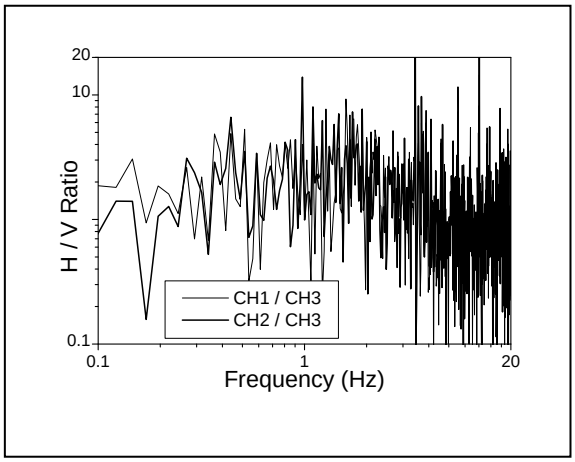

(a) Segment 1: (0-41) Sec

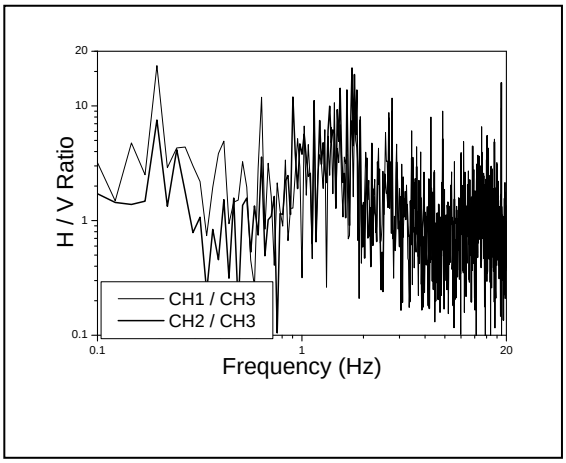

(b) Segment 2: (41-82) Sec

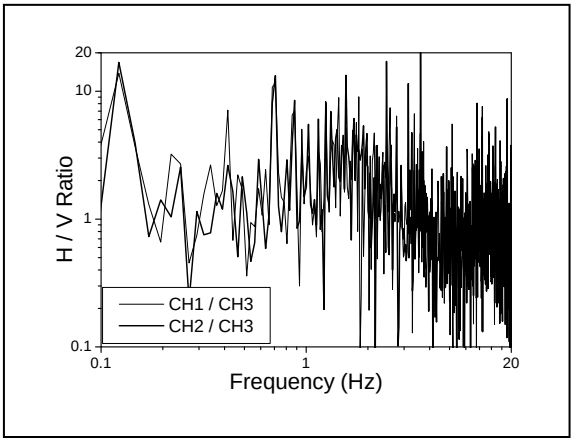

(c) Segment 3: (82-123) Sec

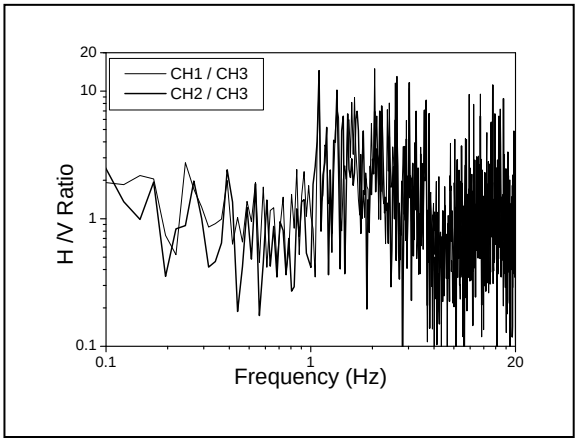

(d) Segment 4: (123-164) Sec

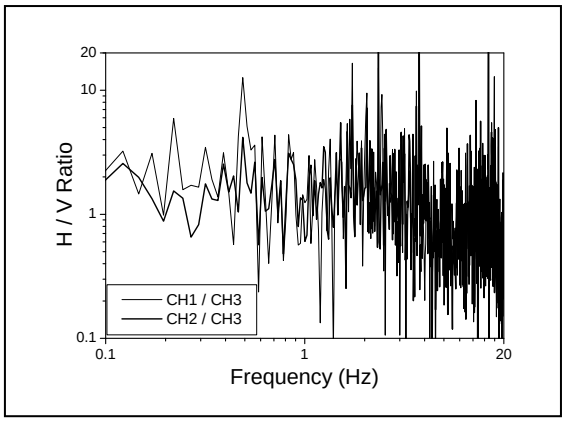

(e) Segment 5: (164-205) Sec

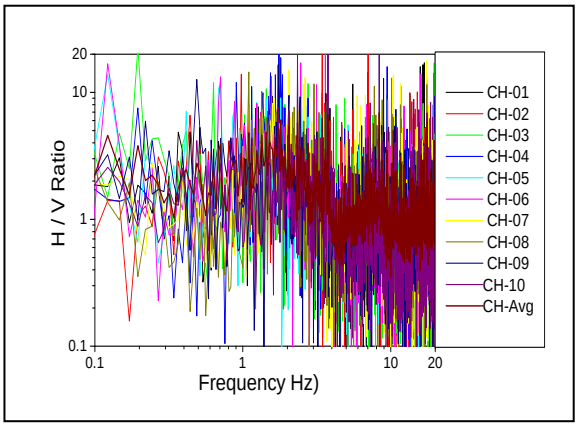

(f) Combined H/ V Ratio at Bogra

Figure 3.21 H / V Ratio of Microtremor analysis at Bogra LGED office in (a) Segment 3: (82-123) Sec (b) Segment 2: (41-82) Sec (c) Segment 3: (82-123) Sec (d) Segment 4: (123-164) Sec (e) Segment 5: (164-205) Sec. and (f) Combined H/ V Ratio at Bogra

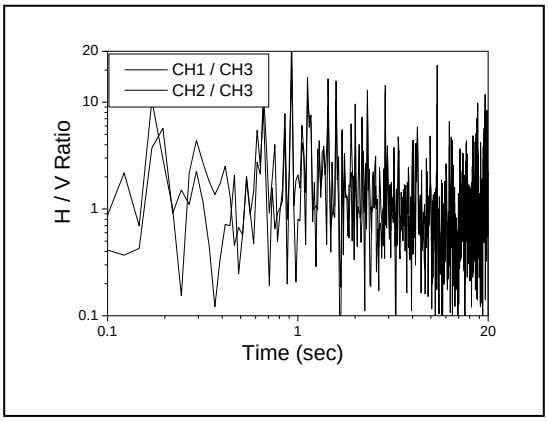

(a) Segment 1: (200-241) Sec

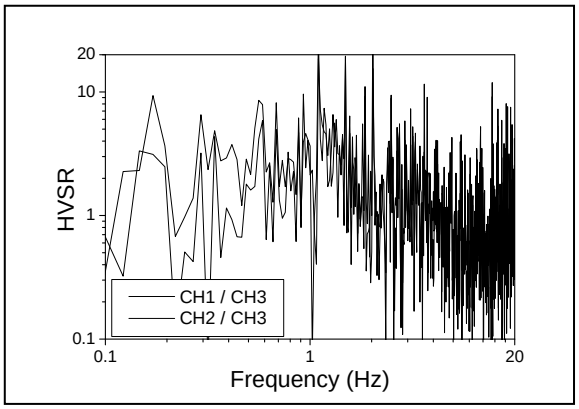

(b) Segment 2: (241-282) Sec

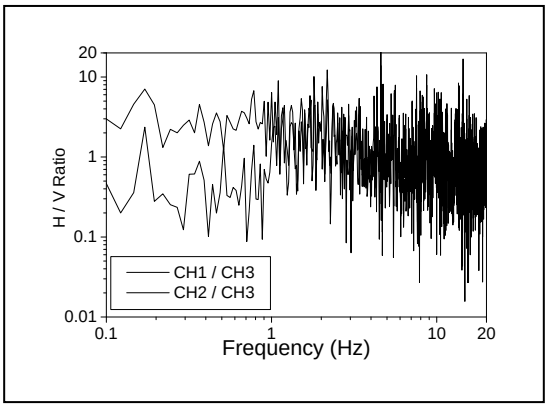

(c) Segment 3: (282-323) Sec

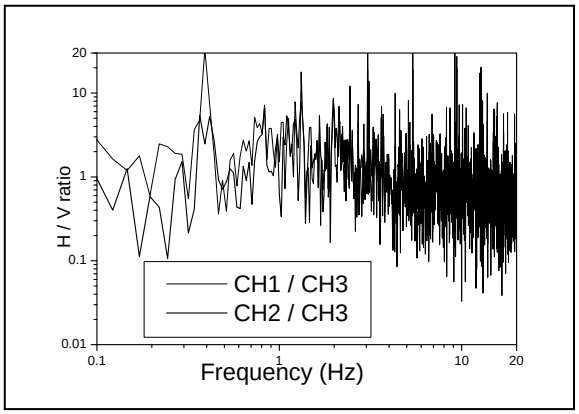

(d) Segment 4: (323-364) Sec

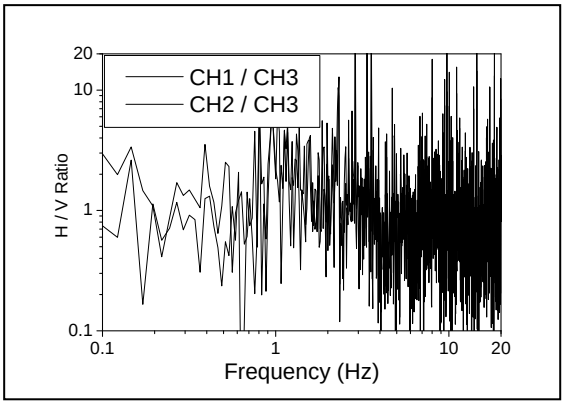

(e) Segment 5: (364-405) Sec

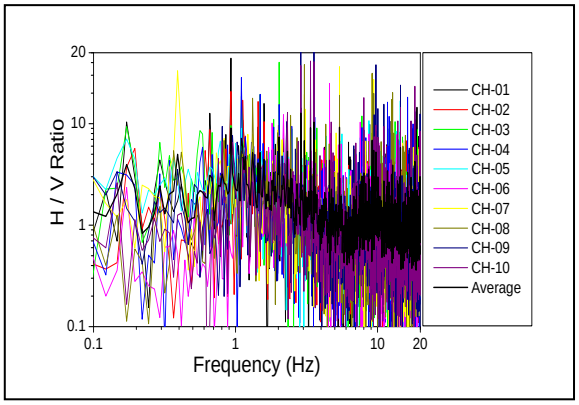

(f) Combined H/ V Ratio at Natore

Figure 3.22 H / V Ratio of Microtremor analysis at Natore LGED office in (a) Segment 1: (200-241) Sec (b) Segment 2: (241-282) Sec (C) Segment 3: (282-323) Sec (d) Segment 4: (323-364) Sec (e) Segment 5: (364-205) Sec. and (f) Combined H/ V Ratio at Natore

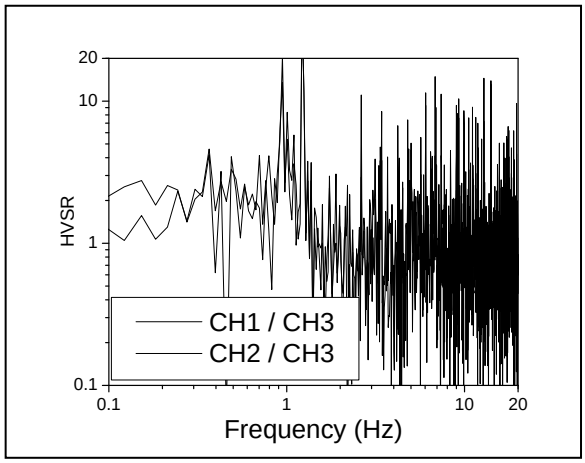

(a) Segment 1: (200-241) Sec

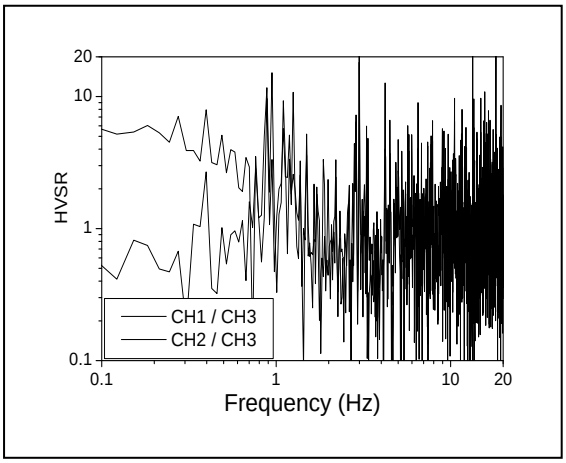

(b) Segment 2: (241-282) Sec

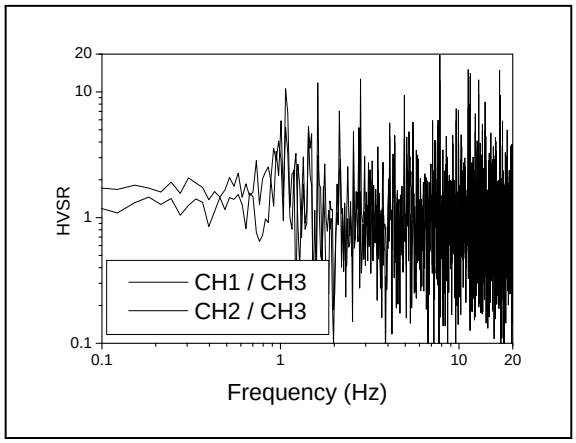

(c) Segment 3: (282-323) Sec

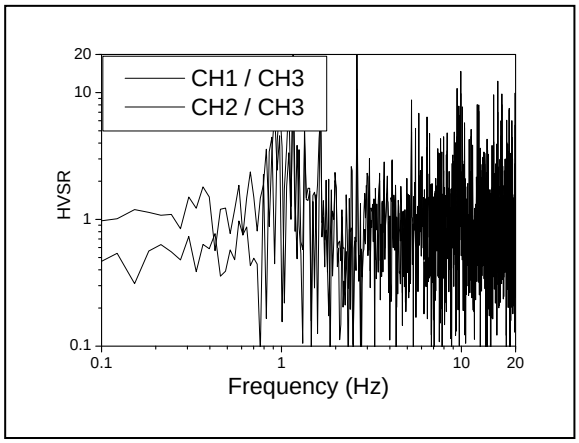

(d) Segment 4: (323-364) Sec

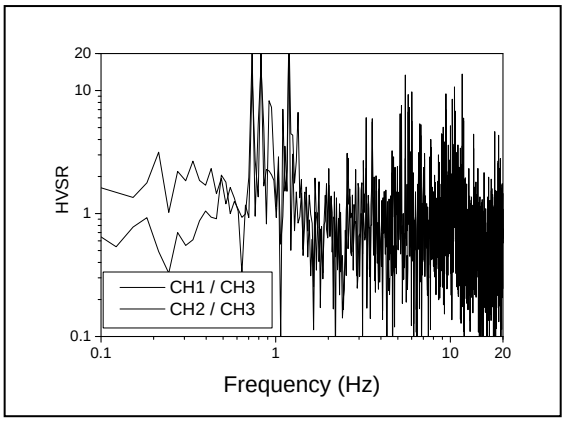

(e) Segment 5: (364-405) Sec

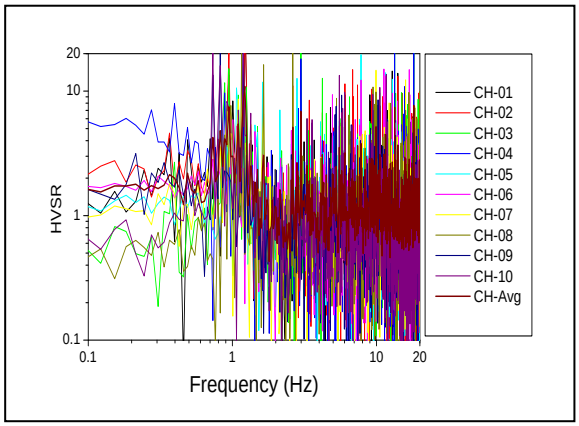

(f) Combined H/ V Ratio at J.B.East side

Figure 3.23 H / V Ratio of Microtremor analysis at Jamuna Bridge East side in (a) Segment 1: (200-241) Sec (b) Segment 2: (241-282) Sec (c) Segment 3: (282-323) Sec (d) Segment 4: (323-464) Sec (e) Segment 5: (464-405) Sec. and (f) Combined H/ V Ratio at Jamuna Bridge East Site

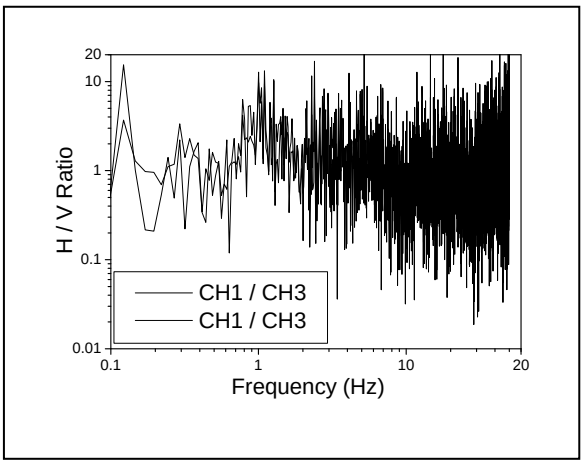

(a) Segment 1: (900-941) Sec

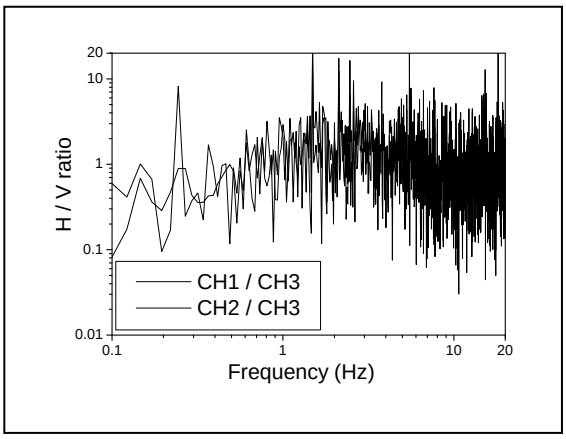

(b) Segment 2: (941-982) Sec

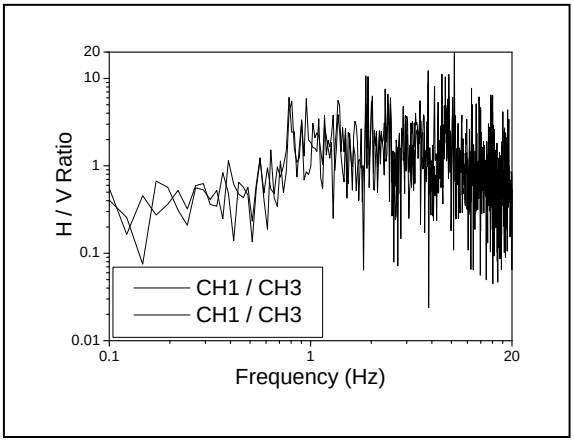

(c) Segment 3: (982-1023) Sec

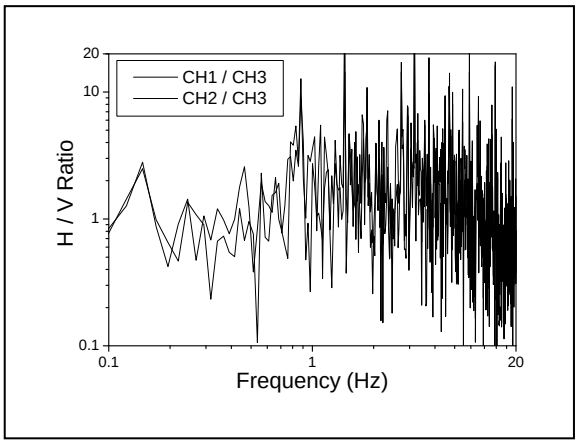

(d) Segment 4: (1023-1064) Sec

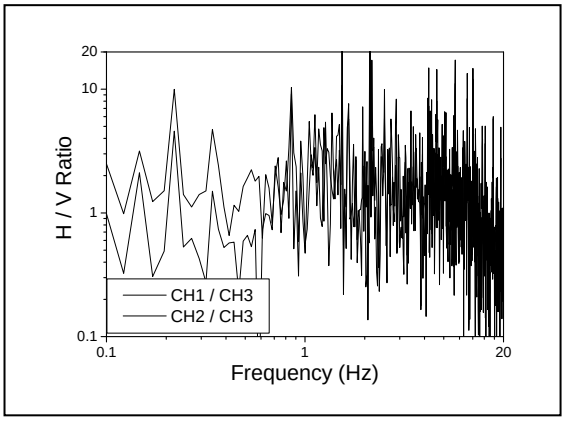

(e) Segment 5: (1064-1105) Sec

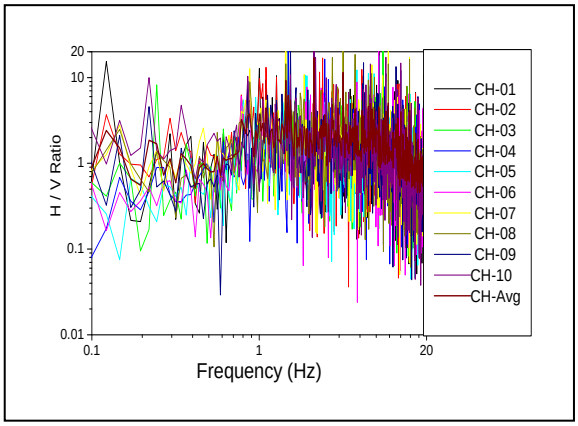

(f) Combined H/ V Ratio at Haji-Camp, Dhaka

Figure 3.24 H / V Ratio of Microtremor analysis at Haji-Camp in (a) Segment 1: (900-941) Sec (b) Segment 2: (941-982) Sec (C) Segment 3: (982-1023) Sec (d) Segment 4: (1023-1064) Sec (e) Segment 5: (1064-1105) Sec. and (f) Combined H/ V Ratio at Airport Haji-Camp, Dhaka

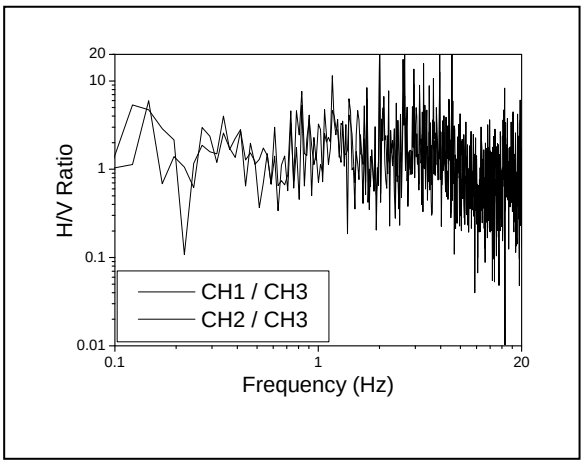

(a) Segment 1: (400-441) Sec

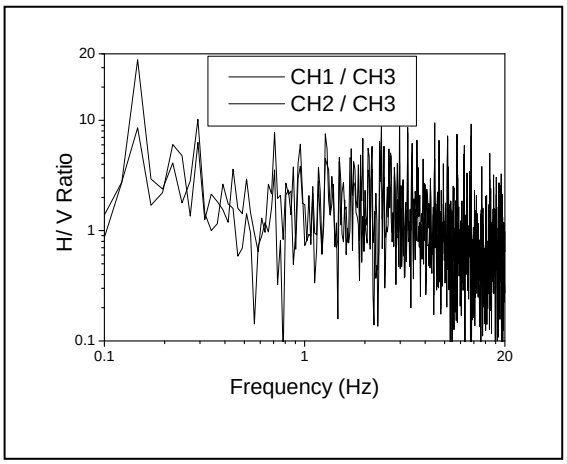

(b) Segment 2: (441-482) Sec

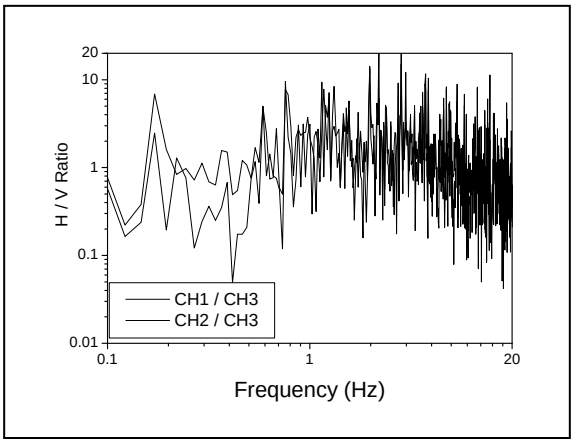

(c) Segment 3: (482-523) Sec

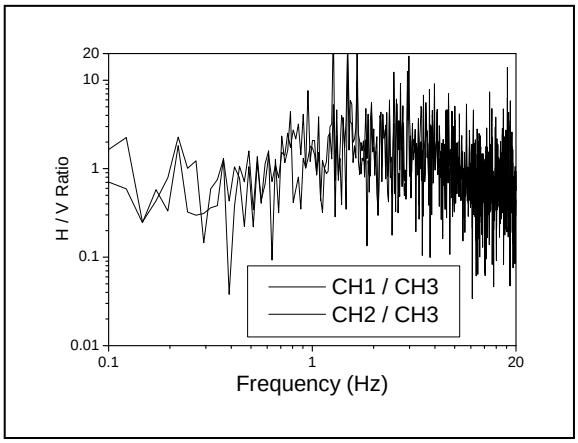

(d) Segment 4: (523-564) Sec

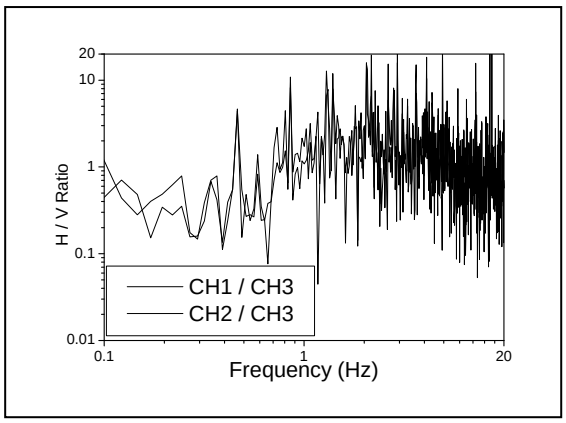

(e) Segment 5: (564-605) Sec

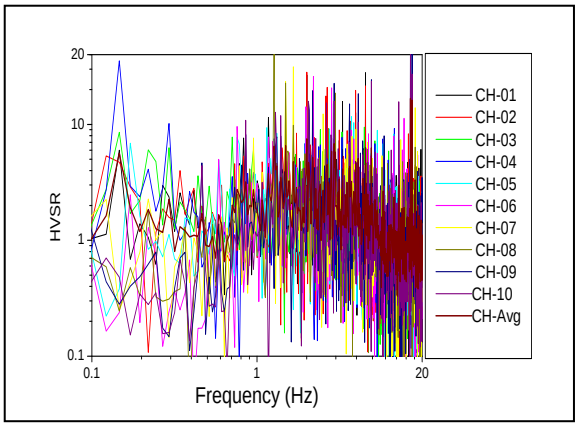

(f) Combined H/ V Ratio at P.S.C, Dhaka

Figure 3.25 H / V Ratio of Microtremor analysis at PSC in (a) Segment 1: (400-441) Sec (b) Segment 2: (441-482) Sec (C) Segment 3: (482-523) Sec (d) Segment 4: (523-564) Sec (e) Segment 5: (564-605) Sec and (f) Combined H/ V Ratio at police Staff College, Mirpur-Dhaka

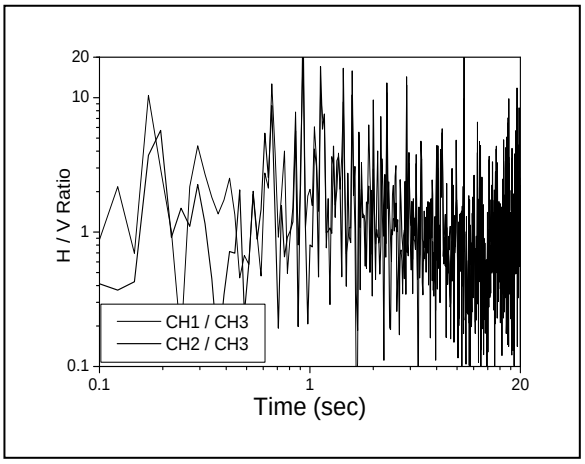

(a) Segment 1: (200-241) Sec

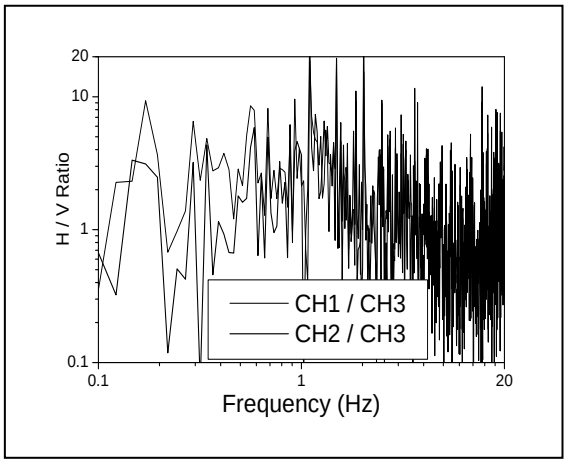

(b) Segment 2: (241-282) Sec

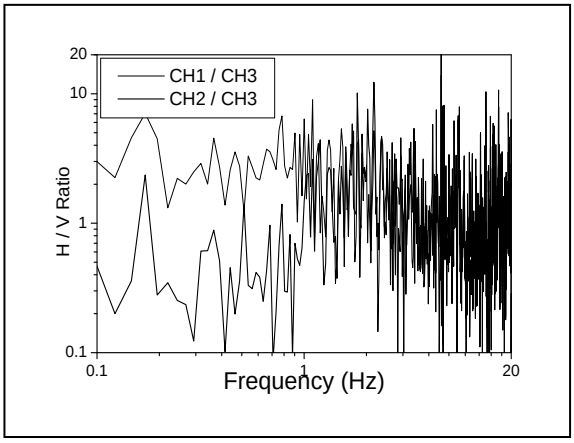

(a) Segment 3: (282-323) Sec

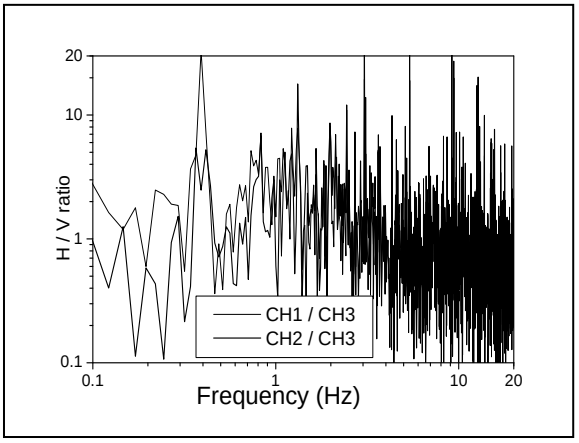

(d) Segment 4: (323-364) Sec

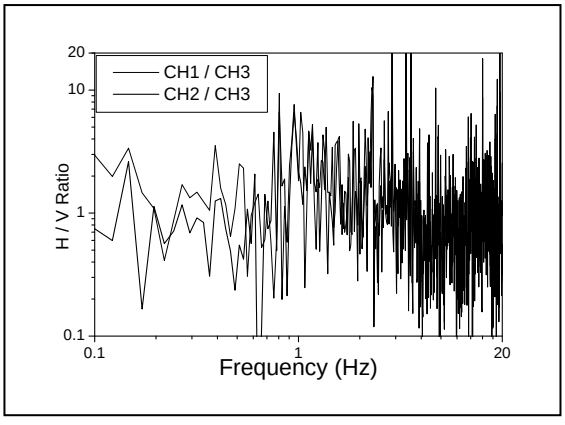

(e) Segment 5: (364-405) Sec

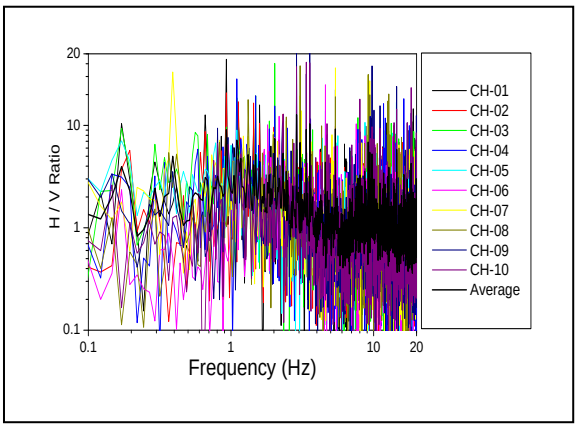

(f) Combined H/ V Ratio at BUET, Dhaka

Figure 3.26 H / V Ratio of Microtremor analysis at BUET in (a) Segment 3: (200-241) Sec (b) Segment 2: (241-282) Sec (C) Segment 3: (282-323) Sec (d) Segment 4: (323-364) Sec (e) Segment 5: (364-405) Sec and (f) Combined H/ V Ratio at BUET-Campus, Dhaka

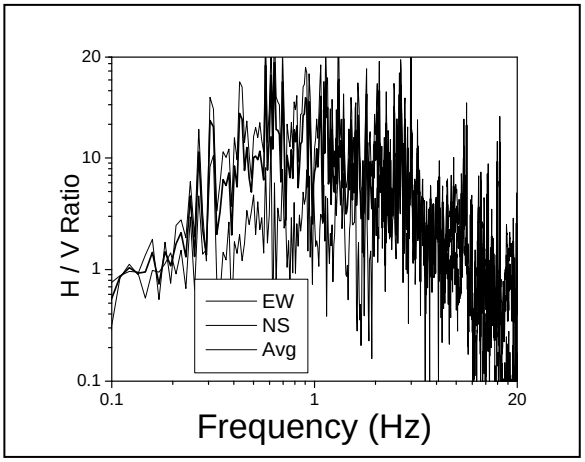

(a) EW, NS and Average HVSR at Bogra

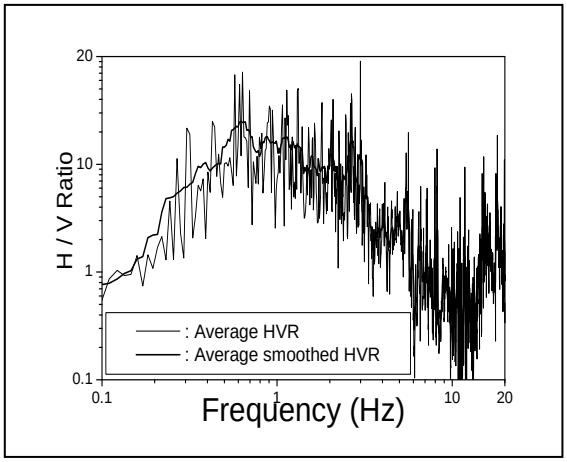

(b) Average and smoothed HVSR at Bogra

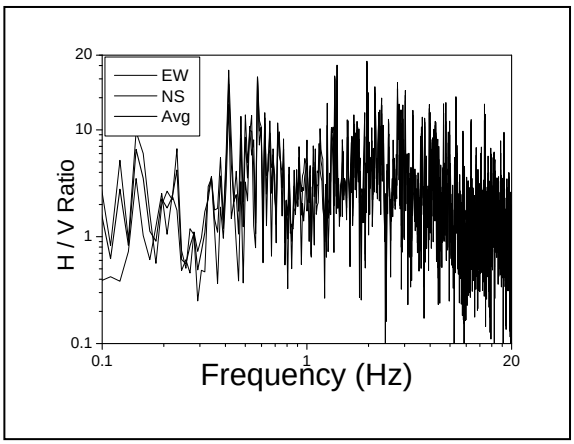

(c) ES, NS and Average HVSR at Natore

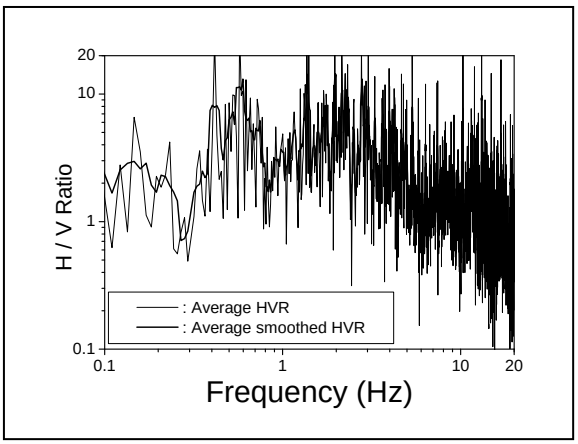

(d) Average and smoothed HVSR at Natore

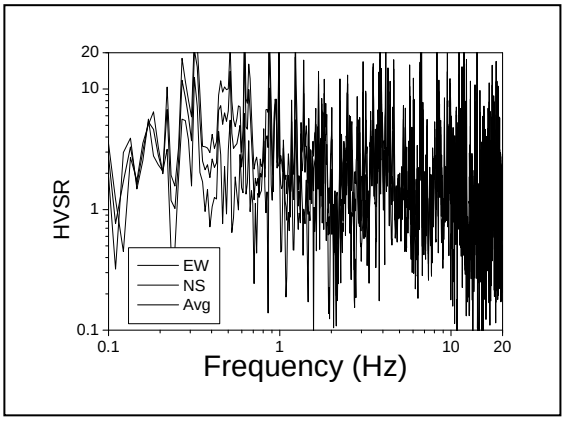

(e) EW, NS and Average HVSR at BUET

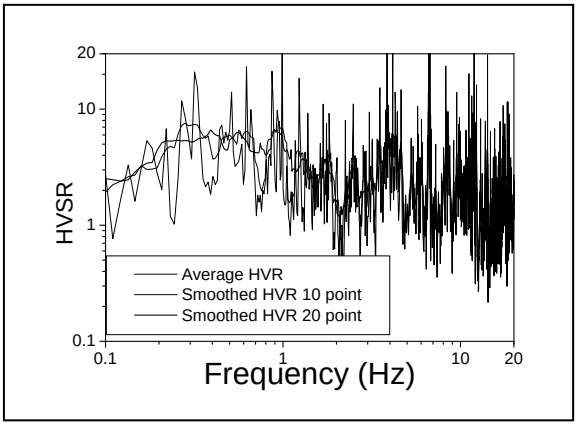

(f) Average and smoothed HVSR at BUET

Figure 3.27 H/ V Ratio and smoothed HVSR analysis of Sikim Earthquake analysis at (a) EW, NS and Average HVSR at Bogra (b) Average and smoothed HVSR at Bogra (c) ES, NS and Average HVSR at Natore (d) Average and smoothed HVSR at Natore (e) EW, NS and Average HVSR at BUET (f) Average and smoothed HVSR at BUET-Dhaka

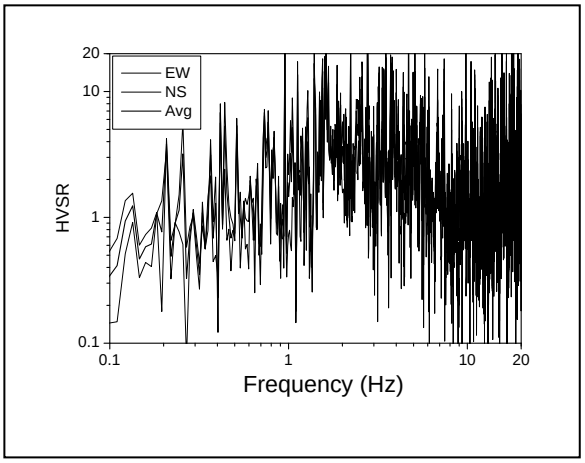

(a) EW, NS and Average HVSR at Bogra

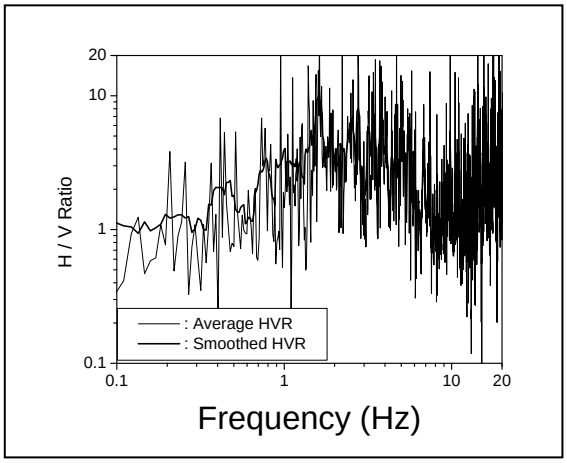

(b) Average and smoothed HVSR at Bogra

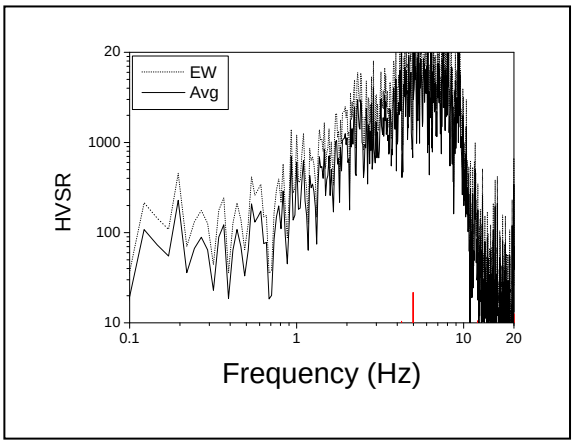

(c) ES, NS and Average HVSR at Natore

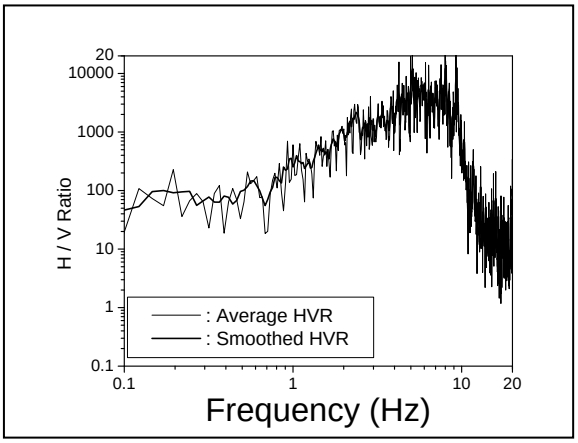

(d) Average and smoothed HVSR at Natore

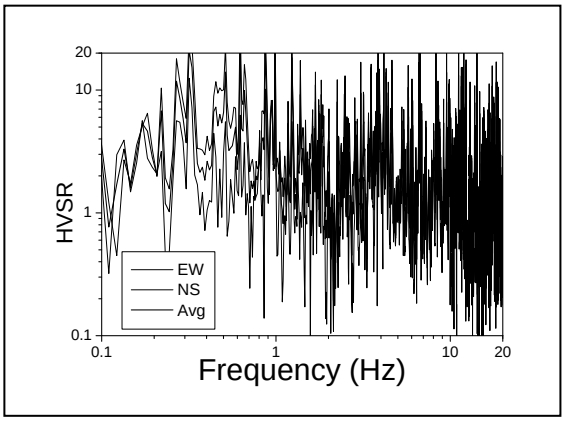

(e) EW, NS and Average HVSR at BUET

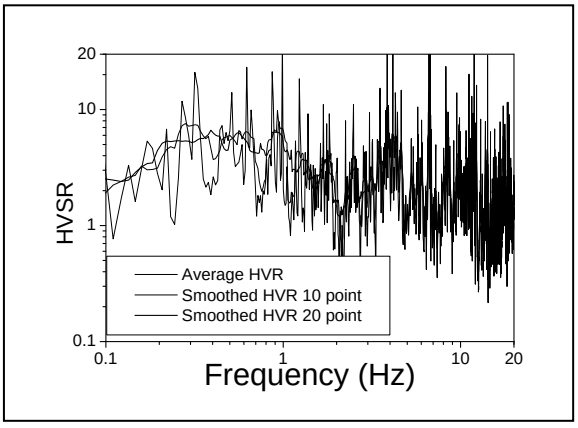

(f) Average and smoothed HVSR at BUET

Figure 3.28 H/ V Ratio and smoothed HVSR analysis of Jessore Earthquake at (a) EW, NS and Average HVSR at Bogra (b) Average and smoothed HVSR at Bogra (c) ES, NS and Average HVSR at Natore (d) Average and smoothed HVSR at Natore (e) EW, NS and Average HVSR at BUET (f) Average and smoothed HVSR at BUET

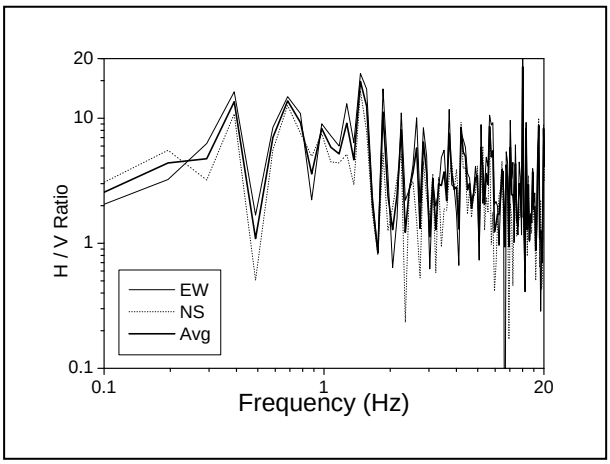

(a) EW, NS and Average HVSR at PSC,Dhaka

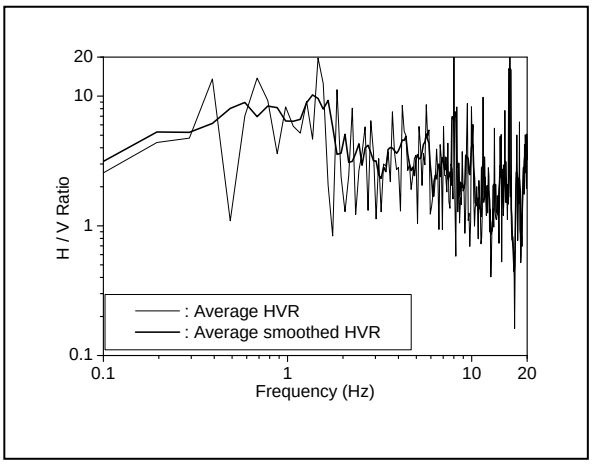

(b) Average and smoothed HVSR at PSC,Dhaka

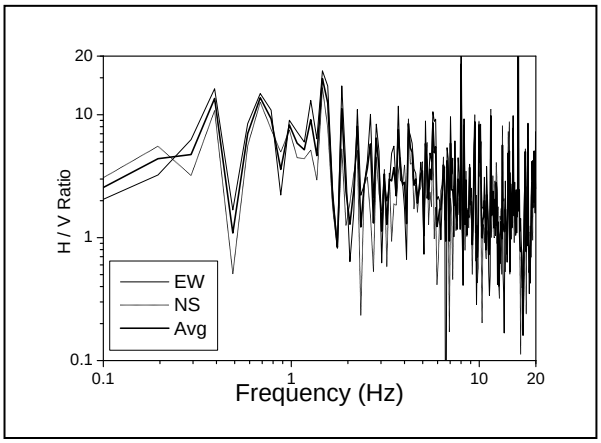

(c) ES, NS and Average HVSR at Haji-Camp

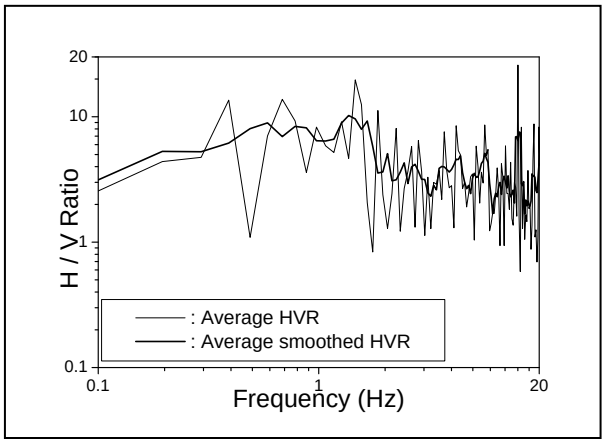

(d) Average and smoothed HVSR at Haji-Camp

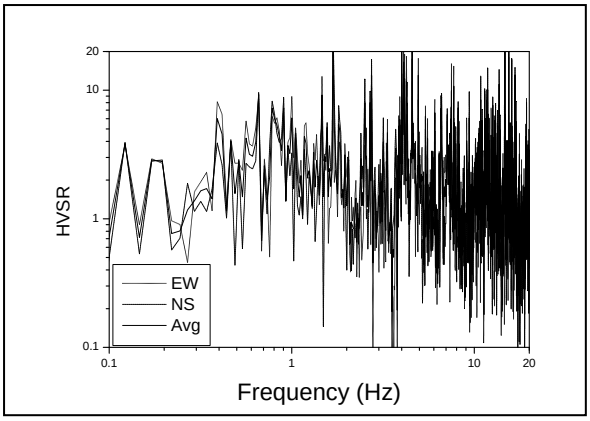

(e) EW, NS and Average HVSR at BUET

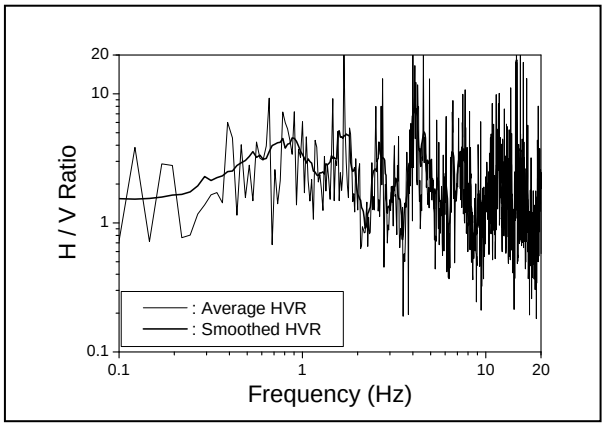

(f) Average and smoothed HVSR at BUET

Figure 3.29 H/ V Ratio and smoothed HVSR analysis of Assam-India and Myanmar-Assam Earthquake analysis at (a) H/ V Ratio at PSC, Mirpur (b) Average and smoothed HVSR at PSC, Mirpur (C) H/ V Ratio at Haji-Camp (d) Average and smoothed HVSR at Haji-Camp (e) H/ V Ratio at BUET (f) Average and smoothed HVSR at BUET, Dhaka

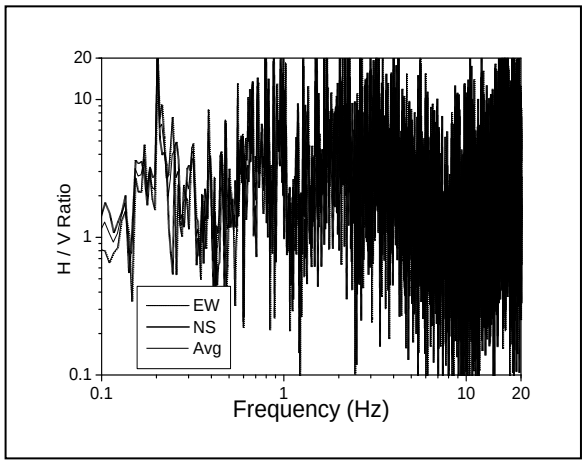

(a) EW, NS and Average HVSR at Bogra

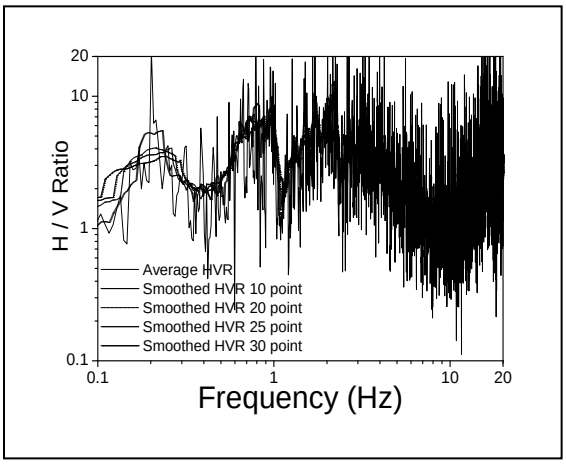

(b) Average and smoothed HVSR at Bogra

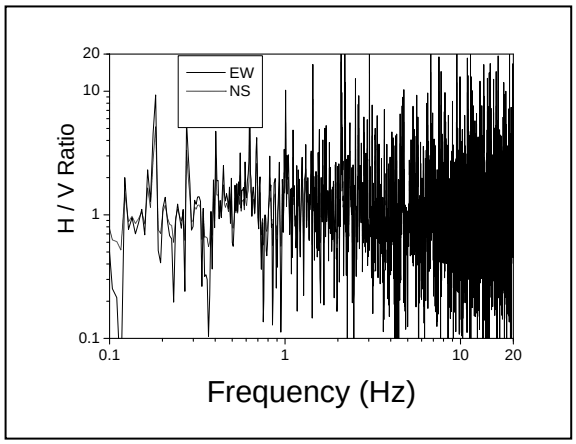

(c) ES, NS and Average HVSR at Natore

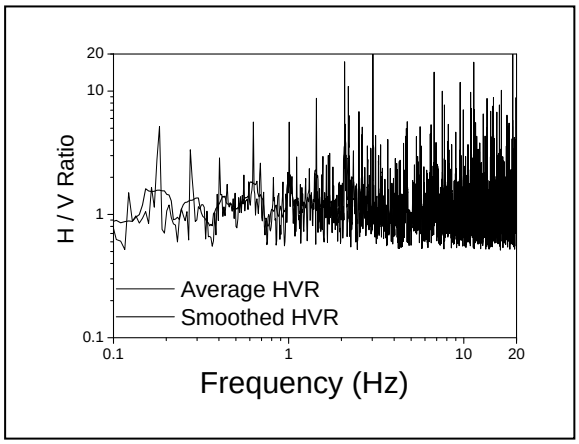

(d) Average and smoothed HVSR at Natore

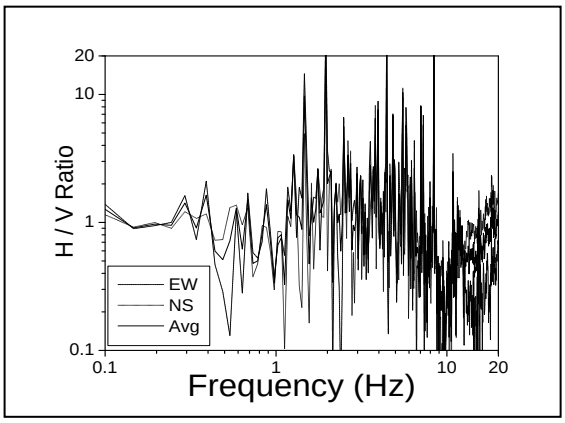

(e) EW, NS and Average HVSR at PSC

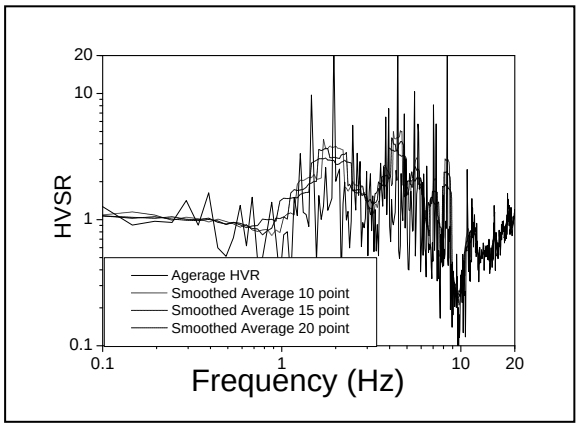

(f) Average and smoothed HVSR at PSC

Figure 3.30 H/ V Ratio and smoothed HVSR analysis of Nepal Earthquake at (a) EW, NS and Average HVSR at Bogra (b) Average and smoothed HVSR at Bogra (c) ES, NS and Average HVSR at Natore (d) Average and smoothed HVSR at Natore (e) EW, NS and Average HVSR at PSC (f) Average and smoothed HVSR at PSC, Mirpur-Dhaka

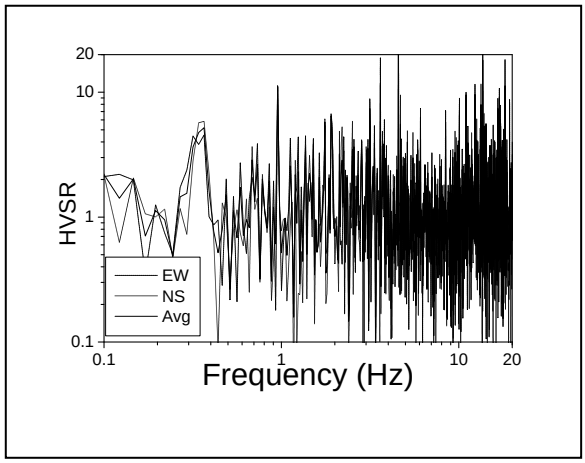

(a) EW, NS and Average HVSR at BUET

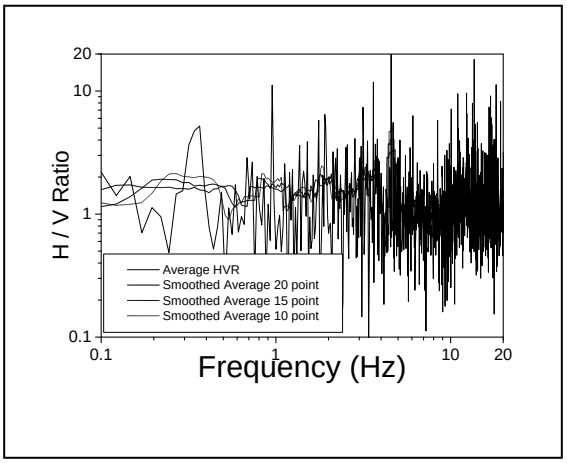

(b) Average and smoothed HVSR at BUET

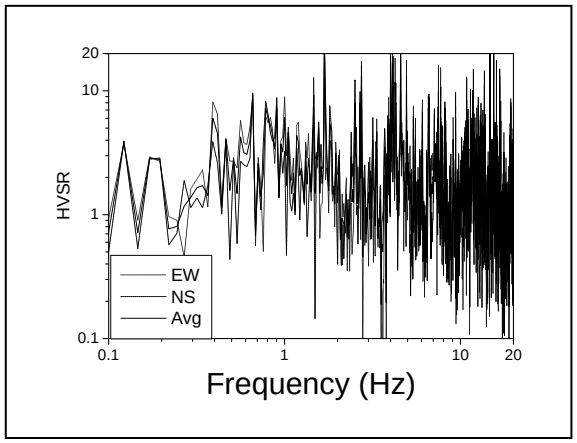

(c) ES, NS and Average HVSR at BUET

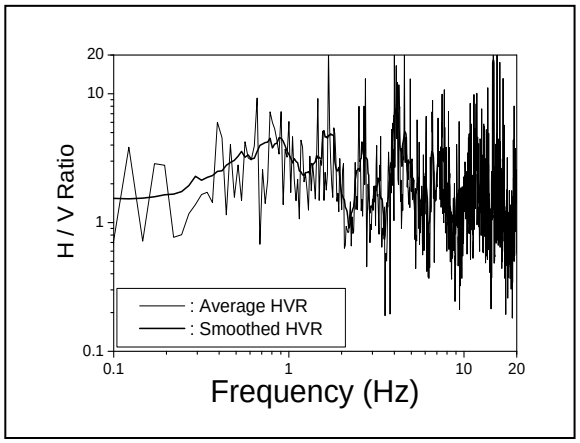

(d) Average and smoothed HVSR at BUET

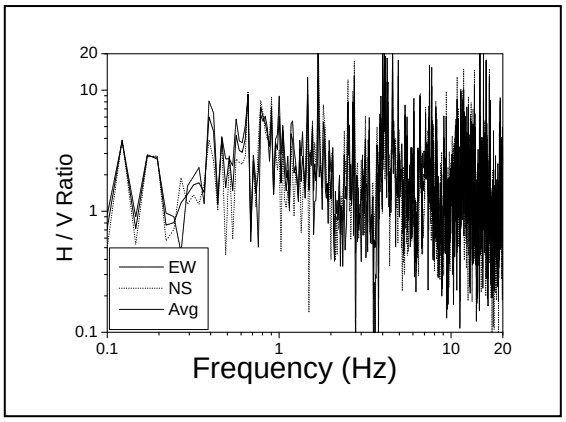

(e) EW, NS and Average HVSR at BUET

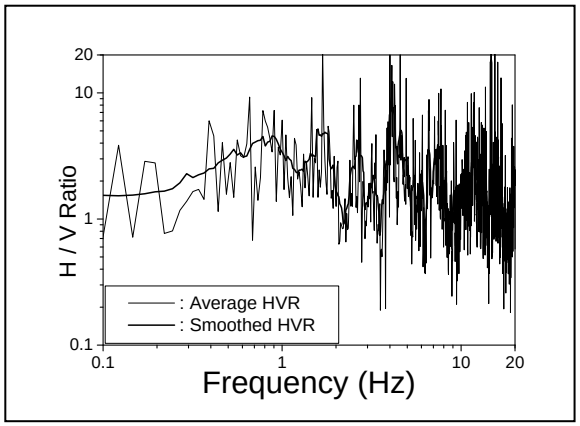

(f) Average and smoothed HVSR at BUET

Figure 3.31 H/ V Ratio and smoothed HVSR analysis of Nepal, Monipur-India and Mynmar-Assam Earthquake analysis at (a) EW, NS and Average at BUET (b) Average and smoothed average HVR at BUET (c) EW, NS and Average at BUET (d) Average and smoothed average HVR at BUET (e) EW, NS and Average at BUET (f) Average and smoothed average HVR at BUET-Dhaka

3.12 SUMMARY

Chapter three is the main body of this research which shows the data collection and analysis result of microtremor and earthquake for selected locations. The characteristics of soil of the investigated locations have been explained also. The shear wave velocity estimated by various empirical correlations has been illustrated. The comparison between shear wave velocity at these locations and the correlated shear wave velocity has been presented in tabular form.

The stability of microtremor data at six different locations has been demonstrated. Fourier spectra and horizontal to vertical (H/V) ratio data has been illustrated in these locations. From this research, it has been found that microtremor and earthquake H/V ratio data is more stable than Fourier spectra in soil at the investigated points. Due to this inference, microtremor and earthquake H/V technique has been applied at selected locations. The effects various factors on microtremor and earthquake result have been demonstrated in this chapter. Five smoothing function have been applied on the microtremor and earthquake H/V ratio and show the effects of smoothing. From these comparision, it has been found that smoothing function has significant effect on the final microtremor and earthquake results.

CHAPTER FOUR

COMPARISON OF MICROTREMOR AND EARTHQUAKE GROUND MOTION ANALYSIS

4.1 GENERAL

Use of Microtremor and Earthquakes data to estimate predominant frequency and H/V ratio of any particular site has been illustrated in Chapter 3. These parameters may be used to assess the response of site soil due to any seismic activities. This chapter provides comparison of these two ratios for microtremor and earthquake data in six locations namely Bogra, Natore, Jamuna Bridge east side at Serajganj, Police staff college at Mirpur, Haji camp at Ashkona and BUET campus have been selected. In these locations from SPT-N value and Microtremor Array data were used and shear-wave velocity has been estimated. Seismic vulnerability index (Kg) for soils has also been estimated using Nakamura (2000) at selected locations.

4.2 COMPARISON OF MICROTREMOR AND EARTHQUAKE GROUND MOTION

Comparison between predominant frequency and average smoothed H/V ratio of microtremor and earthquakes at selected locations Bogra are shown in Figure 4.1 and Table 4.1. Similarly for Natore, Jamuna Bridge East at Sirajganj, Haji-Camp at Ashkona, Police Staff College at Mirpur and BUET-Campus those values as shown in Figures 4.2 to 4.6 and Tables 4.2 to 4.6.

The amplitude ratio of earthquake is similar to microtremor H/V ratio. However, peak H/V of earthquake have been moved into left side and slightly upwards with respect to microtremor. The predominant frequency of microtremor is 1.68 Hz and H/V ratio is 3.36. On other hand predominant frequency of EQ1 is 0.82 Hz and EQ2 is 5.06 Hz and it has been moved into left side and its amplitude slightly upwards with respect to microtremor. And also predominant frequency of EQ3 is 1.57 Hz and EQ4 is 0.83 Hz and

it has been moved into right side and its amplitude slightly upwards with respect to microtremor. The predominant frequency and H/V ratio of microtremor and earthquake at Bogra are shown in Figure 4.1 and Table 4.1

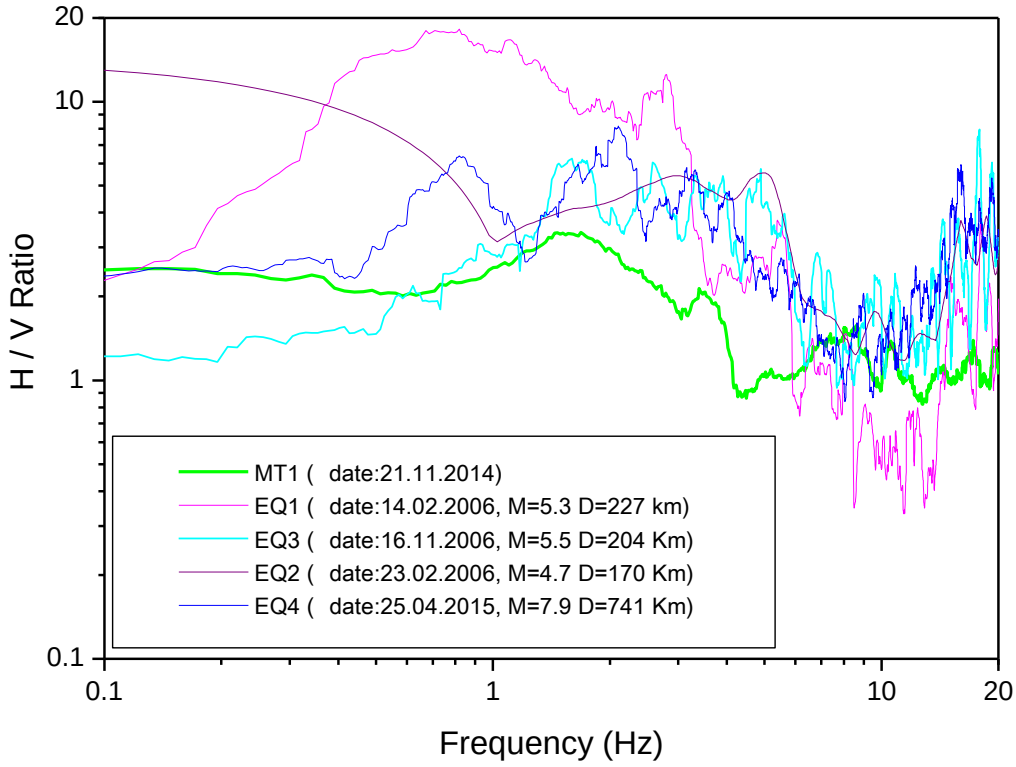

Figure 4.1 Comparison of HVR in Microtremor and Earthquake at Bogra

Table 4.1 The predominant frequency and H/V ratio of microtremor and earthquake at Bogra

Predominant Frequency, F_g(Hz)	MT1	EQ1	EQ2	EQ3	EQ4
	1.68	0.82	5.06	1.57	0.83
H/V Ratio, (A_g)	3.36	18.10	5.54	6.07	6.40

Comparison curves between predominant frequency and H/V ratio of microtremor and earthquakes at Natore as shown in Figure 4.2. It has been demonstrates that the peak amplitude ratio has been moved toward right side of microtremor.

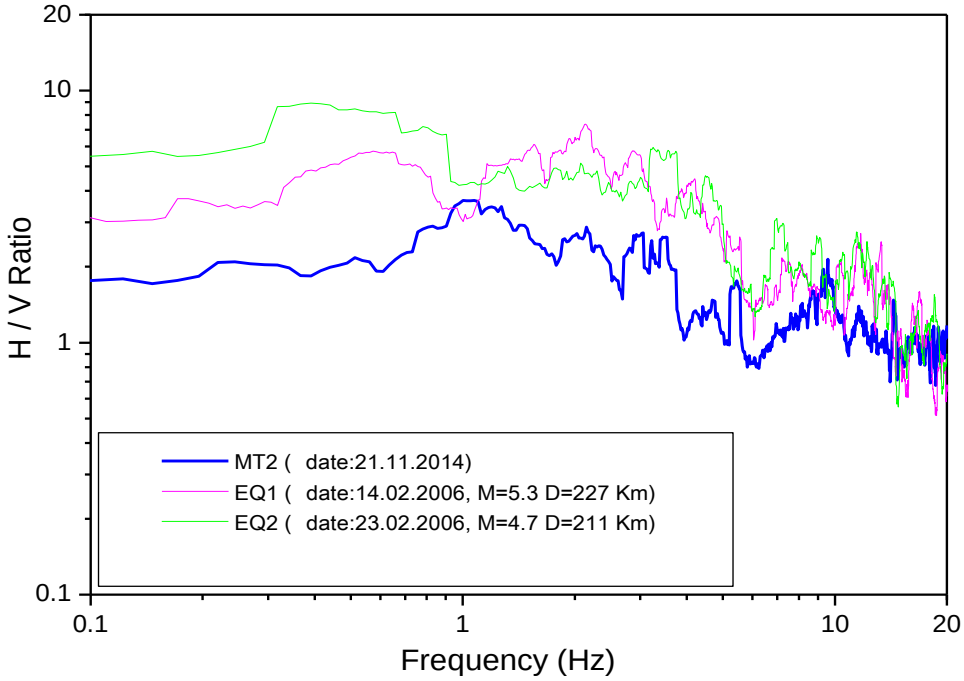

Figure 4.2 Comparison of HVR in Microtremor and Earthquake at Natore

The predominant frequency of microtremor is 1.15 Hz whereas the earthquake is 3.28 Hz. The H/V ratio of microtremor is 3.32 and earthquake is 7.28. The similar pattern of curves between microtremor and earthquake have been observed.

Table 4.2 The predominant frequency and H/V ratio of microtremor and earthquake at Natore.

Predominant Frequency, F_g(Hz)	MT2	EQ1	EQ2
	1.15	2.10	3.28
H/V Ratio, (A_g)	3.32	7.28	5.84

Comparison of HVR in Microtremor and Earthquake in the Jamuna Bridge at Sirajganj as shown in Figure 4.3

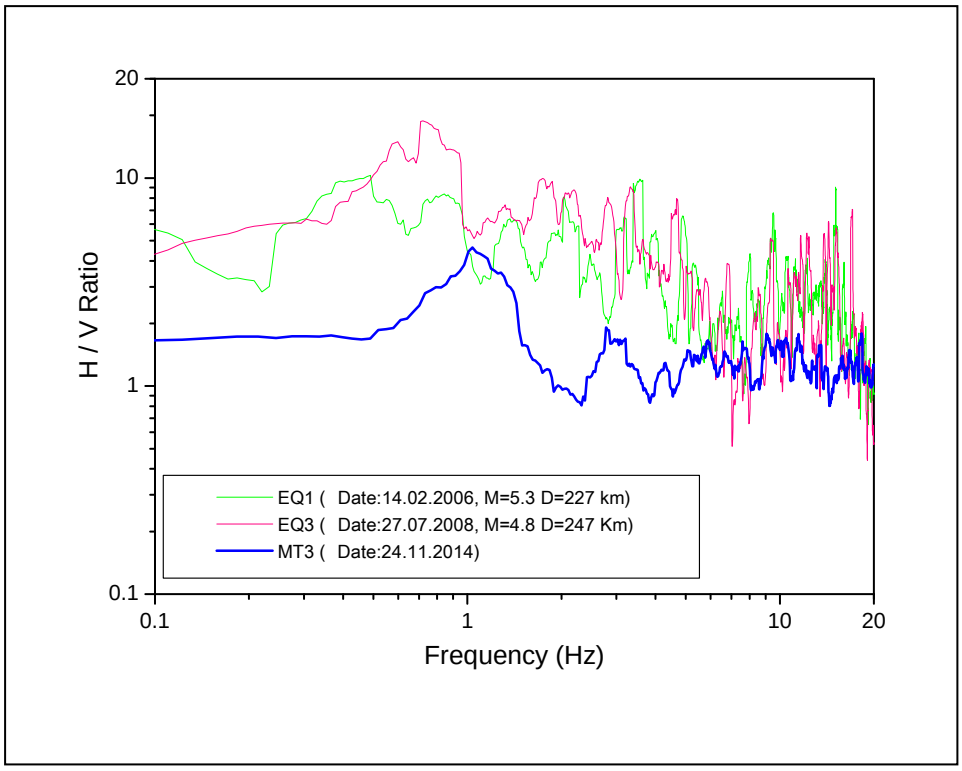

Figure 4.3 Comparison of Microtremor and Earthquake in the Jamuna Bridge East at Sirajganj

The predominant frequency of microtremor is 1.04 Hz whereas the earthquake is 0.83 Hz. The H/V ratio of microtremor is 4.66 and earthquake is 18.61. The similar pattern of curves between microtremor and earthquake have been observed.

Table 4.3 The predominant frequency and H/V ratio of microtremor and earthquakes Jamuna Bridge East at Sirajganj.

Predominant Frequency, F_g(Hz)	MT3	EQ2	EQ3
	1.04	0.83	0.72
H/V Ratio, (A_g)	4.66	8.44	18.61

Comparison of HVR in Microtremor and Earthquake in the Haji-Camp at Ashkona as shown in Figure 4.4

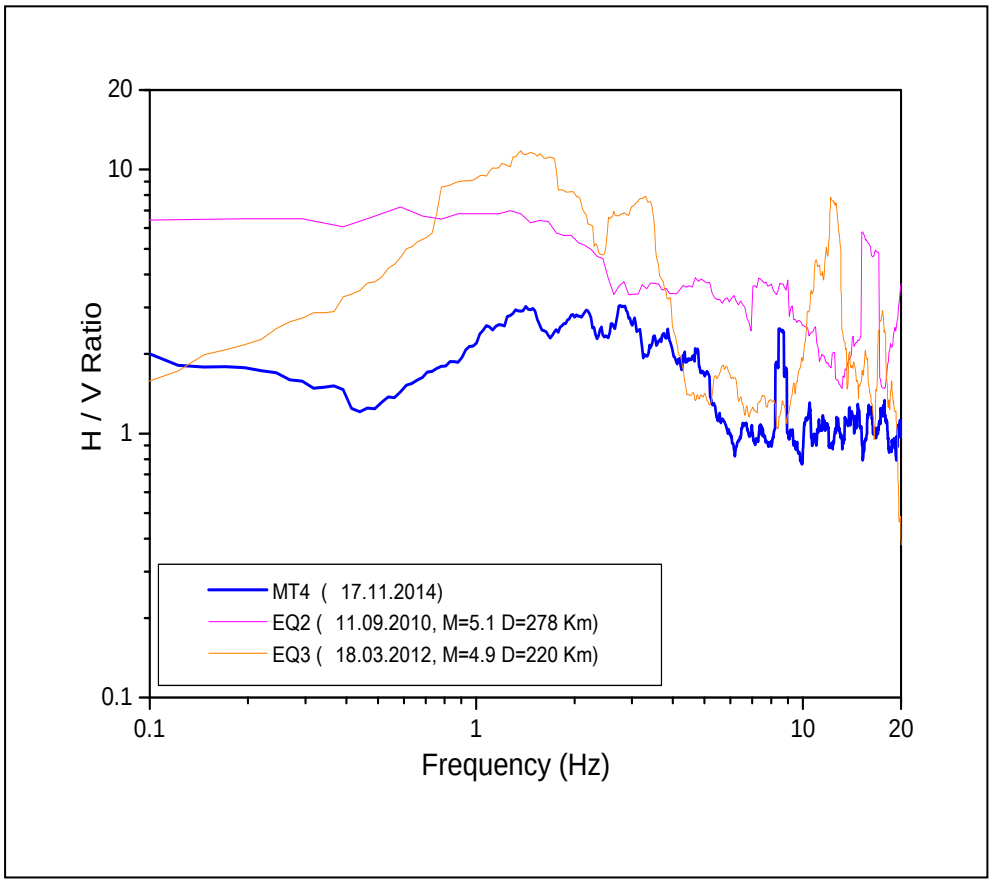

Figure 4.4 Comparison of HVR in Microtremor and Earthquake in the Haji-Camp at Ashkona

The predominant frequency and amplitude ratio of microtremor is 0.74Hz and earthquake is 1.73 Hz where as peak H/V ratio is 2.99 for microtremor and 11.89 for earthquake with respect to microtremor.

Table 4.4 The predominant frequency and H/V ratio of microtremor and earthquakes Haji-Camp at Ashkona.

Predominant Frequency, F_g(Hz)	MT4	EQ2	EQ3	EQ4
	0.74	1.24	1.40	1.73
H/V Ratio, (A_g)	2.99	7.72	11.89	3.64

Comparison of HVR in Microtremor and in the Police Staff College at Mirpur as shown in Figure 4.5

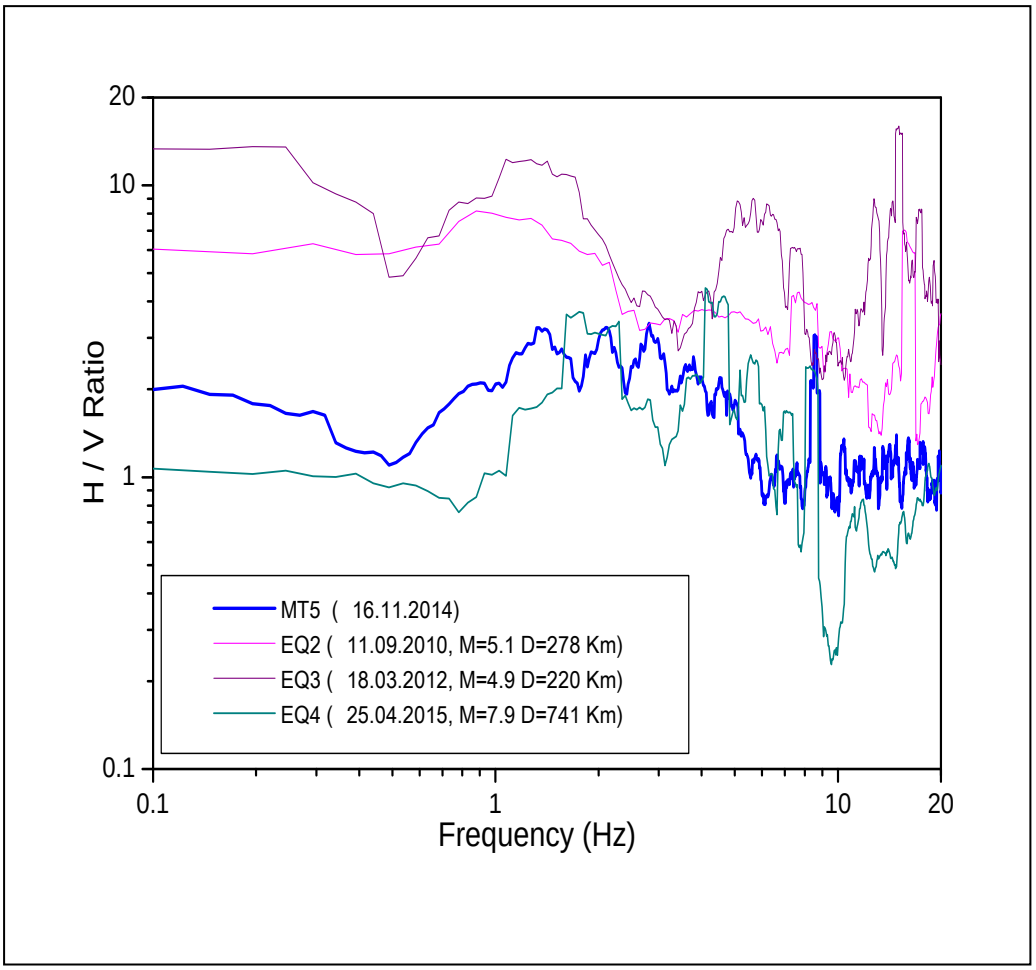

Figure 4.5 Comparison of HVR in Microtremor and in the Police Staff College at Mirpur

Table 4.5 The predominant frequency and H/V ratio of microtremor and earthquakes Police Staff College at Mirpur.

Predominant Frequency, F_g(Hz)	MT5	EQ2	EQ3	EQ4
	1.03	1.28	1.42	1.76
H/V Ratio, (A_g)	3.24	7.70	11.72	3.60

Comparison of HVR in Microtremor and Earthquakes at BUET-Campus as shown in Figure 4.6

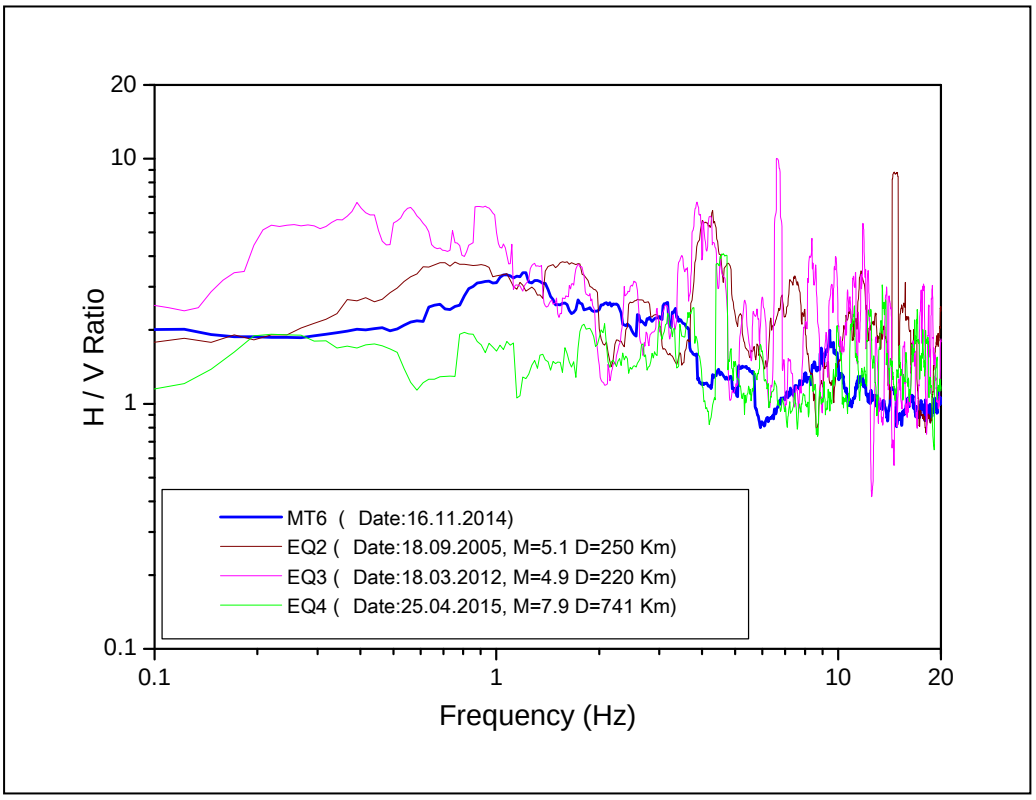

Figure 4.6 Comparison of HVR in Microtremor and Earthquake at BUET-Campus

Table 4.6 The predominant frequency and H/V ratio of microtremor and earthquakes at BUET-Campus.

Predominant Frequency, F_g(Hz)	MT6	EQ2	EQ3	EQ4
	1.31	1.57	0.91	3.71
H/V Ratio, (A_g)	3.41	3.74	6.32	2.42

The predominant frequency in microtremor is 1.31 Hz and EQ2, EQ3 and EQ4 is1.57 Hz, 0.91 Hz and 3.78 Hz. The peak H/V ratio of microtremor is 3.41 Hz whereas the EQ3 is 6.32 and it has been moved into left side and slightly upwards but EQ4 is initially downward with respect to microtremor.

From these result, it can be said that although amplitude values of the ratios are close, the predominant frequency for the two cases differs slightly. The reason of this difference is that microtremor and earthquake consists of different types of waves.

4.3 VULNERABILITY ASSESSMENT

Earthquake and Microtremor data analysis and their vulnerability assessment of six selected locations. The Horizontal to Vertical spectra ratio (HVSR) of these locations have been compared with the predominant frequency of selected site in EW and NS direction, respectively. Article 4.2 shows H/V Ratio and corresponding of microtremor and earthquake at six locations. Chapter 2 shows Vulnerability index (Kg) of soil using Nakamura's (2000).

4.3.1 Seismic Damage assessment of soil using Nakamura's Technique

Seismic vulnerability index (Kg) is an index indicating the level of vulnerability of a layer of soil to deform. Therefore, this index is useful for the detection of areas that are weak zone (unconsolidated sediment) at the time of occurrence of earthquakes. Some studies like Daryono (2009) and Nakamura (2000) showed a good correlation between seismic vulnerability index (Kg) and the distribution of earthquake disaster damage. This index is obtained from the peak value of HVSR squared, divided by the value of the predominant frequency.

The seismic vulnerability index has been classified into four major types. These are Low (0-5), Medium (6-10), High (11-20) and Very High (>20). Damage assessment of site soil at six locations using Nakamura's Vulnerability Index (Kg) is shows in Table 4.7

Table 4.7 Damage assessment of site soil using Nakamura's empirical formula

ID	Location	Predominant Frequency (MT), F_g(Hz)	H/V Ratio (MT-Array), A_g	Vulnerability Index, $K_g = \frac{A_g^2}{F_g}$ (MT)	Remarks (Based on MT data)	Range of Vulnerability index (Kg) for Earthquakes
MT1	Bogra	1.68	3.36	6.72	Medium	6 to 399
MT2	Natore	1.15	3.32	9.58	Medium	10 to 25

ID	Location	Predominant Frequency (MT), F_g(Hz)	H/V Ratio (MT-Array), A_g	Vulnerability Index, $K_g = \frac{A_g^2}{F_g}$ (MT)	Remarks (Based on MT data)	Range of Vulnerability index (Kg) for Earthquakes
MT3	Jamuna Bridge East Side at Sirajganj	1.04	4.66	20.88	Very High	86 to 481
MT4	Haji-Camp at Ashkona	0.74	2.99	12.08	High	14 to 100
MT5	Police Staff College at Mirpur	1.03	3.24	10.19	High	12 to 96
MT6	BUET-Campus	1.31	3.41	8.87	Medium	3 to 43

The seismic Vulnerability Index (Kg) at those six locations varies from 6.72 to 20.88 for microtremor observations. The estimated vulnerability Index from earthquakes are always higher than the microtremor due to high input energy. Microtremor vulnerability Index (Kg) values show higher value for reclaimed area which provides evidence that those sites needs some kind of soil improvement if they want to sustain earthquake load. Both predominant frequency and H/V ratio are required to estimate vulnerability type according to Nakamura's vulnerability index.

4.4 SUMMARY

This chapter shows the comparison of microtremor and earthquake data analysis results. The H/V ratio of microtremor and earthquake ground motion has been compared. From these results, it can be said that although amplitude values of the ratios are close, the predominant frequency for the three cases differs slightly. The reason of this difference is that microtremor and earthquake consists of different types of waves, but the H/V ratio is based on shear-wave only.

The (Kg) value falls within the range of very high in the Jamuna Bridge East side at Sirajganj. Most of the zones having higher Vulnerability Index (Kg) are situated in reclaimed areas.

CHAPTER FIVE

CONCLUSIONS AND RECOMMENDATIONS

5.1 GENERAL

The purpose of this research is to study horizontal to vertical spectral (H/V) ratio of microtremor and earthquake ground motion at six sites. The locations are namely at Bogra, Natore. Jamuna Bridge East, Haji-Camp at Ashkona, Police Staff college at Mirpur and BUET Campus.

The shear wave velocity has also been estimated at those locations using empirical correlation between SPT-N and shear-wave velocity along with using Microtremor Array recordings. Finally, seismic vulnerability index (Kg) of site soil using Nakamura's (2000) technique has been carried out for these sites.

5.2 CONCLUSIONS

The findings may be summarized as shown in bellows.

(a) Stability of Microtremor and Earthquake data

In order to check the stability of microtremor data five time segments of a single record have been used. Each segment is of 41s length. These five segments of time domain data have been converted to frequency domain data using smoothing function with 15 to 60 point. These Fourier spectra of five segments show almost similar pattern.

(b) H/V Ratio of Microtremor and Earthquake at selected Locations

H/V ratio of microtremor and earthquake has been estimated for six locations**.** The maximum predominant frequency of microtremor is 1.68 Hz, where as H/V ratio is 3.36 and Earthquakes predominant frequency is 3.71 Hz, where H/V ratio is 2.42 at BUET Campus. On the other hand, the minimum predominant frequency of micrtremor is 0.74 Hz, where H/V ratio is 2.99 and Earthquake predominant frequency is 0.72 Hz, where H/V ratio is 18.61 in the Jamuna Bridge east at Sirajgang.

(c) Seismic Vulnerability Index (Kg) for soil

Seismic vulnerability index (Kg) is an index indicating the level of vulnerability of a layer of soil to deform. This index is useful for the detection of areas that are weak zone (unconsolidated sediment) at the time of occurrence of earthquakes. The vulnerability index of six selected locations has been classified into four types which are low (0-5), medium (6-10), high (11-20) and very high (>20). From the analysis the highest (Kg) value has been found at Jamuna bridge east site. It can be concluded that this location is weaker than the other locations. The seismic vulnerability index (Kg) for six sites varies between 6.72 and 20.88 for microtremor. Three sites have been classified as low vulnerable of soil layers and other three sites have been identified as having medium to high vulnerable of soil layers to deform.

5.3 RECOMMENDATIONS

Although the study covers the objectives of study, more significant study would be needed to cover other aspects of the research. Specific recommendations are follows:

- Comparison between microtremor in (weak motion) data and earthquake in (strong ground motion) data for more locations.
- Investigation of Microtremor and Earthquake H/V ratio in around Bangladesh using reference site where exposed rock is available.

REFERENCES

Aki, K. (1993). Local site effects on weak and strong ground motion, Tectonophysics, 218, PP. 93-111.

Ali, M.H. and J.R. Choudhury (1992). Tectonics and earthquake occurrence in Bangladesh. *36th Annual Convention of IEB*, Dhaka, January 1992.

Ansary, M. A., Yamazaki, F. and Katayama, T. (1996). Application of microtremor measurements to the estimation of site amplification characteristics, Bulletin of Earthquake Resistant Structure Research Center, IIS, University of Tokyo, No. 29, PP. 95-113.

Ansary, M. A., Rahman, S., Murad, E. M., Chowdhury, S. A. and Shuvra, D. P. (2010). Proposed Time History and Response Spectrum for Dhaka, Chittagong and Sylhet cities, Proceedings, 3rd International Earthquake Symposium, March 5-6, Dhaka, Bangladesh, PP. 349-356.

Arai, H. and Tokimatsu, K. (2000). Effects of Rayleigh and Love Waves on microtremors H/V spectra. Proc. 12th World Conf. on Earthquake Engineering, paper 2232, CD-ROM.

Applied Technology Council (1985). Earthquake Damage Evaluation Data for California, ATC-13. Redwood City, California.

ASTM (2000). Annual Book of ASTM Standards, vol. 04.08: Soil and Rock (I). Standard No. D 1586-99, Standard Test Method for Penetration Test and Split-Barrel Sampling of Soils, West Conshohocken, PA, PP. 139-143.

Bard, P. Y. (1999). Microtremor measurements: A tool for site effect estimation?, Proceedings of the second international symposium on the effects of surface geology on seismic motion, Yokohama, Japan, December 1998, PP. 1251-1279.

Bard, P. Y. (2004). Effects of surface geology on ground motion: Recent results and remaining issues, Proceedings of the 10th European Conference on Earthquake Engineering, Vienna, Austria, August 28 – September 2, 1994, PP. 305-325.

Bilham, R., Gaur, V. K. and Molnar, P. (2001). Himalayan Seismic Hazard, SCIENCE, 293.

Cassidy, J. F., Rosenberger, A., Rogers, G.C., Little, T. E., Toth, J., Adams, J., Munro, P., Huffmann, S., Pierre, J. –R., Asmis, H. and Pernica, G. (2007). Strong motion seismograph networks in Canada, Proceedings of the Canadian Conference on Earthquake Engineering, June 24-27th 2007, Ottawa.

Chouinard, L., Rosset., P., de la Puente, A., Madriz, R., Mitchell, D. and Adams, J. (2004). Seismic hazard analysis for Montreal, Proceedings of the 13th World Conference of Earthquake Engineering, Vancouver, BC, Paper 7010.

Curry, J. R. and Moore, D. G. (1974). Sedimentary and Tectonic processes in Bengal Deep Sea Fan and Geosyncline, The geology of continental margins, Springer-Verlag, New York.

Daryono (2009). Eftek Tapek Lokal (Local site effect) di Graben Bantul Berdasarkan Pengakuran Mikrotremor. International Conference Earth Science and Technology. Yogjakarta.

Dimitriu, P. P., Papaioannou, Ch. and Theodulidis, N. P. (1998). EURO-SEISTEST strong motion array near Thessaloniki, Northern Greece: a case study of site effects. Bulletin of seismological society of America, No. 3, PP. 862-873.

Dravinski, M., Ding, G. and Wen, K. L. (1996). Analysis of spectral ratios for estimating ground motion in deep basins, Bull. Seism. Soc. Am., 86, PP. 843-847.

Enomoto, T., Kuriyama, K., Navarro, M. and Iwatate, T. (2002). Site-effects evaluation by H/V spectra comparing microtremor with strongmotion records observed at ground surface and basement using borehole, 12th European Conference on Earthquake Engineering, paper 596. Londres.

Fah, D., Kind, F. and Giardini, D. (2001). A theoretical investigation of average H/V ratios. Geophys. J. Int., 145, PP. 535-549.

Fahad (2015) “PS logging for site response analysis in Dhaka city” M.Sc.Engg. BUET-Dhaka.

Field, E. H. and Jacob, K. H. (1995). A comparison and test of various site-response estimation techniques, including three that are not reference-site dependent, Bulletin of the Seismological Society of America, 85, PP. 1127-1143.

Ghayamghamian, M. R. and Kawakami, H. (1997). Segmental cross-spectrum in microtremor spectral ratio analysis. 7th International Conference on Structural Safety and Reliability, Kyoto, November 1997, 24-28, PP. 1487-1494.

Grunthal G, editor. (1998). *European Macroseismic Scale*, Luxembourg: Cahiers due Centre European de Geodynamique et de Seismologie, Volumne 15.

Horike, M., Zhao, B. and Kawase, H. (2001). Comparison of site response characteristics inferred from microtremors and earthquake shear waves, Bulletin of the Seismological Society of America, 91, PP. 1526-1536

Kagami, H., Okada, S., Shiono, K., Oner, M., Dravinski, M. and Mal, A. K. (1986). Observation of 1 to 5 second microtremors and their application to earthquake engineering. Part III. A two-dimensional study of site effects in S. Fernando valley. Bulletin of seismological society of America, 76, PP. 1801-1812.

Kanai, K., Tanaka, T. and Osada, K. (1954). Measurements of Micro-tremors 1. Bulletin Earthquake Research Institute, Tokyo University, 32, PP. 199-210.

Konno, K. and Ohmachi, T. (1998). Ground motion characteristics estimated from spectral ratio between horizontal and vertical components of microtremor», Bull. Seism. Soc. Am., 88, N. 1, PP. 228-241.

Lachet, C., Hatzfeld, D., Bard, P. Y., Theodulidis, C. P. and Savvaidis, A. (1996). Site effects and microzonation in the city of Thessaloniki (Greece): Comparison of different approaches, Bulletin of the Seismological Society of America, 86, PP. 1692-1703.

Lermo, J. and Chavez-Garcia, F. J. (1994b). Site effect evaluation at Mexico city: dominant period and relative amplification from strong motion and microtremor records, Soil dyn. Earthquake eng. 13, PP. 413-423., 84, PP. 1350-1364.

Malischewsky and Scherbaum (2004). Numerical analysis suggests that microtremor site response can only be generated when the impedance contrast is greater than 3.5 thus the good correlation at “soft” soil sites.

Malischewsky, P. G. and Scherbaum, F. (2004). Love’s formula and H/V-ratio (ellipticity) of Rayleigh waves, Wave Motion, 40, PP. 57-67.

Matin, M.A., Maroof Khan, M.A., Fariduddin, M., Boul. M.A., Taolad Hossain, M.M. and Kononov, A.I. (1983). The Techtonic Map of Bangladesh-Past and Present, Vol-2, PP. 29-36.

Molnar, S. and Cassidy, J. F. (2006). A comparison of site response techniques using weak-motion earthquake and microtremors, Earthquake Spectra, 22, PP. 169-188.

Molnar, S., Cassidy, J. F. Monahan, P. A. and Dosso, S. E. (2007). Comparison of geophysical methods to determine shear-wave velocity, Proceedings of the Canadian Conference on Earthquake Engineering, June 24-27th 2007, Ottawa, ON, Paper 1173.

Mucciarelli, M. (1998). Reliability and applicability range of the Nakamura's technique. Journ. Earthq. Eng., 2, 4, PP. 625-638.

Mucciarelli, M., Gallipoli, M. R. and Arcieri, M. (2003). The stability of the horizontal to vertical spectral ratio of triggered noise and earthquake recordings, Bulletin of the Seismological Society of America, 93, PP. 1407-1412.

Murthy, V.N.S. (1991). Soil Mechanics and Foundation Engineering. Volume 2, Revised and enlarged third edition, SAITECH, Bengalore, India.

Molnar, S., Cassidy, J. F., Monahan, P. A., Onur, T., Ventura, C. and Rosenberger, A. (2007). Earthquake site response studies using microtremor measurements in southwestern British Columbia, 9th Canadian Conference on Earthquake Engineering, Ottawa, Ontario, Canada, 26-29 June, PP. 410-419.

Molnar, S., Cassidy, J. F., Monahan, P. A., Onur, T., Ventura, C.E. and Rosenberger, A. (2006a). Application of microtremor measurements for earthquake site response studies in southwestern British Columbia, Proceedings 100th Anniversary Earthquake conference, EERI/SSA, San Francisco, April 18-22, 2006.

Molnar, S., Rosenberger, A., Cassidy, J. F. Rogers, G. C. and Ristau, J. (2006c). Digital accelerograph recordings of the July 15 and 19, 2004 earthquakes, west of Vancouver Island, Geological Survey of Canada Open File 5010, PP.76.

Nakamura, Y. (1989). A Method for Dynamic Characteristics of Sub-surface Using Microtremors on the Ground Surface, Quick Report of Railway Technical Research Institute, 30, No. 1, PP. 25-33 (in Japanese).

Nakamura, Y. (2000). Clear identification of fundamental idea of Nakamura's Technique and its applications, Proc. Of the 12th World Conference on Earthquake Engineering, Auckland, New Zealand, PP. 2656-2664.

Ohmachi, T., Nakamura, Y. and Toshinawa, T. (1991). Ground motion characteristics in the San Francisco Bay area detected by microtremor measurements, Proc. 2nd International Conference on Recent Advances in Geotech. Earth. Eng. & Soil Dyn. Saint Louis, Missouri, PP. 11-15 March: PP. 1643-1648.

Rahman (2011) Applicability of H/V Microtremor Tehnique for site response analysis in Dhaka city. M.Sc.Engg. BUET,Dhaka.

Rayleigh, Lord (1885). On waves propagated along the plane surface of an elastic solid, Proceedings of the London Mathematical Society, Vol. 17, PP. 4-11.

Rodriguez, V. S. H. and Midorikawa, S. (2002). Applicability of the H/V Spectral Ratio of Microtremors in Assessing Site Effects on Seismic Motion, Earthquake Engineering and Structural Dynamics, 31, PP. 261-279.

Seo, K. (1994). On the applicability of microtremors to engineering purpose, Preliminary report of the Joint ESG Research on Microtremors after the 1993 Kushiro-Oki (Hokkaido, Japan) earthquake. Proc. of 10th European Conf. on Earthq., 4, PP. 2643- 2648.

Sneider, A. J., Motazedian, D. and Atkinson, G. M. (2005). Seismic soil amplification studies for Ontario Polaris stations, 1st Polaris-Polo Research Workshop, Queen's University, Kingston, January 6th, 2005.

Suzuki, T., Adachi, Y. and Tanaka, M. (1995). Application of Microtremor measurements to the estimation of earthquake ground motions in the Kushiro city during the Kushiro-Oki earthquake of 15 January 1993, Earthquake Eng. Struc. Dyn. 24, PP. 595-613.

Tanvir (2009) "Estimation of earthquake induced liquefaction potential of selected areas of Dhaka city based on shear wave velocity" M.Sc.Engg. BUET, Dhaka.

Taga, N. (1993). Measurement of microtremors in Earthquake Ground Motion and Ground Condition, edited by The Architectural Institute of Japan.

Tokimatsu, K. and Miyadera, Y. (1992). Characteristics of Rayleigh waves in microtremors and their relation to the underground structures, J. struc. consr. Eng, AIJ 439, PP. 81-87 (in Japanese)

TC4 (1993). Manual for Zonation on Seismic geotechnical hazards, published by ISSMFE.

Wakamatsu, K. and Yasui, Y. (1995). Possibility of estimation for amplification characteristics of soil deposits based on ratio of horizontal to vertical spectra of microtremors, J. struct. consr. Eng, AIJ 471, PP. 61-70 (in Japanese).

Yamanaka, H., Takemura, M., Ishida, H. and Niwa, M. (1994). Characteristics of long period microtremors and their applicability in exploration of deep sedimentary layers, Bull. Seism. Soc. Am., 884, PP. 1831-1841.